CIVIL ENGINEERING STUDIES
STRUCTURAL RESEARCH SERIES NO. 153

STRENGTH OF PRESTRESSED CONCRETE BEAMS WITH WEB REINFORCEMENT

A Thesis
by
G. Hernandez

Issued as a Part
of the
SEVENTH PROGRESS REPORT
of the
INVESTIGATION OF PRESTRESSED CONCRETE
FOR HIGHWAY BRIDGES

MAY 1958
UNIVERSITY OF ILLINOIS
URBANA, ILLINOIS

STRENGTH OF PRESTRESSED CONCRETE BEAMS WITH WEB REINFORCEMENT

A Thesis by
G. Hernandez

Issued as a Part of the Seventh Progress Report of the
INVESTIGATION OF PRESTRESSED CONCRETE
FOR HIGHWAY BRIDGES

Conducted by
THE ENGINEERING EXPERIMENT STATION
UNIVERSITY OF ILLINOIS

In Cooperation With
THE DIVISION OF HIGHWAYS
STATE OF ILLINOIS
and
U. S. DEPARTMENT OF COMMERCE
BUREAU OF PUBLIC ROADS

Urbana, Illinois
May 1958

CONTENTS

CONTENTS (Continued)

LIST OF TABLES

LIST OF FIGURES

LIST OF FIGURES (Continued)

LIST OF FIGURES (Continued)

LIST OF FIGURES (Continued)

I. INTRODUCTION

1. General Remarks

While it has been found possible to predict with reasonable accuracy the load carrying capacity of a concrete column and the flexural strength of a concrete beam, one of the greatest difficulties since the advent of reinforced concrete construction has been the formulation of a satisfactory method for the estimation of the "shear" strength of concrete members. This difficulty has been experienced mainly for two reasons:

(1) The complexity of the shear failure mechanism.

(2) The dependence of the "shear" strength of a beam on the tensile strength of concrete.

As is well known, the flexural strength of a beam varies with the tensile strength and area of the steel, the compressive strength and area of the concrete, and the length of the corresponding lever arm between their centers of gravity. The magnitude of these forces, the shape of the compression block etc., can either be determined or reasonably assumed so as to give suitably accurate values. Furthermore, the mechanism of failure is simply and fairly well understood. Thus the flexural strength of a concrete member can be predicted within reasonable limits. The situation is similar for columns, and no further comments are necessary.

In the case of "shear" strength the picture is different. The mechanism of failure and the "shear capacity" depend on factors such as the crack patterns, which are very difficult to predict, and on other factors, such as moment-shear ratio, percentage of longitudinal reinforcement, continuity, span-depth ratio, etc., the influence of which is not well understood. It seems conceivable that a full understanding of the influence of all these factors on

the shear strength could be reached by a very extensive program of investigation. In fact some understanding of many of them already exists, at least qualitatively. But the practicability of such an investigation, and the usefulness of the possible results are doubted by some researchers. They refer to the lack of agreement among the results of many different investigations already performed.

The other factor mentioned in connection with this problem is the tensile strength of concrete. It is the present philosophy in concrete design that the concrete should not be relied upon when it is stressed in tension. Steel reinforcement should be used if tensile stresses exist. This is quite acceptable if the uncertainty of the value of the tensile strength of concrete, the abruptness of failure, and the relatively low strength of concrete in tension are considered. Thus, in predicting the flexural capacity of a reinforced concrete member, the error introduced by neglecting the tensile strength of the concrete is small for all common cases. But again, this is not the case when the shear strength of a member is studied. It is known that a beam without any web reinforcement may fail in flexure, if the "diagonal tensile stresses" are small enough. In this case, the tensile strength of the concrete is carrying all the "shear". At this point it is necessary to remember that, although the term "shear strength" is being used, the stress which really must be considered in dealing with "shear" failures is the so-called "diagonal tensile stress" or "principal tensile stress".

Thus, it is seen that the relative importance of the tensile strength of the concrete in relation to the shear strength of a member is great, and although a practical solution of the shear problem could be achieved by neglecting the contribution of the tensile strength of the concrete, for a full understanding of the phenomenon of shear failures, the relative contribution of both the web reinforcement and the concrete must be considered.

For the special case of prestressed concrete I-beams the relative influence of the tensile strength will be minimized due to other factors such as the reduced cross-sectional area of the web and the presence of the prestressing force.

2. Object and Scope of Investigation

Past experiments have proved conclusively that, contrary to the opinions of some authors, prestressed concrete beams can fail in shear and, in most cases, at considerably lower loads than their flexural capacities.

The present attitude towards shear failures is to try to prevent them. This practice is defended on the grounds of improving the ductility and load-carrying capacity of the beams; that is to say, improved behavior of the member. The purpose of this investigation was to examine the validity of this assumption and to study quantitatively the use of vertical stirrups to prevent shear failures.

The complexity of the "shear" phenomenon has been pointed out. Owing to this and to the obvious limitations of this study, a selection of the variables to be considered had to be made. Thus, the following variables were studied:

a) Amount of longitudinal reinforcement.

b) Web thickness.

c) Amount of web reinforcement.

d) Spacing of stirrups.

e) Yield point stress of web reinforcement.

f) Concrete strength.

g) Shear span.

h) Composite construction with cast-in-place slab.

The results from the 38 beams tested in this investigation are discussed in the following pages. An attempt to determine the amount of web reinforcement necessary for "balanced" design was made, and an empirical expression, based on the variables which seemed to be most significant, is offered. A hypothesis explaining qualitatively the mechanism of failure is stated and discussed. A further use of the results of this investigation is to plan future tests intended for a more comprehensive study of behavior and strength in shear, and suggestions regarding such studies are made in this report.

3. Outline of Tests

A summary of the properties of the 38 beams tested, designated G1 through G38, is presented in Table 1.

All specimens were I-beams with a web thickness of either 1 3/4 or 3 in. The overall dimensions were 6 by 12 in. cross-section, and two of the beams had 2 by 24 in. cast-in-place slabs. The nominal dimensions of the beams are shown in Fig. 1. All tests were conducted on simply supported specimens symmetrically loaded by either one or two concentrated loads on a span of 9 ft. All beams were pretensioned, had straight tension reinforcement and no compression steel.

The web reinforcement for all beams was provided by vertical stirrups having one, two or three legs. The end-blocks were also provided with stirrups at the same spacing as the rest of the beam. The stirrups in the end-blocks were made of the same material used for the other stirrups in each particular beam, although they were of a different type.

The nominal dimensions of the stirrups are shown in Fig. 2, and their spacings in Figs. 3a and 3b. For the first three beams, stirrups were provided only in the shear spans. However, when some cracks between the flanges and the web were observed in the mid-portion of two beams before testing, it was decided to use stirrups throughout the length of the beams to prevent the opening of these cracks.

The nominal effective prestress for all beams was 120,000 psi. The ranges of the other variables are given below:

Beams with 1 3/4-Inch Thick Webs: 26 Beams

Longitudinal Reinforcement Ratio:

0.19 percent . . . . 10 beams

0.40 percent . . . . 16 beams

Concrete Strength: 2310 to 5420 psi

Shear Span:

36 in. . . . . 24 beams

28 in. . . . . 2 beams

Stirrups:

Spacing,

2.5 in. . . . . 12 beams

3.0 in. . . . . 3 beams

3.75 in . . . . 1 beam

5.0 in. . . . . 7 beams

7.5 in. . . . . 1 beam

9.0 in. . . . . 2 beams

Ratio (based on overall area); 0.048 to 0.382 percent.

Yield Point: 30.7 to 42.5 ksi.

Cast-in-Place Slab: . . . 2 beams

Beams with 3-Inch Thick Webs: 12 Beams

Longitudinal Reinforcement Ratio:

0.19 percent . . . . 1 beam

0.40 percent . . . . 11 beams

Concrete Strength: 2680 to 5520 psi

Shear Span:

54 in. . . . . 1 beam

48 in. . . . . 2 beams

36 in. . . . . 9 beams

Stirrups:

Spacing,

2.5 in. . . . . 3 beams

5.0 in. . . . . 7 beams

7.5 in. . . . . 1 beam

10.0 in. . . . . 1 beam

Ratio (based on overall area); 0.048 to 0.196 percent.

Yield Point: 33.6 to 42.5 ksi.

In spite of the wide range of concrete strengths shown in the preceding summary, it should be noted that for most of the beams a value of about 3000 psi was used.

4. Acknowledgment

The studies reported herein were made as a part of an investigation of prestressed concrete for highway bridges conducted in the Structural Research Laboratory of the Civil Engineering Department of the University of Illinois in cooperation with the Illinois Division of Highways and the Bureau of Public Roads, U. S. Department of Commerce.

This program of investigation has been guided by an advisory committee on which the following personnel have served during the period covering the work reported herein: W. E. Chastain, W. J. Mackay, and C. E. Thunman, representing the Illinois Division of Highways; E. L. Erickson and Harold Allen, representing the Bureau of Public Roads; C. P. Siess, I. M. Viest, and N. Khachaturian, representing the University of Illinois.

General direction of the investigation was provided by Dr. C. P. Siess, Professor of Civil Engineering. The work was carried out under the immediate supervision of Dr. M. A. Sozen, Assistant Professor of Civil Engineering.

The prestressing reinforcement used in this investigation was donated by the American Steel and Wire Division of the United States Steel Corporation.

The following research personnel, graduate students in Civil Engineering, gave valuable assistance in conducting the tests and reducing and presenting the data: E. Alfieri, N. M. Hawkins, and T. J. Larsen.

This report was written as a thesis under the direction of Professor Siess, whose instruction and assistance are gratefully acknowledged.

5. Notation

(a) Designation of Test Specimens

Each specimen has been designated by a letter and a number. The letter is the same for all specimens and is used to distinguish this series of tests from the other series which compose the investigation of prestressed concrete for highway bridges. The series reported herein is G. The number was assigned to each specimen according to the order of testing and has no other meaning.

(b) Symbols

Cross-sectional Constants

A_c = gross area of cross-section

A_s = total area of longitudinal reinforcement

b = top flange width of beam without any slab

b' = web thickness

d = effective depth of the longitudinal reinforcement

Loads

C = total compressive force in the concrete

F_{se} = effective prestressing force

M_c = bending moment at inclined tension cracking (Eq. 4)

M_t = total ultimate moment measured in tests

M_u = total ultimate bending moment

P_c = applied load at inclined tension cracking

P_u = ultimate applied load

T = total tensile force in the longitudinal reinforcement

V_c = shear at inclined tension cracking

V_u = total ultimate shear

Stresses

Concrete

E_c = assumed modulus of elasticity of concrete

f'_c = compressive strength determined from 6 by 12-in. control cylinders

f_{cu} = average concrete stress in compression zone at failure

f_r = modulus of rupture determined from 6 by 6 by 22-in. control beams loaded at the third-points over an 18-in. span

f_t = assumed tensile strength of concrete

v = nominal shear stress

Steel

E_s = modulus of elasticity of steel

f'_s = ultimate tensile strength of longitudinal reinforcement

f_{se} = effective prestress

f_{su} = stress in longitudinal reinforcement at failure of beam

f_y = yield point stress of web reinforcement

Strains

Concrete

ϵ_c = concrete strain

ϵ_{ce} = concrete strain at level of longitudinal reinforcement, due to effective prestress

ϵ_u = limiting strain at which concrete crushes in a beam

Steel

$\epsilon_{sa} = \epsilon_{su} - (\epsilon_{se} + \epsilon_{ce})$ = increase in steel strain after zero concrete strain at level of longitudinal reinforcement is reached

ϵ_{se} = steel strain corresponding to effective prestress

ϵ_{su} = steel strain at failure of beam

Dimensionless Factors

a/d = ratio of shear span length to effective depth

k_u = ratio of neutral axis depth at failure to effective depth

k_2 = ratio of depth of the compressive force to neutral axis depth

$p = A_s/bd$ = longitudinal reinforcement ratio

$Q = p\, E_s/f'_c$

$r' = A_v/bs$ = web reinforcement ratio, based on flange width

$r = A_v/b's$ = web reinforcement ratio, based on web width

Miscellaneous

a = length of shear span

A_v = cross-sectional area of one stirrup

s = spacing of the stirrups

Δ_u = midspan deflection at ultimate load

II. MATERIALS, FABRICATION, AND TEST SPECIMENS

6. Materials

(a) Cement

Marquette brand Type I portland cement was used for all the specimens. The cement was purchased in lots of 20 or 40 paper bags from local dealers.

(b) Aggregate

Wabash River gravel and Wabash River sand were used as aggregate for all the specimens. Both aggregates have been used in this laboratory for many previous investigations and have passed the usual specification tests. Because of the geometry of the specimens the maximum size of the coarse aggregate was limited to 3/8 in. The sieve analyses for the various lots of aggregates are listed in Table 2.

The origin of these aggregates is an outwash of the Wisconsin glaciation. The major constituents of the gravel are limestone and dolomite with minor quantities of quartz, granite, gneiss and others. The sand consists mainly of quartz. The absorption of both fine and coarse aggregate was about one percent by weight of surface-dry aggregate.

(c) Concrete Mixes

Mixes were designed from available data for similar mixes used in this investigation during the past six years. Minor corrections were necessary in some cases. The mixes were designed for a 3-in. slump. At the time of mixing of the concrete, moisture samples were taken from the sand and gravel, and their results were used to determine the proportions of the mixes. These proportions by weight are reported in Table 3 which also includes information on slump, compressive strength, modulus of rupture at time of beam test, age, and aggregate lot.

To facilitate comparison with similar mixes used in other phases of the general investigation of which this study is a part, a summary of the characteristics of the mixes is included. Figure 4 shows the relationship between interpolated seven-day compressive strengths and the corresponding water-cement ratios. The increase of concrete strength with age, expressed as a ratio of the seven-day strength, is shown in Fig. 5.

The modulus of rupture was determined for each batch from tests of 6 by 6-in. beams, loaded at the third-points on a 18-in. span. In Fig. 6 the moduli of rupture are compared with the corresponding compressive strengths of the concrete. As expected, the scatter is quite large but in general the results seem to agree reasonably well with the following expression based on experience with the same type of concrete (1)*:

$$f_r = \frac{3000}{4 + \frac{12000}{f'_c}} \qquad (1)$$

In this formula, f_r and f'_c are both in pounds per square inch. The values of f_r used in this study were all computed by formula (1) and were not the observed ones.

(d) Prestressing Wire

All the prestressing reinforcement used in this investigation was manufactured by the American Steel and Wire Division of the United States Steel Corporation. The manufacturer designated this steel as "Hard Drawn Stress Relieved Super-Tens Wire", and it was received in two different shipments designated as Type X and Type XI upon arrival.

Type X wire was delivered in a coil about six feet in diameter and weighing approximately 300 lb. Type XI wire was delivered in a 260-lb. coil, of

---

* Numbers in parentheses refer to entries in the Bibliography at the end of this volume.

54-in. diameter. The following steps were involved in the manufacture of the wire: (1) hot rolling, (2) lead patenting, (3) cold drawing, and (4) stress relieving. The following heat analyses were furnished by the manufacturer:

Type	C percent	Mn percent	P percent	S percent	Si percent
X	0.81	0.76	0.010	0.027	0.23
XI	0.85	0.65	0.010	0.027	0.18

The stress-strain characteristics for the two types of wire are shown in Figs. 7 and 8. The curves are based on the average results obtained by testing several samples cut from different portions of each coil. All samples were tested in a 120,000-lb. capacity Baldwin-Southwark-Tate-Emery hydraulic testing machine, and the strains were measured with an 8-in. extensometer employing a Baldwin "microformer" coil and recorded by an automatic device.

The surfaces of all wires were wiped with a rag dipped in a solution of hydrochloric acid and the wires were then stored in a moist room for several days in order to rust them. This produced a slightly pitted surface which improved the bond characteristics. The intended locations of the electric strain gages were protected from rusting by wrapping them with insulating tape. All wires were cleaned with a wire brush to remove loose rust before they were used in a beam.

(e) Stirrups

The stirrups for all beams were made of black annealed wire of five different nominal diameters. This wire was received in two shipments, designated here as lot A and lot B, consisting of straight pieces of wire 15 ft long. After cutting the wires to the proper lengths for stirrups, they were rusted and samples were tested in the same way as indicated for the prestressing steel. The

stress-strain characteristics together with the diameters and yield-point stresses are shown in Figs. 9 and 10. The type of wire used for the stirrups of each particular beam is identified in Table 1 by its yield point stress.

(f) Reinforcing Bars

Intermediate grade No. 3 deformed bars were used to reinforce the slabs cast on the tops of two beams. These bars were taken from the laboratory stock and samples were tested in the same way indicated in Section 6(d). The bars had a "flat" yield point, at an average stress of 52,000 psi.

7. Description of Specimens

All the specimens were pretensioned I-beams with nominal overall cross-sectional dimensions of 6 by 12 in. and total lengths of 10 ft - 10 in. Of the 38 beams tested, 12 had 3-in. webs and 26 had 1 3/4-in. webs. These webs were formed by metal inserts placed in standard rectangular forms. The inserts were shorter than the full length of the beam in order to form end-blocks about 18 in. long at each end of the beam.

The longitudinal reinforcement consisted of straight single wires, and the bond between them and the concrete was relied upon for anchorage. No other anchorage device was used, and no slip was ever detected. Vertical stirrups were used in all beams at a constant spacing for each beam, but varying from beam to beam.

The nominal dimensions of the beams are shown in Fig. 1. However, in the actual beams, although metal forms were used to cast them, the dimensions varied slightly from beam to beam. The measured dimensions are listed in Table 1.

Two beams had 2 by 24-in. slabs cast on the top. These slabs were reinforced by intermediate grade No. 3 deformed bars at 6-in. spacing in both directions. The bars were placed at midheight of the slab. The continuity of the shear flow between the slab and the beam was maintained by using longer

stirrups with the upper ends protruding from the beam (Fig. 2, Type B) and also shear keys along the top of the beam. The shear keys for both beams were 3/4 in. deep, 2 in. long in the direction of the length of the beam, and extended the full width of the upper flange. The center-to-center spacing of the keys was 5 in. for G34 and 6 in. for G38. For a view of the shear keys and the slab reinforcement see Figs. 11 and 12.

8. Prestressing

(a) Wire Anchorages

Threaded connections were used to grip both ends of the wires during the tensioning process and thereafter until "transfer" took place. Threads were cut on the end 3 in. of the wires by specially heat-treated, 24 threads to the inch, chasers mounted in an automatic threading machine. In spite of the heat treatment, the chasers became dull after threading about twenty-five wires, and required resharpening. The threads on the wires were cut to provide a medium fit with the threads in the nuts, requiring a thread slightly larger than a No. 10 which has a basic major diameter of 0.190 in. The nominal diameter of the wires was 0.196 in.

To fit the conditions required for these connections, 5/8-in. long hexagonal nuts were specially manufactured in the laboratory machine shop. They were sub-drilled with a No. 16 tap drill and tapped with a standard No. 12, 24 threads to the inch tap. This provided a full No. 12 thread in the nuts. Nuts with a No. 10 thread required too much material to be cut from the wires to be practical. The thread cut on the wires to fit the No. 12 thread in the nuts was sufficient to develop at least 160,000 psi in the wires for several days and was considered to be the most suitable.

The nuts were made from 1/2-in. diameter "Buster" alloy punch and chisel steel having the following analysis range: Carbon 0.56-0.60 percent;

Chromium 1.10-1.30 percent; Silicon 0.60-0.80 percent; Tungsten 2.00-2.30 percent; Vanadium 0.20-0.30 percent. The nuts were hardened by the following procedure. (1) Pack in charcoal in a closed steel box. (2) Heat for 20 minutes at 1200° F. (3) Heat for 45-60 minutes at 1650° F. (4) Oil quench to slightly above room temperature. (5) Temper 30 minutes at 1000° F. (6) Remove from furnace and air cool. To avoid any time delay in this process two furnaces were used.

(b) Tensioning Apparatus

Since all the beams were pretensioned, a prestressing frame was used to provide a reaction for the tensioning force until "transfer" took place. This frame was made from two lengths of standard 3-in. pipe and two 6 by 2 by 21-in. bearing plates. The plates had four rows of six 0.206-in. diameter holes spaced at 11/16-in. vertically and laterally to accommodate various positions of the wires. The prestressing frame had enough room between the pipes and the wires to accommodate the form of the beam.

A thirty-ton capacity Simplex centerhole hydraulic ram operated by a 10,000-psi capacity Simplex pump was used to tension the wires. A U-shaped frame supported by a bearing plate of the prestressing frame provided a reaction for the jack. To tension the wires, the ram reacted against the U-frame and a 5/8-in. diameter rod. This rod was placed through the centerhole of the ram and had one end directly connected to the threaded prestressing wire, and the other end bearing against the ram through a stiff plate attached to the rod with a nut. Consequently, the thrust was transferred from the ram to the rod, and from the rod to the wire. When the wire was tensioned to the desired stress, a split shim was slipped onto the wire and a nut was turned up tight against it. The shims were used to fill the space between the nut and the bearing plate created by the elongation of the wire and thereby reduce the required length of thread on the wires. The complete tensioning arrangement is shown in Fig. 13.

(c) Measurement of the Tensioning Force

Aluminum dynamometers were used to determine the tensioning force in the wires. These dynamometers consisted of 2-in. lengths of 1/2-in. aluminum rod, with 0.2-in. diameter holes drilled through their centers. Two type A7 SR-4 electric strain gages were attached to opposite sides of each dynamometer and wired in series. Consequently the strain reading was the average of the strains in the two gages. This arrangement was such that small eccentricities of the load would not affect the strain reading.

The dynamometers were placed on the wire between the nut and the bearing plate at the end of the prestressing frame opposite to that at which the tension was applied. Therefore, the prestress was transferred from the wire to the dynamometer through the nut, and from the dynamometer to the prestressing frame through the bearing plate. In this arrangement the dynamometers are acted upon by a compressive force equal in magnitude to the tension in the wires. The relationship between this compressive force and strain reading was determined by calibrating each dynamometer individually. They were calibrated using the 6000-lb range of a 120,000-lb capacity Baldwin hydraulic testing machine. The strain allowed a fairly precise measurement of stress in the wires, since the strain indicator used had a sensitivity of 2 or 3 millionths.

Figure 15 shows a schematic drawing of the reinforcement anchorage at the dynamometer end of the prestressing frame.

(d) Tensioning Procedure

The prestressing frame was used to tension the reinforcement prior to casting the beam. The ends of the wires were slipped through the end plates of the form and through the bearing plates of the prestressing frame. The dynamometers were then slipped on one end of the wires and finally the anchoring nuts were put on both ends of each wire. Two wires of each beam had Type A7 SR-4

electric strain gages located at midspan. After readings were taken on all the dynamometers in an unstressed condition, the wires were tensioned individually. The jacking frame was placed in position resting against the bearing plate, and the pull-rod connected to the wire. The centerhole ram was placed over the pull-rod and each wire in turn was tensioned to the desired value of stress. The anchor nut was turned up snug against the shim, and the pressure on the ram was released. As the prestressing frame underwent an elastic shortening with the tensioning of the wires, the first wires to be tensioned were overstressed a certain amount dictated by the experience with previous beams. In spite of that, minor adjustments were needed after tensioning all wires, and the overstressing was such that these adjustments were generally made by releasing the nuts with a wrench rather than by tensioning again with the ram.

The initial prestress was 132,000 psi for all the beams, which gave a nominal effective prestress of about 120,000 psi after all the losses took place.

(e) Stirrups

The stirrups of Types A, B and D (Fig. 2) were slipped on the prestressing wires before anchoring the latter to the end-blocks. Upon tensioning the wires, the position of each stirrup was marked on the longitudinal reinforcement, and each stirrup was tied in position using baling wire (Fig. 16). When Type E stirrups were required, they were placed in two operations: First, Type D stirrups were placed as indicated above, and then a third leg was added to each stirrup to make up the three-leg stirrups. Type C stirrups could be placed in position after tensioning the longitudinal steel because they had only one leg. The position of the stirrups was always carefully referred to the prestressing frame before casting the beam, and afterwards the position of each stirrup was marked on the sides of the beam by vertical broken lines, which can be seen in all photographs of the beams.

In order to keep the stirrups in position during casting, a provisional steel bar was tied to the top of all stirrups, keeping them vertical and at the proper spacing. After the concrete was placed and vibrated this bar was removed.

9. Casting and Curing

After prestressing and tying the stirrups in position, the prestressing frame was placed around the form with the reinforcement correctly aligned inside it.

Prior to this operation, the form was cleaned and greased. Two metallic inserts were put in place inside the form to shape the I-Beam. No wooden inserts were used because past experience showed that the concrete adhered more strongly to them than to the metallic ones.

Two clamps were placed externally at the third points of the form to prevent bulging out of the sides. After this operation, the position of each stirrup was carefully checked. This was important because the concrete cover of the stirrups in many cases was less than 1/4 in.

The prescribed amount of each component of the concrete mix was measured by weight and placed in the hopper of a 6-cu ft nontilting drum mixer in the following order: coarse aggregate, cement, and sand. The hopper was emptied into the rotating drum as the water was being added. From time to time the mix was checked and if it appeared dry, one or two pounds of water were added. The mixing lasted about 2 1/2 minutes. Two 4-cu ft batches were used to cast each beam and the corresponding control cylinders and control beams. In spite of the use of a butter mix, the two batches were usually different in strength and consistency, thus, to ensure as much uniformity of material in the compression flange as possible, the first batch was placed in the bottom half of the beam and the second batch in the top half. Four 6 by 12-in. control cylinders and one

6 by 6 by 22-in. control beam were cast from the first batch. Eight control cylinders and one beam were cast from the second batch.

After casting each batch, the concrete was vibrated with a high frequency internal vibrator. While the concrete was still fresh, two hooks were embedded in the beam at about 11 in. from each end to facilitate handling.

During the batching operation samples of the aggregates were taken to determine the free moisture. The slump of each batch was measured immediately after mixing.

The tops of the test beam and the control beams were troweled smooth and the cylinders capped with a paste of neat cement four hours after casting. Four of the cylinders cast from the second batch were tested within the first six days in a 300,000-lb hydraulic Riehle testing machine to estimate the time of release of the tensioned wires. The remaining cylinders and the control beams were tested on the day of the test to determine the concrete strength and the modulus of rupture, respectively.

Since cracks between the web and the flanges were detected in the first specimens cast, it was decided to pull the sides of the form away from the beam about six hours after casting after which the beam was covered with wet burlap for two days. Usually the specimen was removed from the form six days after it was cast and kept in laboratory air until it was tested. The control specimens were stored under the same conditions as the test beams.

When the concrete in the beam was strong enough, the prestress was transferred to the concrete beam. This was accomplished by slowly loosening the nuts so that the tension in each of the wires was approximately equal at all times. In spite of this precaution, some wires fractured at the threads during this operation. Before releasing the wires, all beams were prestressed externally at the top to counteract the tensile stresses caused by the prestressing

force in the top fibers. This was very desirable in order to move the specimens safely about the laboratory. The "top prestress" was removed either before the test was started or after the first few increments of load were applied.

The beams which were to have a slab cast on top were manufactured in the same manner as indicated in the preceding paragraphs, except for the following difference. The top of the beam was not troweled smooth and beveled pieces of wood were pressed into the concrete to shape the shear keys. After transfer, the protruding parts of the stirrups were thoroughly cleaned, and the coarse aggregate of the concrete was exposed on the top of the beam by using a special hammer and a wire brush. Finally the top surface was cleaned by compressed air (Fig. 11). At this stage the beam was supported at two points, corresponding to the reactions during the testing, and the form for the slab was built up around the beam. The slab reinforcement was put in place and the top surface of the beam was wetted before casting the slab (Fig. 12). One batch of concrete was used for the whole slab, four 6 by 12-in. control cylinders, and one 6 by 6 by 22-in. control beam. The slab was finished and cured following the procedure already indicated for the beams.

III. INSTRUMENTATION, LOADING APPARATUS, AND TEST PROCEDURE

10. Loading Frame

All specimens were tested in a steel frame composed of two steel columns anchored to the laboratory floor and supporting a cross beam against which a 30-ton capacity Simplex hydraulic ram operated by a Blackhawk pump reacted. Two concrete piers were used as the end supports of the beams. Details of the frame are shown in Fig. 17. The load was measured with a 50,000-lb elastic-ring dynamometer, which was placed between the ram and the distributing beam. The dynamometer was equipped with a dial indicator which was calibrated at 111 lb per division; it was sensitive to about one-tenth of a division.

Two loading blocks were used to apply the load to the beam. These blocks were 8 by 6 by 2-in. steel plates and a 4 by 4-in. piece of leather was inserted between each block and the beam, in order to have a uniform distribution of the load. The loading blocks received the load from the distributing beam, one through a roller and the other through a ball. This combination assured a central application of the load and allowed for changes of the distance between the loading blocks. The distributing beam was omitted when the load was applied only at midspan. Each reaction had a bearing block which was also an 8 by 6 by 2-in. steel plate. At one end of the beam, the bearing block was supported on a "half-round" and at the other end on a roller in order to provide for the elongation of the lower fiber of the beam during test.

11. Strain Gages

(a) Electric Strain Gages on the Longitudinal Wires

Two of the longitudinal prestressing wires in each beam were instrumented with Type A7 SR-4 electric strain gages which have a nominal gage length of 1/4 in., and a minimum trim width of 3/16 in. These gages were chosen for

their narrow width, short length, flexibility, and above all, because past experience with them had been satisfactory. The gages were mounted at the midpoint of each wire.

When rusting the wires, rusting was prevented on a small portion of each wire by insulating tape. Afterwards, the tape was removed and the surface smoothed with emery cloth and cleaned thoroughly with acetone. Duco cellulose acetate cement was used as the bonding agent, and after application, the gage was kept in position by applying pressure with the thumb for one or two minutes. Only enough pressure was applied to squeeze out the excess cement and hold the gage to the contour of the wire. After a short period of air drying, heat lamps were used to accelerate drying of the cement.

Each gage was connected to No. 18 Type FL solid wires by soldering. These lead wires were securely attached to the reinforcing wires to prevent pulling out of the gage filaments. The gage and its connections were covered with small pieces of insulating tape. All these operations were performed without turning off the heat lamps, and after they were concluded the gages were ready to be water-proofed. Petrolastic, an asphaltic compound produced by Standard Oil of California, was melted at a low temperature, and then applied to the gages in several layers. After it is applied, Petrolastic solidifies quickly, and gives a very good, flexible, waterproof coating.

The lead wires from the gages were carried at the level of the steel to one end of the beam and then brought up and out of the top flange.

(b) Electric Strain Gages on Concrete

Type A3 SR-4 electric strain gages were used to measure the concrete strains in all the specimens. They have a nominal gage length of 3/4 in. and a minimum trim width of 3/16 in. The gages were mounted on the top surfaces of all the beams, and also on the sides of the two beams with slabs cast on top. The

locations where the gages were to be applied were smoothed with a portable grinder and thoroughly cleaned with acetone. A thin layer of Duco cement was then applied and allowed to dry for fifteen or more minutes. The gages were mounted using additional Duco cement. This type of gage needed only a very slight pressure to squeeze out the excess cement and air bubbles. One-pound steel weights were left on the gages for about 15 minutes. These gages were mounted on concrete at an age of about eight days, and although concrete at this age has some moisture in it, no effort was made to waterproof the gages because they were mounted only about 24 hours before testing the specimens.

Figures 18a, 18b, and 19 show the different patterns used in placing the gages. The pattern was changed as the tests progressed either in order to obtain a better representation of the strain distribution in the shear spans after the formation of the inclined cracks, or to fit the different loading patterns.

(c) Mechanical Strain Gages

A 10-in. Whittemore strain gage was used to measure the distribution of concrete strain in the pure flexure region of the beams with cast-in-place slabs. Although these measurements were not strictly related to the shear strength of the beams, it was considered that they would be helpful in obtaining a better understanding of the behavior of those specimens, since only a few tests of this type have been reported so far. The Whittemore gage was equipped with a 0.0001-in. dial indicator, which was sensitive to about one-tenth of one division, and since a 10-in. gage length was used, the strains measured were estimated to one millionth. Measurements on all the gage lines were taken twice, and if both readings did not agree within 10 millionths, additional readings were taken until agreement was reached. A mild steel standard bar was used to compensate for the changes in temperature during the test.

The gage lines were placed symmetrically on both sides of the specimen, and their location is shown in Fig. 19. These gage lines were established by cementing steel plugs 3/8 in. in diameter and 1/4 in. thick to the sides of the specimen. Each plug had a cylindrical gage hole drilled to a depth of about 1/8 in.

12. Measurements

The load was measured with an elastic-ring dynamometer as described in Section 10.

Deflections were measured at midspan and at the third-points by means of 0.001-in. dial indicators.

Strains in the longitudinal reinforcement were measured by Type A7 SR-4 electric strain gages as described in Section 11(a). Type A3 SR-4 electric strain gages were used to measure the strains on the top surface of all beams and the sides of the beams with cast-in-place slabs as described in Section 11(b). In both cases a Baldwin Portable Strain Indicator was used to read the strains to the nearest 10 millionths, and dummy gages mounted on unstressed steel blocks were used for temperature compensation.

Strains in the region of pure flexure for the beams with cast-in-place slabs were measured with mechanical gages as described in Section 11(c). These beams also had 0.0001-in. dial indicators mounted at the ends of the span to measure any possible slip between the slabs and the beams. Since no measurable slip was observed no readings are reported.

After each increment of load, the cracks were marked and each one was identified by a number corresponding to the load increment. Photographs were taken during the test and after failure and were then kept as a permanent record of the development of the crack pattern.

The widths of inclined cracks at different stages of the test were measured for some beams, but these measurements are not reported, since they were not made for all beams and no use was found for them in explaining, or interpreting the results of the tests.

After each beam was tested, the following measurements were taken near the section of failure: depth of the longitudinal reinforcement, web thickness, and width of the upper flange. These dimensions are reported in Table 1.

13. Test Procedure

The load was applied in ten to fifteen increments to failure. Three or four readings of midspan deflection and applied load were made on the run during the application of each increment. After the application of each increment, all deflection and strain measurements were taken and the cracks were marked. The first few load increments were equal, but after the formation of the first crack they were based on deflection measurements and crack pattern.

The loads corresponding to the formation of the first flexural crack and the first inclined crack were observed as carefully as possible. Usually three load increments were applied before the first flexural crack occurred.

A certain amount of drop-off in load and increase in deflection occurred while readings were being recorded. Therefore, the load and midspan deflection were measured both immediately after the interruption and before the resumption of loading.

All beams were loaded to failure, each test taking from three to six hours.

IV. BEHAVIOR OF TEST BEAMS

14. Load-Deflection Relationships

The structural value of a member depends mainly on two factors: its strength, and its behavior under load. The load which is applied to a member under working conditions is usually a fraction of the total load required to produce failure. The value of this fraction is governed by the so-called factor of safety, and depends mainly on the behavior of the member under loading. The salient characteristics of behavior are ductility and mode of failure. Ductility, measured by the magnitude of the deformation produced by the loads, is a highly desirable quality because of its influence on such important properties as energy absorption and moment redistribution. It is therefore understandable that a knowledge of the relationship between load and deformation is fundamental to the study of any structural member.

The load-deflection curves for all the beams are shown in Figs. 20 through 28. The curves have been grouped according to the longitudinal reinforcement and shear span. Figures 20 and 21 show the curves corresponding to the beams with four wires, and Figs. 22 through 26 those for beams with eight wires. All these beams had 36-in. shear spans. The curves for beams with shear spans different from 36 in. are presented in Fig. 27, and the curves for beams with cast-in-place slabs in Fig. 28. All the curves, except those for beams with cast-in-place slabs, are plotted to the same scale so that direct comparisons can be made among them. Different symbols are used to differentiate the type of failure, and the points corresponding to the observed flexural and inclined cracking loads are indicated on each curve. In all curves the deflections measured at midspan were plotted versus the total live load, that is, the weight of the test beam was not included.

Two distinct stages can be defined on the basis of the behavior of the test beams. The first corresponds to the part of the load deflection curve up to flexural cracking, which is practically linear for all beams. This stage is referred to as the "elastic" range. The second corresponds to the part of the curve beyond the formation of the first flexural crack, and is characterized by an almost constant change in slope until the curve becomes practically horizontal in some cases.

In the first stage, the beam is completely uncracked and the deflections can be computed by using an elastic analysis. The following well-known formula was used to compute the midspan deflections for all beams corresponding to an observed load before first cracking occurred,

$$\Delta = \frac{P\,a}{48EI}\,(3L^2 - 4a^2) \qquad (2)$$

This load was selected instead of the observed cracking load because this load was definitely in the "elastic" range. To use Eq. 2 it is necessary to know the value of the modulus of elasticity of the concrete. Strictly speaking, the modulus of elasticity for concrete does not have a constant value and consequently, the proper stress-strain relationship should be used in each case. However due to the inherent variation in the properties of concrete, this refinement is not justified, and in accordance with common practice, an approximation was used. When the control cylinders were tested, stress-strain readings were taken from two cylinders of each batch, and these data were used to plot a stress-strain curve for the concrete. From these curves, a modulus of elasticity was arbitrarily obtained as the slope of a secant passing through the origin and the point on the curve corresponding to a stress of 1000 psi. The initial tangent was not used because of the inherent difficulties in determining such a line and because the secant was considered more representative of the magnitude under study. Since

more than one batch of concrete was used for each beam, the corresponding average value of the moduli of elasticity was used in each case. Figure 29 shows the relationship between the modulus of elasticity and the concrete compressive strength for all the beams. The curve in the figure represents a modified form of Jensen's expression for the modulus of elasticity, as follows:

$$E_c = \frac{30 \times 10^6}{6 + \frac{10{,}000}{f'_c}} \qquad (3)$$

which has been often used in the course of this investigation for similar concretes. The values of the modulus of elasticity, E_c, and the compressive strength, f'_c, are in pounds per square inch. The agreement between Eq. 3 and the experimental points in Fig. 29 is quite good.

The computed and observed deflections are compared in Table 4. The average observed deflection was five percent greater than the computed. This difference and the scatter obtained are quite acceptable for tests involving concrete.

An important development in the second stage was inclined tension cracking. This was accompanied by a slight drop in the load, similar when plotted to the drops in load which occurred between loading operations. Since these drops were not critical they were omitted in the curves presented. No other significant changes in the load-deflection curves occurred as a result of inclined tension cracking. Some beams with 1 3/4-in. web and the higher percentage of longitudinal reinforcement, and thus higher prestress force such as G26, G32, and G38, reached the inclined tension cracking before a flexural crack had been observed.

The ultimate deflection reached by each test beam appeared to depend mainly on the following variables: the percentage of longitudinal reinforcement, or more properly the value of Q, the type of loading, and the mode of failure.

The smaller the value of Q, the greater was the deflection. This is easily explained since the smaller the value of Q, the higher is the position of the neutral axis at failure, which results in a greater rotation for the same concrete strain at the top fiber, and consequently a greater deflection. Accordingly, the smallest deflections correspond to the beams with eight wires and the largest deflection to beam G38 which had the smallest value of Q. The type of loading influenced the ultimate deflections by changing the length of the region of constant moment, since this region becomes "plastic" at ultimate and most of the rotations take place there. Therefore, for a constant span, the closer the loads are to each other, the smaller is the deflection. Beam G31 which had only one load at midspan had the smallest deflection of all beams. In general, it can be stated that a beam must fail in flexure in order to develop its maximum deflection. Any premature failure would prevent this, and since shear failures can be considered in this category, the beams failing in shear had smaller deflections than similar beams failing in flexure. The reduction in ultimate deflection for beams failing in shear was greater for the smaller values of Q. This is illustrated in Fig. 28 for beams G34 and G38, which had very small values of Q (about 7), and were alike except for the amount of web reinforcement. Beam G38 failed in flexure at a deflection which was more than twice the deflection of beam G34, which failed in shear. The same difference, but to a smaller degree, can be noticed in the case of the beams with four wires, which had Q-values of about 20 (Figs. 20, 21). On the other hand, for the beams with eight wires and a corresponding Q-value of about 40, no significant differences in the load-deflection curves can be observed (Figs. 22-26). This behavior agrees with the hypothesis that states that shear failures take place at a load smaller than that corresponding to the flexural capacity, since for a beam failing in shear at slightly less than its flexural capacity the reduction in the ultimate deflection

will depend on the shape of its load-deflection curve. For low values of Q this curve is relatively flat and hence the corresponding reduction in deflection will be greater than for a beam with a higher value of Q.

Except for almost negligible differences in moment of inertia of the uncracked section the web thickness had no effect on the load-deflection curves other than governing the formation of the inclined tension cracks, and consequently affecting the amount of web reinforcement needed to avoid a shear failure.

Probably the most significant variable affecting the overall behavior was the web reinforcement. To study its influence, comparisons are made with beams similar to those tested, but without web reinforcement. Figures 30a and 30b show load-deflection curves and properties for beams B.12.35 and C.12.44 tested by Sozen (1), compared with similar curves for beams G4, G6, and G12. The curves in Fig. 30a show that after cracking beam B.12.35 deflected at a faster rate than beam G12 which had stirrups to restrain the opening of the inclined cracks. The ultimate deflections were comparable, but G12 failed in flexure at a greater load than beam B.12.35 which failed in shear. In the case of beam C.12.44 (Fig. 30b) which had no stirrups, failure occurred simultaneously with the formation of the inclined tension cracks. Beam G4 had enough web reinforcement to induce a flexural failure. It carried twice as much load as beam C.12.44 and failed at about four times the ultimate deflection. Another interesting comparison can be made using curves for beam C.12.44 and beam G6 which had only half as much web reinforcement as beam G4. Although beam G6 failed in shear, it shows how even a small amount of web reinforcement improves considerably the behavior of the beam.

15. Measured Concrete Strains

(a) Procedure

As described in Section 11(b), electric strain gages were used to measure the concrete strains on the top surface of all beams. The use of these

gages on concrete surfaces has proved successful in similar investigations in the past fifteen years. Mechanical strain gages were used to measure the strain distribution over the depth of the beams with cast-in-place slabs. These measurements agreed fairly accurately with those given by the electric strain gages. Similar agreement has been also reported by Warwaruk (2).

No attempt was made to measure the distribution of strains over the depth of the beams since this has been done by others in the past and, furthermore, it was not considered important to this investigation. On the other hand, the strain measurements at the tops of the beams were very useful in determining the crushing strain of the concrete, and the variation of the strain distribution with the development of the cracks. To accomplish this, 1-in. gages were used at a fairly close spacing.

The measured strains at each gage point were plotted versus the midspan deflection. Several of these curves were drawn in the same graph in order to compare them more easily, observe any possible trends, and detect any inconsistencies in the readings. Figure 31 shows several of these plots for the north half span of beam G15. Several points of interest can be observed. At a deflection of about 0.11 in., the first flexural crack was observed and a change in the slope of the curves took place. This was due to the upward displacement of the neutral axis because of cracking. Another change in slope for the gages near the loading points took place when the first inclined crack was formed at a deflection of 0.46 in. At the first "change" the slope decreased and at the second it increased, due to the concentration of strains in those locations. At a deflection of 1.6 in. crushing was observed at a point in the south half span, the strains for which are not shown in the figure. Consequently, part of the deflection from there on was due to the rotation in the crushing zone, and the slope of the curves for strain in the other half of the span began to decrease.

Finally, from a deflection of 1.9 in. up to failure the load was fairly constant, and so were the strains. The strains in the shear span were affected by the formation of the inclined cracks to the extent of changing the strains at gages A and B from tension to compression.

(b) Strain at First Crushing

Figure 32 shows the crushing strains plotted against the compressive strength of the control cylinders. When the concrete started to crush and collapse did not follow immediately the crushing strain was recorded directly. In other cases, it was determined by extrapolation, and for a few beams which failed in shear without any definite crushing of the flange, it was omitted. It must be said that these strains were not always the maximum attained by the concrete. They were the concrete strains at the location where crushing took place, measured at the moment when crushing was first observed. In some cases, greater strains were recorded at other locations, usually at the loading points. Apparently the confinement of the concrete under the loads prevented its crushing in spite of the greater strains.

The crushing strain ranged from 0.0035 to 0.0070, and the mean is about 0.0050. The crushing strain seems to be independent of the concrete strength and any other variable studied. This is in agreement with the usual reasonable assumption that concrete fails in flexure at constant limiting concrete strain. Previous investigators have assumed values for this strain from 0.003 to 0.004. Warwaruk (2) adopted a value of 0.004 after studying his results and those of Gaston, Billet, Feldman, and Allen. The scatters in the tests studied by Warwaruk and in the results reported here are of the same order, although the average values do not agree. To understand this difference, it should be remembered that the concrete strain readings are dependent on the technique used to measure them. Some of the values included by Warwaruk in his study were obtained by using 6-in.

strain gages, while all the values reported here were measured with 1-in. strain gages. In the first case an average strain over a 6-in. length was obtained, which can be different from a reading over a 1-in. length if the strain distribution is not uniform.

No difference between the crushing strains for flexural failures and those for shear failures can be seen in Fig. 32.

(c) Distribution of Concrete Strain on Top of Beam

The distribution of concrete strains on the top surface of the beam as measured by SR-4 gages was plotted for each beam at different stages of loading. As already pointed out in Section 15 (a) there is a definite relation between the strains at different points on the top surface and the stage of development of the crack pattern. This relation was very helpful during the tests, and afterwards, when the behavior or modes of failure of different specimens were compared.

Figures 33, 34, and 35 show typical distributions of concrete strains for three different beams and the related developments of the crack patterns. Three strain distributions and the corresponding crack patterns are shown for each beam. The one at the top of each figure corresponds to a load before inclined cracking, the one in the middle corresponds to a load after inclined cracking, and finally, the bottom one corresponds to the ultimate load. Some of the strains shown in this last distribution were obtained by extrapolation.

Beam G2 (Fig. 33) failed in flexure since it had about 2.8 times the minimum amount of web reinforcement needed to prevent a shear failure. Hereafter, this minimum amount of web reinforcement will be referred to as "balanced web reinforcement". A view of the failure of beam G2 is shown in Fig. 36. Beam G16 (Fig. 34) also failed in flexure, but the amount of web reinforcement was only about 12 percent greater than balanced. Therefore, there were many indications

that the failure was in the transition range between a shear and a flexural failure. Finally beam G21, having only 77 percent of the balanced web reinforcement failed in shear (Fig. 35). Views of the failures of beams G16 and G21 are shown in Figs. 37 and 38, respectively.

It can be seen in Figs. 33-35 that the strains were generally not proportional to the moments. This is due mainly to the distortion of the strain pattern produced by the cracks. Thus, in the shear spans, the strain distribution was in fairly good agreement with the moment diagram until the formation of cracks, especially inclined cracks. Afterwards, the strain distribution varied in accordance with the development of the inclined cracks. An inclined crack lowers the line of action of the compressive force in the shear span of the beam and consequently the strains in the top surface are reduced, even changing sign in some cases of shear failures. The greatest rotations occurred near the upper ends of the inclined cracks, under the loads and the maximum strains were recorded there. All these distortions were in direct proportion to the severity of the inclined cracks, as can be observed in the figures presented. Before inclined cracking, the distribution of strains in the flexural span was fairly uniform for all beams, although these strains were proportionally greater than the ones in the shear spans, owing to the presence of flexural cracks. After inclined cracking, the magnitude of the inclined cracks was sharply reflected in the strains. In the case of beam G2 (Fig. 33) because of its heavy web reinforcement, the inclined cracks did not open appreciably and the strain distribution remained unaltered. At loads approaching failure, the strains became greater and crushing occurred at a point between the loads, presumably where the concrete was weakest.

The behavior of beam G21 (Fig. 35) was different. Its stirrups were not able to prevent the opening of the inclined cracks, and the concentration

of strains at the loading points was therefore very marked. The strain distributions after inclined cracking show clearly the change in sign of the strains in the shear span.

Beam G16 (Fig. 34) was an intermediate case; it failed in flexure, but its stirrups permitted some opening of the inclined cracks with the related concentrations of strains. In this aspect it resembles a shear failure. On the other hand, the distribution of strains in the shear spans was not noticeably affected by the inclined cracks.

The three examples presented do not cover all the possible cases; some other "patterns" are possible. Some of the beams which failed by distress or crushing of the web did not develop high concentrations of strains under the loading points; they failed before they reached that stage. Nevertheless, these examples seem to be enough to emphasize the following points: (a) Some beams which otherwise would fail in shear can fail in flexure and behave "flexurally" if enough web reinforcement is provided. (b) The behavior of a beam which has some web reinforcement but still fails in shear is greatly improved by the presence of the web reinforcement.* (c) There is no clear-cut boundary between shear and flexural failures. Instead, there is a transition range, and the beams that fall in this range manifest "hermaphrodite" characteristics involving properties of both shear and flexural failure. In this transition zone the behavior changes gradually from one type of failure to the other. In fact, the definitions of shear and flexural failures become academic in this zone. This point will be discussed in greater detail later.

---

* For the behavior of beams without web reinforcement see a thesis by Sozen (1).

(d) Relation of Concrete and Steel Strains

One of the basic assumptions made in the theory of flexure for beams of homogenous and elastic materials is that the strains are linearly distributed over the depth of a cross-section. This assumption holds true for reinforced concrete beams if the bond between the steel and the concrete is perfect and the concrete remains uncracked. When the concrete cracks, the bond is usually broken, and this assumption is no longer true. However, for practical purposes it can be used, provided that the cracks are uniformly distributed and no inclined cracks are present. To study the influence of the crack pattern on the relationship between the steel strains and the concrete strains at the top surface of the beam, plots like those in Fig. 40 were prepared. This figure shows the relation between the steel strain measured at midspan and the concrete strains measured at the three points indicated in the figure. Below the flexural cracking load, the relation was linear and the concrete strain increased rapidly. After flexural cracking, but before inclined cracking, the concrete strain increased more slowly, due to the shifting of the position of the neutral axis. However, the strain distribtution could still be considered practically linear.

Three different beams were used to plot the curves on this figure. There are two curves for beam G3, one corresponding to a point at midspan and the other to a loading point. This beam failed in flexure, and the amount of web reinforcement in it was enough not only to prevent a shear failure but also to prevent any appreciable opening of the inclined cracks. Consequently, the two curves are almost identical and fairly straight for the full range beyond first flexural cracking.

Beam G6 failed in shear and had a very small amount of web reinforcement. It is seen that after the formation of the inclined cracks, the concrete strain increased at a faster rate than before, although there was no definite break in

the curve, probably because of the presence of stirrups. The increase in concrete strains indicates a non-linear distribution of strain. Beam G13 also failed in shear. However, the amount of web reinforcement in this beam was only slightly less than that required for a flexural failure. Thus, the inclined cracks affected the relation between the concrete and steel strains to a smaller extent than they did in G6. These trends agree in general with the results reported by Sozen who has described these phenomena in more detail for beams without web reinforcement (1).

16. Crack Patterns

In reinforced concrete members tensile steel reinforcement is provided because of the intrinsic weakness of concrete in tension.

This reinforcement prevents the total collapse of the member when the tensile stresses in the concrete exceed the tensile strength of this material. However, the reinforcement does not prevent the cracking of the concrete under those stresses. The study of these cracks is extremely helpful in determining the adequacy of the steel reinforcement used and the behavior of test specimens. For example, the location and width of cracks can indicate whether the reinforcement was placed in the proper position, or the state of bond between the steel and concrete. Because of these reasons, special care was taken to mark the position and development of the cracks in all the specimens as can be seen in the photographs.

Usually the first cracks formed at the section of maximum moment. These were called flexural cracks and they were practically vertical since the direction of the principal tensile stresses in this zone was parallel to the axis of the beam. The cracks appeared in the bottom fiber at a load which depended on the total prestressing force, the loading arrangement, the moment of inertia of the cross-section and the modulus of rupture. The observed values

of the cracking load agreed with the predicted ones. As the load increased the flexural cracks progressed upward. The rate of this progress depended mainly on the amount of longitudinal reinforcement. The smaller the longitudinal reinforcement ratio, p, the faster the crack progressed upward immediately after cracking; this rate decreased with subsequent applications of load increments. In fact, for the beams with the smaller value of p, the cracks developed suddenly from the bottom fiber to about mid-depth of the beam. On the other hand, the greater the value of p, the more uniform the progress of the cracks was with respect to the load. All the flexural cracks in a given beam were fairly uniformly spaced, opened at the same rate, and had approximately the same height in all stages of the test. This indicates that the bond between the steel and the concrete was satisfactory. Since in the region between the loading points the longitudinal reinforcement was placed perpendicularly to the cracks, the stability of the beam was not endangered at any moment by the progress of the cracks.

The formation and development of the cracks in the shear spans was by far more significant. Here the cracks were not vertical, since the principal tensile stresses were no longer horizontal owing to the presence of shear stresses. Three different types of cracks were observed in this region. Some cracks started from the bottom, like the flexural cracks, but instead of being vertical, their paths were inclined towards the loading points. These cracks were generally fairly close to the loading points; consequently their inclination was not great and, although they penetrated somewhat into the compression zone, the longitudinal reinforcement was in general enough to prevent any harmful effect. One of these cracks can be seen in Fig. 37. A more important type of crack is the one shown in Fig. 41, which formed suddenly in the web without starting from the bottom of the beam. These are the so-called inclined

cracks and they appeared when the principal tensile stresses at some region in the web exceeded the tensile strength of the concrete. It has already been established (1) that for beams without web reinforcement the formation of this crack marks the limit of usefulness of the beam. Practically, it means collapse or a stage very near to it. However, in the case of the beams tested, the stirrups prevented the collapse of the member and additional load could be applied. As the load increased, the critical stress condition was reached in different zones of the web, and additional inclined cracks were formed parallel to the first crack and nearer the support. This successive formation of inclined cracks, which continued until failure occurred, is shown in Fig. 42. It must be said that in some cases failure took place when only one of these cracks had been formed. In general, the inclined cracks were not confined to the web, but extended upward into the compression zone and downward to the bottom of the beam as more load was applied. It is interesting to notice the break in the slope of these cracks when they progressed from the web into the lower flange. This shows quite clearly how the direction of the principal tensile stresses is changed at that point because of the great difference between the values of the shear stresses in the flange and in the web. The inclined cracks will be discussed further in relation to the failure of the beams.

The third type of crack was observed in some beams with 1 3/4-in. webs and greater percentages of longitudinal reinforcement. It consisted of a series of small inclined cracks which appeared suddenly at the junction of the web and the upper flange and near the end-block, as shown in Fig. 43. This appears to be a stress phenomenon similar to the formation of the inclined cracks since high tensile stresses exist in this region. However, these cracks did not appear to have much influence on the failure of the beam since the presence of the stirrups seemed to stop effectively their propagation and opening.

17. Flexural Failures

The existence of beams whose properties place them in a transition range where the behavior of the beams is practically independent of the type of failure has already been pointed out in Section 15(c). Although most of those beams finally failed either in shear or in flexure, some of them exhibited an intermediate or transition type of failure. Consequently, an explanation of the criteria used to classify the failures is necessary. In general, a beam is said to have failed in flexure if the concrete in the compression zone crushes or the longitudinal reinforcement fractures due to bending stresses. If a beam fails by fracture of the longitudinal reinforcement there is no difficulty in applying the above definition, but if the beam fails by crushing of the concrete at a section near the shear span it may be difficult to distinguish whether the crushing is due to bending stresses alone or if it has been influenced by the presence of inclined tension cracks. In such cases, the failure was classified as flexural if the concrete started to crush in the region of pure bending before any inclined tension crack opened appreciably.

A beam is said to have failed in shear if its failure is due to the presence of an inclined tension crack resulting from a combination of shearing and bending stresses. These failures can take different forms, but it is always possible to recognize the influence of a well developed inclined tension crack. When a beam did not fall clearly within either one of these two groups, its failure was termed a "transition failure". Transition and shear failures will be discussed in Sections 18 and 19.

Twenty-three beams out of the thirty-eight tested failed in flexure. The behavior of these beams has already been explained in the preceding sections except for the description of the failure. If the beam failed in flexure, the inclined tension cracks did not open sufficiently to influence the failure. The

flexural cracks progressed upward at a decreasing rate until either the concrete in the top flange crushed in a region of maximum moment or the steel fractured.

Crushing started at the top and progressed downward, while the load dropped as a consequence of the reduction in the internal lever arm. However, as soon as the neutral axis moved back down into the web, the compression zone was drastically reduced and crushing over the remaining depth of the flange followed suddenly. This type of failure was typical of the beams with the smaller reinforcement ratio and is illustrated in Figs. 36 and 37. Although the failures in these two examples are basically similar, they appear different because the arrangement of the stirrups was not the same in both cases. Beam G2, in Fig. 36, had no stirrups between the loading points, so that, when the concrete crushed, the upper flange was partially separated from the web. On the other hand, beam G18, in Fig. 37, had stirrups for the full length of the span which kept the concrete in one piece, except at the location of crushing.

In the case of beams with the higher reinforcement ratio, the neutral axis was already in the web before crushing started. Therefore, as soon as the concrete started to crush, the compression zone was greatly reduced, and the crushing progressed downward violently. This failure was sudden, without warning, and quite different from the flexural failures of rectangular beams. This fact must be kept in mind when flexural and shear failures are compared. Figure 38 shows a photograph of one of these failures.

Photographs of beam G38 with a cast-in-place slab are shown in Figs. 44, 45 and 46 as an example of a very ductile flexural failure. The value of Q for this beam was seven, based on the flange width and it failed by fracture of six out of the eight wires in it, after initial crushing of the concrete. Figure 44 shows the well developed crack pattern after failure. Figure 45 shows in detail the position of the cracks on the underside and edges of the slab, and

Fig. 46 shows the crushing in the slab. In these last two figures the large opening of the crack in which the wires fractured can also be seen.

Beam G31 is used as an example to explain how the definition of flexural failure was applied to a "doubtful" case. This beam was tested with only one load applied at midspan and Fig. 47 shows the crack pattern after extensive crushing started under the loading point. The crushing is indicated by cross-hatching. After this stage in the test, the load started to drop and the crushing progressed downward. No appreciable distress could be observed in the web, and the inclined cracks remained as hair-line cracks. All these features fit the definition of a flexural failure, and at this moment, it was considered that the beam had already failed by crushing of the concrete at the zone of maximum bending moment. The fact that the crushing subsequently interacted with the inclined cracks, and resulted in a sudden collapse as shown in Fig. 48 was considered secondary in nature. This type of behavior appears to be typical for beams loaded at midspan, since they do not have a region of pure bending, and consequently, any flexural failure will be influenced by the closeness of more or less developed inclined cracks.

18. Shear Failures

The definition of shear failure given in Section 17 indicates the importance of inclined tension cracking in this type of failure. When an inclined tension crack is developed in a beam without any web reinforcement, "beam" action is completely disrupted, and the specimen becomes a more complex structure, which usually collapses before it reaches a load comparable to its flexural capacity. If the beam has web reinforcement, its presence across the inclined cracks partially restores beam action by providing a path for the stress flow between the upper flange and the longitudinal reinforcement. In some cases the stirrups can induce so much "beam-like" action that a flexural failure can take place, but in

other instances that is not so, and the beam fails in shear in a manner similar to that of a beam without stirrups.

When the stirrups were insufficient to prevent a shear failure, the inclined tension cracks opened appreciably, progressed into the compression zone, and signs of distress were observed in the web, usually at the intersections of the stirrups and the cracks. In these cases, the stirrups yielded where the cracks crossed them. Final collapse was a result of one of the following phenomena:

(a) Fracture of the Stirrups. In beams with very small amounts of web reinforcement the inclined cracks kept opening until some stirrups fractured. Usually, before fracture of the stirrups, signs of crushing under the loading point and/or tensile cracks in the shear span starting from the top flange and progressing downward could be observed. Upon fracture of the stirrups a great distortion took place in the web with the consequent collapse of the member. This type of failure is shown in Fig. 39.

(b) Crushing of the Web. As the inclined cracks opened, the character of the specimen was changing from that of a beam to that of an arch. Consequently the position of the thrust line was moving downward in the zone above the inclined cracks, inducing greater compressive stresses in the web and tensile stresses in the top flange. As a result, tensile cracks formed in the upper flange and eventually the web crushed as shown in Fig. 49.

(c) Crushing of the Top Flange Above an Inclined Crack. At this point it should be explained that, although many inclined tension cracks formed in most beams, usually one crack developed more than the others and finally triggered the failure. Sometimes this crack penetrated into the compression zone, reducing it appreciably, and creating a concentration of strain above the crack. As a

result, crushing took place in the reduced compression zone above the crack in a fashion similar to a flexural failure, but at a smaller load. As the concrete crushed, a relative sliding displacement of the concrete on each side of the crack was observed. This type of failure is usually referred to as shear-compression and is illustrated in Fig. 50.

A type of failure somewhat different from any of those just described was observed in beam G29, which had a shear span of 28 in., a web thickness of 1 3/4 in., and eight wires as longitudinal reinforcement. Consequently, the shear force in this beam was great. After inclined cracking, one of the inclined cracks developed faster than the others until it extended from the lower region of the end-block to a point beneath the loading block. As the load increased, tensile cracks formed in the upper flange near the end-block, and signs of crushing were observed and marked in the flexural span near the load. However, the beam continued to take more load and after another increment of load had been applied and while readings of the electrical strain gages were being taken, the beam failed so violently that seven stirrups were exposed and severely distorted (Fig. 51).

An unusual phenomenon was observed in this failure, the crushing of the concrete in the web below the upper end of the major inclined crack. Whether this was the initial cause of failure or not, is open to question. However, if that were the case, this phenomenon has deeper theoretical implications. It could mean that there is an upper limit to the amount of web reinforcement which can be used efficiently in a beam. This possibility will be discussed in detail in Section 24. On the other hand, it is possible that this crushing was a secondary effect, which took place after the concrete in the web crushed above the crack.

In most cases it is not possible to predict the final mode of shear failure of a beam. This mode may be influenced by factors such as the thickness of the web and the crack pattern. Failure by crushing of the web is more likely to occur in a beam with a thin web than in a beam with a thick web. However, the mode is largely determined by the development of the crack pattern and although this pattern is known to be influenced among other factors by the magnitudes of the shear span and the prestressing force, it is still in general unpredictable. Even companion beams can fail in different modes owing to different crack pattern developments. For certain combinations of the critical variables, a combination of various modes caused by all the above factors could be present in the same beam.

19. Transition Failures

Four of the thirty-eight test beams exhibited the type of failure which was designated as transition failure in Section 17. The failures of these beams are briefly described in the following paragraphs.

Figure 52 shows a view of beam G15 after failure. This beam had four wires and the concrete started crushing in the flexural span near a loading point. The crushing progressed downward simultaneously with widening of the inclined cracks, and some distress was observed in the web. The crushing of the concrete was evidently influenced by the inclined cracks as in a shear-compression failure. On the other hand, the web distortion in this beam was not as extensive as would be expected in a definite shear failure. Beam G21 had properties similar to those of G15, and failed definitely in shear as shown in Fig. 39. These two identical beams failed in different modes apparently because of slight differences in the locations of the major inclined tension cracks.

Another transition failure was that of beam G26, a view of which is shown in Fig. 53. In this case the crushing of the concrete in the shear span

took place rather violently, starting from the top and progressing downward until it reached the lower flange. It was very similar to crushing in a flexural failure, and apparently was not influenced noticeably by any inclined crack. The only unusual characteristic of this failure was that it took place outside the flexural span, that is, at a point where the bending moment was not a maximum. It is conceivable that an unusually weak spot in the concrete triggered the failure at such a location. This beam was tested in order to study the influence of the stirrup spacing on the efficiency of the stirrups. A fairly large spacing, 7.5 in., was used, but no conclusion was obtained because of the type of failure.

Beam G33 also was tested in order to investigate the influence of stirrup spacing. It had enough stirrups to prevent a shear failure, but they were spaced at 7.5 in. Figure 55 shows where crushing was observed on the west side of the beam. However, on the east side, the crushing was observed directly beneath the loading point, as shown in Fig. 56. This figure also illustrates the failure, showing the combination of crushing well into the pure flexure span together with distress of the web in the shear span.

The case of beam G35 is different from the preceding ones. This beam had long shear spans and only 12 in. in between the loading points. Even if such a beam fails in flexure, it is difficult to avoid any influence of the inclined cracks on the crushing of the concrete because of the geometry. Therefore it is difficult to classify its failure. Figure 54 shows that the crushing did not start at midspan but near one loading point. Whether this crushing was due to bending stresses alone, or was a shear-compression failure is difficult to determine. Finally the concrete crushed at midspan and one inclined crack opened appreciably.

In conclusion, it can be said that all of these beams behaved as if they were going to fail in flexure up to the instant when failure took place.

They exhibited all the properties of beams with flexural failures except for their appearance after failure. For structural purposes, these beams were as good as those which failed in flexure.

20. Comparison of Shear and Flexural Failures

The present philosophy regarding shear failures can be summarized as follows: Beam design is based on the flexural capacities of the cross-sections of the beam. Any premature shear failure which can prevent the beam from attaining its ultimate flexural capacity should be avoided. This line of thinking is in accordance with the results of tests of ordinary reinforced concrete beams failing in shear and flexure. In a flexural failure the concrete or the steel or both reach large strains before the beam fails. Thus, the beam can develop large deflections, moments can be redistributed in continuous beams, and in general failure does not mean total collapse of the structure. After the beam reaches its maximum moment, its carrying capacity does not decrease suddenly, but slowly. All these features are very desirable.

On the other hand, if an ordinary reinforced concrete beam fails in shear it does so at a more or less unpredictable load and usually before the beam develops considerable deflection. Furthermore, the failure is relatively sudden and brittle, and the collapse is complete. No redistribution is possible. All the flexural capacity of the beam beyond the shear failure is useless. This behavior is highly undesirable.

In prestressed concrete I-beams, however, the characteristics of shear and flexural failures are different from those indicated in the preceding paragraphs for ordinary reinforced concrete beams. The flexural failures observed in the tests were not as ductile as the failures of rectangular beams. In many cases the collapse was sudden and complete. As explained in Section 17, this was due to the position of the neutral axis in the web of the beam when it failed.

Also, while reinforced concrete beams are usually far removed from being over-reinforced, it is common to find over-reinforced prestressed concrete beams. Some of the test beams were slightly over-reinforced.

In the case of the beams which had web reinforcement and failed in shear, it was observed that they carried about the same load as comparable specimens which failed in flexure. This is true, for instance, in the case of bean G5, which had a value of $r f_y$ equal to 60 percent of that required for flexural failure. Also, the beams which failed in shear were ductile enough to reach deflections comparable to those for the beams which failed in flexure. This is not completely true for the beams with the smaller percentage of longitudinal steel, but it is remarkably so for the ones with the higher value of p.

To recapitulate, it can be said that all the beams which failed in flexure did not exhibit the desirable behavior at failure which is generally attributed to this type of failure. On the other hand, the beams which failed in shear had a greater ductility and carried a greater load than anticipated. Consequently, these results seem to indicate that it may not be absolutely necessary to avoid shear failures completely but only to provide an amount of web reinforcement sufficient to produce either a flexural failure or a "gentle" shear failure.

V. STRENGTH OF PRESTRESSED CONCRETE BEAMS WITH WEB REINFORCEMENT

21. Inclined Tension Cracking

A knowledge of the inclined tension cracking is of primary importance in order to study the strength of prestressed concrete beams either with or without web reinforcement. If a beam has no web reinforcement, the formation of an inclined tension crack produces either immediate collapse of the beam or such distortion of the stress distribution that only a small additional load is needed for collapse. If a beam has web reinforcement, the formation of an inclined tension crack has a different effect. It marks a change in the manner in which the shear force is resisted. Any additional shear applied after inclined cracking is "carried" by the web reinforcement. Therefore, the difference between the ultimate load and the cracking load for a given beam failing in shear depends on the amount of web reinforcement.

The inclined tension cracking phenomenon in prestressed beams without web reinforcement has been studied extensively by Sozen. He found that the main variables affecting inclined cracking were the geometry of the cross-section, the tensile strength of the concrete, the ratio of the shear span to the effective depth of the beam, and the average compressive stress produced by the prestress. He proposed the following empirical expression to predict the cracking moment:

$$\frac{M_c}{f_t\, bd^2\sqrt{b'/b}} = 1 + \frac{F_{se}}{A_c\, f_t} \qquad (4)$$

where: M_c = bending moment at inclined tension cracking

f_t = assumed tensile strength of concrete

b = width of top flange of beam without a slab

b' = web thickness

d = effective depth of the longitudinal reinforcement

F_{se} = effective prestressing force

A_c = gross area of cross-section

The tensile strength of concrete had to be determined in order to apply Eq. 4 to the test beams. Since no direct tests had been made, the tensile strength of concrete was assumed to be two-thirds of the modulus of rupture. The moduli of rupture for the concrete used in the tests discussed herein have been studied in Section 6 (c). In accordance with the data presented there, the following expression was used to evaluate the tensile strength:

$$f_t = \frac{1000}{2 + \frac{6000}{f'_c}} \qquad (5)$$

The values of the tensile strength, f_t, and the compressive strength, f'_c, are both in pounds per square inch.

The computed and observed values of the cracking moment are presented in Table 5. The observed values are compared graphically with Eq. 4 in Fig. 57. The observed cracking moments are consistently greater than predicted, the average increase being about 13 percent. Since Eq. 4 was derived empirically using test data of beams without any web reinforcement and all the beams reported here had vertical stirrups, it seems logical to assume that the discrepancy in the magnitude of the cracking moment is caused by the presence of web reinforcement. To substantiate this statement it can be said that in general the inclined cracks for the test beams started between two stirrups, and sometimes even several cracks formed simultaneously in the spaces between stirrups without crossing them. When loading was continued, the inclined cracks crossed the stirrups and sometimes several of them joined together. This seems to indicate that the presence of the stirrups retarded the formation of the inclined cracks. However, an attempt made to relate the difference between the observed and the computed cracking moments to the amount of web reinforcement was unsuccessful.

Apparently, the magnitude of the variables was of the same order as the experimental errors and no trend could be detected.

In spite of the differences between the observed and computed cracking moments, the observed values follow the trend indicated by Eq. 4. This fact indicates that Eq. 4 includes the variables which affect the inclined cracking phenomenon and therefore supports the validity of that equation. Perhaps a constant could be used to modify the equation in order to apply it to beams with web reinforcement. On the other hand, it is felt that if the increase in the inclined cracking load observed is due to the web reinforcement, Eq. 4 without any modification should be used to predict that part of the shear strength of a beam contributed by the tensile strength of the concrete. This criterion was adopted and used throughout the rest of this report.

It should be noted that in Fig. 57 there are only three points below the line representing Eq. 4. Two of these points seem to be within the natural scatter, but the third for beam G26 is undoubtedly too low. The failure of this beam was discussed in Section 19, where the possibility that the beam could have had weak concrete in the location where crushing occurred was pointed out. It is interesting to observe in Fig. 53 that the first inclined crack formed at the location where the concrete crushed, and that if the concrete was weaker there, this would also explain the low value of the inclined cracking load.

The values of the inclined cracking moment for the beams with cast-in-place slabs reported in Table 5 were computed by using Eq. 4 for the I-beams only, and neglecting the presence of the slabs. There is no rational justification for this procedure and therefore the results obtained are not reliable. In fact, the point corresponding to beam G34 is extremely high, the largest discrepancy in Fig. 57. However, it is included in this report for comparison purposes.

22. Effectiveness of Stirrups

The overall result of the presence of vertical stirrups in the test beams was an increase in the load carried by the beams beyond inclined tension cracking. Several studies of the test data were made in order to find out the significant properties of the web reinforcement. From these studies, it was concluded that, within the range covered in this investigation, the strength contributed by the web reinforcement is a function of the total cross-sectional area of the stirrups per unit of length and the yield point stress of the stirrups. Other variables studied, such as the diameter and number of legs of the stirrups, did not alter the effectiveness of the web reinforcement. The spacing of the stirrups was also studied and the results are discussed later in this Section.

Figure 58 shows, in terms of dimensionless quantities, the relationship between the web reinforcement index, $r\ f_y$, and the corresponding increment in total shear beyond inclined cracking. In order to make all the results compatible and to detect possible trends more easily, ratios of the variables rather than absolute values were used. The ratios between the quantity $r\ f_y$ corresponding to the stirrups actually present in each beam and the same quantity $r\ f_y$ for the computed balanced web reinforcement, as defined in Section 15 (c), corresponding to each beam were plotted as abscissas. Actually, the proper parameter should be $\frac{A_v}{s} f_y$, but $r\ f_y$ was used instead for simplicity and because the change did not affect the numerical values of the ratios. The ratios plotted as ordinates had in the numerator the difference between the observed shear at failure and the computed shear at inclined cracking, and in the denominator the difference between the shear corresponding to the computed flexural capacity and the computed shear at inclined cracking. By definition, any value of the ratio $(r\ f_y)/(r\ f_y)_b$ in Fig. 58 greater than 1.0 refers to a flexural failure and

should correspond to an ordinate equal to 1.0. Therefore, the locus of the predicted flexural failures is a horizontal line starting at the point (1.0,1.0) and extending to the right, as shown in the figure. Also shown is a straight line from the origin to the point (1.0, 1.0) which would represent the locus of the shear failures if the increase in shear beyond cracking were directly proportional to the quantity $(r\ f_y)/(r\ f_y)_b$. Different symbols were used on this figure to indicate the type of failure of each beam only in order to facilitate this discussion. However, a comparison between the actual and predicted modes of failure will be made in Section 27.

It can be observed in Fig. 58 that, while the points representing flexural failures agree fairly well with the horizontal portion of curve A, the points corresponding to shear failures do not agree with the inclined portion of the same curve. The "dashed" curve B was plotted in Fig. 58 to represent better the trend shown by the points corresponding to shear failures. Since the purpose of this investigation was not to study the effect of relatively small amounts of web reinforcement, not enough points were available to extend curve B down to the origin. Nevertheless, the data presented here indicated that the "efficiency" of the stirrups decreases as the amount of web reinforcement increases until the balance point is reached. The main practical consequences of this behavior are that (a) a relatively small amount of web reinforcement improves the strength of a beam proportionally more than the balanced amount of web reinforcement does and (b) if a beam has somewhat less web reinforcement than balanced its strength is not appreciably smaller than its flexural capacity.

In studying the scatter of the points in Fig. 58, it is important to notice that the magnitude of the ordinates depends on the difference of two comparable quantities the shear at failure and the shear at cracking. Consequently, the experimental error of the observed shear at failure is included in

this difference, and since this difference is relatively small, the error may be proportionally large. In spite of this possibility the scatter is not great and in general the points follow a definite trend.

Because of its practical importance, the spacing of the stirrups was studied in relation to the strength of the web reinforcement. It is generally accepted that the stirrups should be closely spaced for efficient utilization of their strength and, theoretically, there is no reason why the stirrups cannot be closely spaced. Therefore, the spacing requirement is not a basic problem. However, in practice the greatest possible spacing is usually preferred for economic reasons. In this investigation several spacings were used, and from a study of the results it can be concluded that spacings of 5 in. or smaller did not affect the efficiency of the web reinforcement noticeably. This spacing of 5 in. is approximately equal to the clear depth of the web. Although only a few beams with stirrups spacings from 5 to 10 in. were tested, their results seem to indicate that the strengths of these beams were detrimentally affected by these large spacings.

23. Analysis of Flexural Strength

The flexural strength of prestressed concrete beams has been studied by Billet and Appleton (3), who developed a semi-empirical procedure for computing the ultimate flexural moment. In accordance with this procedure the ultimate flexural moment, M_u, is given by the following expression:

$$M_u = A_s f_{su} d \, (1 - 0.42 \, k_u) \qquad (6)$$

where A_s = total area of longitudinal reinforcement

f_{su} = stress in longitudinal reinforcement at failure of beam

d = effective depth of the longitudinal reinforcement

k_u = ratio of neutral axis depth at failure to effective depth

In order to use Eq. 6, the values of f_{su} and k_u must first be computed. This can be accomplished by solving the following two equations together with the stress-strain relationship for the longitudinal steel:

$$\epsilon_{su} = \epsilon_u \frac{1 - k_u}{k_u} + \epsilon_{ce} + \epsilon_{se} \tag{7}$$

$$k_u = \frac{pf_{su}}{f_{cu}} \tag{8}$$

where ϵ_{su} = steel strain at failure of beam

ϵ_u = limiting strain at which concrete crushes in a beam

ϵ_{ce} = concrete strain at level of longitudinal reinforcement due to effective prestress

ϵ_{se} = steel strain corresponding to effective prestress

p = longitudinal reinforcement ratio

f_{cu} = average concrete stress in compression zone at failure

It should be noted that the notation for the parameter $k_1k_3f'_c$ used by Billet and Appleton is changed here to f_{cu}.

The value of the limiting strain, ϵ_u, has been assumed to be 0.004. Any reasonable value can be assumed for this parameter since the results are insensitive to fairly large variations in the assumed value for the limiting strain at practical ranges of the variables involved.

The average concrete stress in the compression zone at failure has been assumed to be that given by the following empirical expression derived by Billet and Appleton:

$$f_{cu} = \frac{f'_c}{2} \left[\frac{f'_c + 6000}{f'_c + 1500} \right] \tag{9}$$

where the units of the average concrete stress, f_{cu}, and the cylinder strength, f'_c, are pounds per square inch.

24. Analysis of Shear Strength

Before analyzing the shear failures quantitatively, a qualitative discussion of the mechanism of failure will be presented. This discussion applies to prestressed concrete I-beams with straight tendons and two symmetrically placed concentrated loads, although it need not necessarily be restricted to this case only. For convenience, the mechanism of shear failure for beams without web reinforcement is considered first.

As explained in Section 18, when an inclined tension crack forms in a concrete beam, beam action is destroyed in the shear span and the specimen becomes a very complex structure. The analysis of this "structure" is troublesome to say the least, and very complicated, thus some simplifying assumptions are usually made. A common assumption is to regard the portion of the beam above the inclined crack as an arch with the steel reinforcement acting as a tie rod. This structure is able to carry an appreciable amount of load, and in some cases even a load greater than the cracking load. In accordance with this assumption of arch action, the position of the compressive force, or thrust line, in the shear span is shown in Fig. 59 (a). To draw this line it was assumed that the steel stress in the region beneath the inclined crack, region A, was constant, and therefore the thrust line above the crack is straight. In order to satisfy statics this condition requires that the longitudinal steel does not transfer any shear across the inclined crack. At present the opinions of investigators are divided in relation to this question. While some think that an important amount of dowel action takes place across the crack, others consider that amount negligible. The writer believes that dowel action is critical in understanding the behavior of the beam and must be considered. This opinion is based mainly on two points.

First, if dowel action is neglected, it is easily seen that the portion A (Fig. 59 (a)) of the beam will carry no load. In fact, that portion could be removed leaving only the steel reinforcement. Under these circumstances the portion A does not "follow" the deformations of the upper part of the beam, or of the "arch", and there would be a "fault" in the longitudinal steel where it crosses the inclined crack, as illustrated in Fig. 59 (b). In the beams tested, such a "fault" was not observed, consequently some sort of dowel action transfering shear across the crack must have been present. This shear force subjects the portion A to the action of a force F, equal and opposite to another force F' acting upon the "arch", as shown in Fig. 59 (b).

The second point is based on observations of beams tested by Sozen (1). In some of those beams, the upper portions of the inclined crack was very flat and in some sections of the arch, such as that corresponding to the plane BB' in Fig. 59 (a), the eccentricity of the thrust line drawn without considering any dowel action was so great that the magnitude of the stresses in the arch would limit the load-carrying capacity of the structure to a value much smaller than observed in the tests. On the other hand, if dowel action is considered, the force F' (Fig. 59 (b)) will change the position of the thrust line upward, and consequently the eccentricity in the arch will decrease. Thus, by considering this load-carrying pattern it can be explained why the beams mentioned were able to carry fairly large loads.

The beneficial consequences of dowel action are apparent. It is reasonable to assume that the influence of dowel action upon the behavior of the beam is in direct proportion to the magnitude of the force F' (Fig. 59 (b)). The determination of this magnitude is extremely complicated since it depends on factors such as the stiffnesses of the arch, of the "portion A", and of the longitudinal reinforcement, which are very difficult to evaluate in advance of

the formation of the inclined crack. In addition to these, there is a detrimental consequence of dowel action, which usually makes the magnitude of the force F' even more uncertain: the formation of a horizontal crack observed in many beams between the web and the lower flange starting at the inclined crack, as shown in Fig. 59 (b). This crack is caused mainly by the vertical tensile stresses induced in that location by the dowel action, and its formation depends among other factors on the magnitude of those stresses, the tensile strength of the concrete, the thickness of the web, and the stiffness of the portion of concrete beneath the crack, in this case the lower flange. When this horizontal crack forms, the value of the force F' decreases as the length of this crack increases.

From this presentation, it is inferred that the magnitude of the dowel force can be negligible in some cases, and fairly unpredictable in general. Nevertheless, the dowel force contributes to the strength of the beam in two ways. One, by transferring some shear and therefore decreasing the magnitude of the thrust force in the arch, although this contribution seems to be of little importance in most cases. Two, by "improving" the location of the thrust line, and consequently reducing the stresses in the arch. This contribution is important since even a relatively small force can change the location of the thrust line significantly.

Collapse may take place either simultaneously with inclined tension cracking or after some additional load has been applied, depending among other factors, on the location and shape of the inclined cracks, the formation of a horizontal crack between the arch and the lower flange, and the magnitude of the dowel action. The final collapse of the beam can occur in different modes, all of which are related to the failure of the arch. Usually the arch fails either by excessive tension in the top fibers near the end-block, or by crushing in

the zones under compression, mainly near the loading point, or in the web of the beam. Sometimes combinations of these phenomena occur in one particular failure.

Once the mechanism of failure for beams without web reinforcement has been described, it is possible to discuss more easily the mechanism of failure for beams with web reinforcement. Fundamentally, each stirrup transfers some shear across the inclined crack, resulting in forces acting on the arch and displacing the thrust line in a manner similar to that of the dowel force of the longitudinal steel, as illustrated in Fig. 59 (c). However, the stirrups can transfer shear more efficiently than the longitudinal steel and are more reliable. Also the amount of shear transferred by the stirrups can be much greater than that transferred by dowel action, and consequently, the effects on the thrust-line location are much more important. If enough stirrups are provided, this line can be moved up to a location close enough to that corresponding to beam action in order to prevent a shear failure. Another consequence of the use of stirrups is to diminish the possibility of horizontal cracking between the web and the lower flange, because of a better distribution in the shear transfer; if cracks do form in that location, their influence is greatly reduced by the presence of the stirrups which limit the propagation of the cracks.

Actually the action of the stirrups has been simplified in the previous discussion. It is assumed that the stirrups are stressed in tension only, but they seem to be subjected to some dowel action also, because of the nature of the relative displacement between the arch and the region A shown in Fig. 59 (b). However, the overall result is to move the thrust line in the arch upward, and consequently restore beam action to some extent.

Beams with web reinforcement can develop shear failures similar to those already described for beams without stirrups, if the shear transferred by the stirrups is not enough to keep the thrust line in the proper location. In

this case, the stirrups usually yield and sometimes even fracture. Also, there is another possible cause of the final collapse of the beam: crushing of the concrete beneath the upper part of the inclined crack, or zone C in Fig. 59 (c). In this zone there are compressive stresses induced by the action of the stirrups in zone A, and it is conceivable that these stresses could be large enough to produce crushing in some cases. Whether the conditions for such a failure can be present in practice is not known, and should be investigated because of the implications of this type of failure. The crushing of the concrete in such a location cannot be avoided by merely increasing the strength of the stirrups, but the stiffness of the stirrups also must be increased. Practically, this type of failure means that there could be an upper limit to the amount of vertical stirrups which can be used efficiently, as has been observed for ordinary reinforced concrete beams (4).

From this analysis of the mechanism of shear failures the complexity of a purely rational theory to predict the shear strength of the beams is evident. Such an attempt was beyond the scope of this investigation and consequently a purely empirical approach was used in order to derive an expression for the shear strength of the beams tested. It was decided that this expression should include only the most significant variables since the number of tests made was not enough for a careful study of all the variables involved. Also, because of the natural inaccuracies of any empirical expression, it is reasonable to omit any variable whose influence on the phenomenon being studied is slight.

The difference between the ultimate shear and the shear corresponding to inclined tension cracking was found to be by far the most significant variable governing the amount of web reinforcement necessary to prevent a shear failure, and the following empirical expression relating these two variables was found:

$$V_u - V_c = \frac{5}{4} A_v \frac{d}{s} f_y \tag{10}$$

where: V_u = ultimate shear corresponding to flexural failure

V_c = shear corresponding to inclined tension cracking load

A_v = cross-sectional area of one stirrup

d = effective depth of the beam

s = spacing of the stirrups

f_y = yield point stress of the stirrup steel

Equation 13 can also be written as follows:

$$r f_y = \frac{4}{5} \frac{V_u - V_c}{b'd} \tag{11}$$

where: $r = A_v/b's$ = web reinforcement ratio, based on web thickness

b' = web thickness

The value of the empirical coefficient, which is 4/5 in Eq. 11 depends on how the values of V_u and V_c are determined. In these studies Eqs. 10 and 11 were obtained using measured values of V_u and computed value of V_c based on Eq. 4.

Equation 11 is represented graphically in Fig. 60 and compared with the observed data. It must be pointed out that Eq. 11 represents the locus of the points corresponding to balanced failures. Points corresponding to shear failures can lie to the left of that line although not far away from it, if the amount of web reinforcement is smaller than balanced, and points corresponding to flexural failures must be to the right of the plotted line. It can be seen that the agreement between the plotted line and the test data is excellent.

VI. COMPARISON OF MEASURED AND COMPUTED QUANTITIES

25. Comparison of Measured and Computed Ultimate Strengths of Beams Failing in Flexure

The ultimate flexural moment was computed for all beams by the following equations which were presented in Section 23:

$$M_u = A_s f_{su} d (1 - 0.42 k_u) \tag{6}$$

$$\epsilon_{su} = \epsilon_u \frac{1 - k_u}{k_u} + \epsilon_{ce} + \epsilon_{se} \tag{7}$$

$$k_u = \frac{p f_{su}}{f_{cu}} \tag{8}$$

Equation 7 and 8 can be solved for f_{su}, ϵ_{su}, and k_u by a simple trial and error procedure provided that the properties of the beams and the stress-strain relationship for the longitudinal steel are known. In this study, the method used involved the following steps: (1) a reasonable value for f_{su} was selected; (2) this value was substituted in Eq. 8 to determine k_u; (3) ϵ_{su} was evaluated from Eq. 7; (4) f_{su} and ϵ_{su} were checked for compatibility with the measured stress-strain relationship. If f_{su} and ϵ_{su} were not compatible, the operation was repeated for different values of f_{su} until a reasonable agreement was reached. In each trial, the selection of the value of f_{su} was guided by the results of the previous trials.

After the values of f_{su} and k_u are known, it is possible to compute the moment from Eq. 6. The moments thus obtained for all the beams are tabulated in column 4 of Table 6. This moment computation procedure was originally derived for beams with rectangular compression zones at failure, but can also be applied without correction to I-beams if the neutral axis lies in the upper flange. Consequently, the position of the neutral axis, as given by Eq. 8, was

determined for all the beams and the computed moments were corrected if the neutral axis was found to be in the web. The correction was made by multiplying each moment by the ratio of the actual area of the compression zone to the rectangular area assumed in the computations, and the corrected moments are marked with asterisks in Table 6. This rather crude procedure was used since all the corrections were less than 10 percent and therefore a more refined method was not justified.

The moments measured in the tests and the observed modes of failure are also listed in Table 6, columns 6 and 9, respectively, and the ratios of the quantities in column 6 to the quantities in column 4 are tabulated in column 7. From an examination of the ratios in column 7 it can be concluded that for the beams failing in flexure, the capacities computed on the basis of the flexural analysis agree with the test results within reasonable limits; the mean is 0.98 and the mean deviation 0.021. It is evident that for the range of variables employed, the method of computation was satisfactory in determining the flexural strengths of the beams studied.

Columns 2 and 3 in Table 6 show the computed and measured stresses in the longitudinal steel at failure. It can be seen that the computed stress is consistently greater than the measured stress. Actually, the measured stresses were not the true stresses at failure since the readings of the electric strain gages on which those stresses are based were taken at a load slightly less than the failure load. Moreover, if the concrete carries any tension at all at the location of the gages, the measured stresses should have a value smaller than the computed.

26. Comparison of Measured and Computed Ultimate Strengths of Beams Failing in Shear

The procedure presented in Section 24 was derived exclusively for the determination of the amount of web reinforcement necessary to produce a balanced

design. However, Eq. 10 can be written as follows for the determination of the strength of beams failing in shear:

$$M_u = M_c + \frac{5}{4} A_v \frac{d}{s} f_y a \qquad (12)$$

where all the symbols except a have been defined in the preceding sections. Symbol a designates the length of the shear span.

In accordance with the discussion of the effectiveness of the stirrups presented in Section 22, Eq. 12 gives conservative values for M_u when the value of A_v is smaller than that required for balanced design. If A_v is greater than the value required for balanced design, the value of M_u given by Eq. 12 does not have any direct meaning, since the beam would fail in flexure at a smaller moment. However, if under those circumstances the shear span a is shortened, the value of M_u decreases and a value of a for which M_u is equal to the flexural strength can be found. This value of a can be regarded as the minimum shear span for that particular beam for which a flexural failure can still be obtained. However, it should be noted that under this new loading arrangement the beam carries a greater load than for a longer shear span.

The resisting moment based on the shear capacity was computed for all the beams using Eq. 12, the properties of the beams, and the values of M_c given by Eq. 4. The results are tabulated in column 5 of Table 6, and a comparison of these computed values with those measured in the tests for all the beams which had either shear or transition failures is made in column 8. The mean of the ratios in column 8 for all beams failing in shear except G20 is 1.04, and the mean deviation is 0.043. These results indicate that the predicted moments, as expected, were slightly smaller than the measured moments, and consequently Eq. 12 can be safely used to predict the shear strength of a beam. Beam G20 was

not included in the average because, although it failed in shear, according to the analysis it should have failed in flexure.

27. Prediction of Mode of Failure

The mode of failure of a beam can be predicted by comparing the computed values of the flexural and shear strengths, since the beam should fail in the mode indicated by the smaller of those values. Accordingly, the values in columns 4 and 5 of Table 6 were compared and the predicted modes of failure are listed in column 10. The observed modes of failure are indicated in column 9. The predicted modes of failure were strictly correct for all except eight beams, but, in a broader sense, only one prediction may be considered incorrect because of the following considerations:

(a) Four of the "incorrect" predictions correspond to transition failures. This type of failure is not predictable by the method used and it is not really necessary to predict it since in the transition range the behavior and capacity of a beam is practically independent of the mode of failure. The average computed flexural strength of the four beams with transition failures was 0.99 of their average computed shear capacities.

(b) Three of the other four beams with incorrectly predicted failures exhibited very small differences between the computed flexural and shear capacities. These differences were less than two percent of the beam strength, and in this range it is not possible to predict the mode of failure with certainty, because of the inherent properties of concrete beams.

The predicted mode of failure for beam G20 was flexure. It failed in shear but at a load corresponding to its predicted flexural capacity.

Another way of comparing the predicted and observed modes of failure is illustrated in Fig. 61. Equation 11 is represented in this figure by a straight line which defines two zones, one corresponding to shear failures and

the other to flexural failures. If for a given beam, the quantity $(V_u-V_c)/b'd$, based on computed values of V_u and V_c, is plotted versus the quantity $r f_y$, the position of the point in relation to the plotted line would indicate the predicted mode of failure. These points were plotted in Fig. 61 for the beams tested using different symbols in order to distinguish the observed types of failure. The relation between the predicted and observed modes of failure can then be readily examined in Fig. 61.

28. Discussion of the Strength of Prestressed Concrete Beams

In this investigation the strength of prestressed concrete beams has been studied, mainly in relation to the mode of failure and the use of web reinforcement. The results obtained are summarized and discussed briefly in the following paragraphs.

The strength of a prestressed concrete beam depends on the relative magnitudes of three main factors: the flexural capacity, the inclined cracking moment, and the amount of web reinforcement.

If the flexural capacity is smaller than the inclined cracking moment the beam will fail in flexure and its strength will be equal to its flexural capacity. This case is usually associated with beams which have small longitudinal reinforcement ratios and either rectangular cross-sections or fairly thick webs. The amount of web reinforcement has no influence on the failure and could therefore be omitted.

If the flexural capacity is greater than the inclined cracking moment, the beam will fail either in flexure or in shear depending on the amount of web reinforcement. Within the range of the variables used in this investigation it is possible to find the minimum amount of web reinforcement which a beam can have and still fail in flexure. If a beam has less web reinforcement than this minimum amount, it will fail in shear, and its strength will vary from a value

equal to or slightly greater than the inclined cracking moment to the flexural capacity, depending on the amount of web reinforcement. Because of the nature of prestressed concrete beams and because of the assumptions made in the derivations of the strength formulas, it is not possible to establish precise boundaries between the preceding cases. In practice, these precise boundaries are not necessary, since the strength of a beam does not change abruptly if the failure mode of the beam is changed from one case to another by varying slightly its properties. Instead there will be a continuous gradual change in strength.

Expressions to compute the strength of the beams for the different cases are presented in this report. They are in general semi-empirical expressions and therefore their ranges of application depend on the ranges of variables considered in their derivation. This range is quite wide in the case of the expression for flexural strength. However, the expression given for the shear strength of beams with web reinforcement was derived only from the test results reported herein, and consequently its reliable application is limited at present to beams similar to those tested.

Besides the factors already discussed, there are other factors which can influence the strength of a beam. Usually they are not considered legitimate factors but are associated with poor design. Thus, a very large spacing of the stirrups can cause a premature shear failure, or a poor arrangement of the longitudinal steel can initiate a bond failure. End-block failures in prestressed concrete beams also can be considered in this category. In this investigation, the behavior of the end-blocks was observed and, although no conclusive results were obtained, it can be said that the end-blocks used were quite satisfactory, and it is reasonable to expect that similar end-blocks should be satisfactory in other cases.

VII. FUTURE TESTS

The results reported herein were obtained from tests on prestressed concrete beams with web reinforcement made as a part of a more general investigation of prestressed reinforced concrete for highway bridges. This program of tests will be continued in order to obtain more general results and consequently it is appropriate, after studying these first tests, to make recommendations for future tests.

Since the actual layout of the test programs should be decided at the time of initiation of each particular program and since it is desirable to be able to change the range of the variables during the tests in accordance with developments, only general areas of investigation are suggested here.

(a) Balanced Web Reinforcement

An expression for the balanced web reinforcement was derived from the results of the beams tested so far. This expression indicates that the additional shear that a beam can carry beyond inclined cracking depends only on the parameter $r\ f_y$. The validity of this expression for prestress levels other than 120,000 psi should be investigated.

(b) Beams with Cast-in-Place Slabs

The advantages of this type of construction are obvious, and although only two specimens of this type were tested in this investigation, they showed a highly desirable behavior. Apparently, the slab gives extra toughness to the specimens and even the one which failed in shear exhibited a rather gentle failure. A procedure to predict the inclined cracking load for these beams is needed and an adaptation of Sozen's method to this case should be investigated.

(c) Web Reinforcement

Since the effectiveness of the web reinforcement depends on the parameter $r\ f_y$ it seems convenient to investigate the validity of this finding for

stirrups with yield points higher than that used in this investigation. The possibility of using stirrups made of high strength steel should be explored in order to see how the stiffness of the stirrups affects quantitatively their effectiveness.

In Section 24 the possibility of the existence of an upper limit to the efficient use of vertical stirrups was mentioned, this phenomenon may need further investigation.

Tests conducted by J. MacGregor (5) suggest the necessity of further investigations in relation to the use of web reinforcement in beams with draped longitudinal steel.

Since all of the beams tested had uniform spacing of stirrups throughout the shear span, the variation of the spacing of the stirrups along the span of the beam in accordance with the type of loading deserves further attention.

(d) End-Blocks

The present practice tends to the elimination of end-blocks in order to simplify the construction procedures, especially in precasting. Consequently, some beams should be tested without end-blocks, and if this practice is satisfactory, the end-blocks could be eliminated in all future tests.

(e) Type of Loading

Only beams with symmetrically placed concentrated loads have been tested so far. Although from these tests it is possible to infer the behavior of similar beams under some other loading arrangement, this is not possible for all other types of loading. Consequently, tests of beams under moving loads simulating traffic conditions and possibly under distributed loads are recommended.

(f) Continuous Beams

Tests of continuous beams should be made in order to relate and facilitate the application of the data accumulated for simply supported beams to the case of continuous beams.

VIII. SUMMARY

29. Outline of Investigation

The purpose of this investigation was to study the behavior of prestressed concrete I-beams with web reinforcement, with special attention to the influence of the web reinforcement on the mode of failure. In total, 38 beams with overall cross-sectional dimensions of 6 by 12 in. were tested. All the beams had webs either 1-3/4 in. or 3 in. thick. Two beams had cast-in-place slabs 2 in. thick and 24 in. wide. The concrete strength varied from 2310 to 5520 psi, being about 3000 psi for most of the specimens. Two longitudinal reinforcement ratios were used, either 0.00192 or 0.00400, and the nominal prestress was kept at 120,000 psi for all the beams. Vertical stirrups were used in all beams, with the ratio, based on web thickness and effective depth, varying from 0.00098 to 0.0135. The stirrup spacing varied from 2.5 to 10 in. All beams had symmetrically placed concentrated loads, the shear spans ranging from 28 to 54 in.

Load increments were applied to each beam until failure was reached. The load, deflections at three points, concrete strains at the top, steel strains, and crack pattern were recorded for each increment of load. Each test took about four hours.

Web reinforcement proved to be a suitable means of improving the behavior of the beams failing in shear, and of preventing shear failures if used in proper amounts. From studies of the data, a hypothesis for the mechanism of failure was developed.

30. Behavior of Test Beams

Of the 38 beams tested, 11 failed in shear, 23 in flexure, and 4 in a "transition" failure. Before cracking, all beams behaved "elastically" and

similarly. After the first flexural cracks, the stiffness was appreciably reduced but the beams still behaved rather elastically until the formation of inclined cracks or the development of long flexural cracks. Before the formation of inclined cracks, it was considered that the stresses in the stirrups were negligible. After inclined cracking the stirrups prevented the opening of the cracks and immediate failure. As the load was increased, the stirrups either yielded or fractured and a shear failure took place, or they were capable of preventing this and the beam failed in flexure.

The beams which had enough stirrups to develop the flexural capacity failed in flexure by crushing of the concrete or fracture of the longitudinal reinforcement. Some of these failures, especially those for the beams with the greater longitudinal reinforcement ratio, were fairly violent.

Beams failed in shear in several different ways: (1) by crushing of the compression zone above the end of one of the inclined cracks, similar to a flexural failure; (2) by crushing of the web, due to the thrust induced by arch action; or (3) by general distortion of the web, usually accompanied by tension cracks in the top flange and fracture of the stirrups.

In general, shear failures were violent, although in most cases the beam reached a deflection and carried a load comparable to those of the beams which failed in flexure.

31. Test Results

An empirical expression, Eq. 11, for the amount of stirrups required to prevent shear failures was derived from the test data. For the range of variables used, this amount was found to be proportional to the difference between the shear at inclined cracking and the ultimate shear. With this expression it was possible to predict the mode of failure of all the beams except one. It was also found that Eq. 11 can be rewritten in the form given

by Eq. 12 and used to predict conservatively the strength of the beams which failed in shear. The average ratio of the measured to computed strengths of the beams which failed in shear was 1.04, and the mean deviation 0.043.

In summary, it was found that, at least for the cases covered in this investigation, it was possible to prevent shear failures by using adequate amounts of vertical stirrups, and that even a small amount of web reinforcement improved considerably the behavior and load carrying capacity of a beam. If a beam fails in shear, but the amount of web reinforcement is not much less than that required for a flexural failure, the behavior and strength of the beam are practically equal to those of a similar beam failing in flexure. Therefore, a beam should have enough web reinforcement either to fail in flexure or to have a "desirable" shear failure in order to utilize its optimum strength.

IX. BIBLIOGRAPHY

1. Sozen, M. A., "Strength in Shear of Prestressed Concrete Beams Without Web Reinforcement," Ph. D. Thesis, University of Illinois, August 1957. Issued as a part of the Sixth Progress Report of the Investigation of Prestressed Concrete for Highway Bridges, Civil Engineering Studies, Structural Research Series No. 139, August 1957.

2. Warwaruk, J., "Strength in Flexure of Bonded and Unbonded Prestressed Concrete Beams," M. S. Thesis, University of Illinois, August 1957. Issued as a part of the Sixth Progress Report of the Investigation of Prestressed Concrete for Highway Bridges, Civil Engineering Studies, Structural Research Series No. 138, August 1957.

3. Billet, D. F. and Appleton, J. H., "Flexural Strength of Prestressed Concrete Beams," Journal of the American Concrete Institute, V. 25, No. 10, June 1954.

4. Hognestad, E. and Elstner, R. C., "An Investigation of Reinforced Concrete Beams Failing in Shear," Department of Theoretical and Applied Mechanics, University of Illinois, October 1951.

5. MacGregor, J. G., "Effect of Drapped Reinforcement on Behavior of Prestressed Concrete Beams," M. S. Thesis, University of Illinois, May 1958.

TABLE 1

PROPERTIES OF SPECIMENS

Mark	Concrete Strength f'_c psi	Type of Reinf.	Flange Width b in.	Web Thickness b' in.	Effect. Depth d in.	Steel Area A_s in.^{2}	Longit. Reinf. p %	Effective Prestress f_{se} ksi	Web Reinf. r' %	Stirrup Spacing s in.	Yield Pt. Stirrups** f_y ksi	Type of Stirrup (***)	Shear Span a in.
G1	3100	X	6.00	1.70	10.50	0.121	0.192	125.5	0.382	2.5*	33.6	D	36
G2	3280	X	6.00	1.70	10.50	0.121	0.192	125.5	0.277	2.5*	35.5	D	36
G3	2640	X	6.00	1.65	10.13	0.242	0.397	119.2	0.277	2.5*	35.5	D	36
G4	2840	X	5.95	1.70	10.10	0.242	0.402	116.5	0.192	2.5	42.5	D	36
G5	3240	X	5.95	1.70	10.11	0.242	0.401	120.8	0.140	2.5	35.5	C	36
G6	3010	X	6.00	1.75	10.12	0.242	0.397	119.2	0.095	2.5	42.5	C	36
G7	4660	X	5.95	1.71	10.14	0.242	0.400	121.6	0.193	2.5	33.6	C	36
G8	2310	X	6.00	1.70	10.50	0.121	0.192	126.1	0.139	2.5	35.5	C	36
G9	3080	X	6.00	1.78	10.48	0.121	0.192	125.9	0.095	2.5	42.5	C	36
G10	2535	X	6.00	1.70	10.14	0.242	0.396	118.8	0.191	5.0	33.6	D	36
G11	3020	X	6.00	1.70	10.49	0.121	0.192	127.1	0.095	5.0	42.5	D	36
G12	3050	X	5.95	2.90	10.11	0.242	0.401	120.6	0.193	2.5	33.6	C	36
G13	3140	X	6.00	1.76	10.49	0.121	0.192	125.9	0.048	5.0	42.5	C	36
G14	3110	X	6.00	2.95	10.11	0.242	0.398	120.0	0.095	2.5	42.5	C	36
G15	2990	X	6.00	1.70	10.52	0.121	0.191	125.7	0.069	5.0	35.5	C	36
G16	2810	X	5.98	2.96	10.14	0.242	0.398	121.0	0.139	2.5	35.5	C	36
G17	2780	X	6.00	2.95	10.12	0.242	0.397	120.3	0.196	5.0	39.3	D	36
G18	2870	X	6.00	2.95	10.47	0.121	0.192	126.8	0.048	5.0	42.5	C	36
G19	2860	X	6.00	2.95	10.15	0.242	0.397	121.8	0.139	5.0	35.5	D	36
G20	2400	X	6.00	1.75	10.15	0.242	0.397	121.5	0.261	5.0	30.7	D	36

* Stirrups in the shear spans only
** See Figs. 9 and 10 for other properties of the steel used for stirrups
*** See Fig. 2 for description of types of stirrups

TABLE 1 (Continued)

Mark	Concrete Strength f'_c psi	Type of Reinf.	Flange Width b in.	Web Thickness b' in.	Effect. Depth d in.	Steel Area A_s in.^{2}	Longit. Reinf. p %	Effective Prestress f_{se} ksi	Web Reinf. r' %	Stirrup Spacing s in.	Yield Pt. Stirrups** f_y ksi	Type of Stirrup (***)	Shear Span a in.
G21	2690	X	6.00	1.75	10.48	0.121	0.192	125.8	0.069	5.0	35.5	C	36
G22	3300	X	6.00	1.80	10.11	0.242	0.399	112.5	0.261	3.75	39.3	D	36
G23	2680	X	6.05	1.75	10.47	0.121	0.191	125.5	0.108	9.0	39.3	D	36
G24	3010	XI	6.00	1.75	10.14	0.242	0.397	120.2	0.347	5.0	41.5	D	36
G25	3230	XI	6.00	1.75	10.47	0.121	0.193	127.3	0.077	9.0	35.5	D	36
G26	3420	XI	6.05	1.75	10.06	0.242	0.398	118.5	0.230	7.5	41.5	D	36
G27	5050	XI	6.00	1.80	10.15	0.242	0.397	121.2	0.277	2.5	35.5	D	36
G28	3870	XI	6.00	3.00	10.02	0.242	0.402	116.8	0.147	10.0	39.3	E	36
G29	4330	XI	6.00	1.75	10.03	0.242	0.402	118.5	0.277	2.5	35.5	D	28
G30	5430	XI	6.00	3.00	10.10	0.242	0.399	119.7	0.139	5.0	35.5	D	36
G31	3160	XI	6.00	3.00	10.05	0.242	0.401	122.0	0.097	5.0	36.6	D	54
G32	3200	XI	6.00	1.80	10.03	0.242	0.402	119.0	0.327	3.0	39.3	D	28
G33	2680	XI	6.00	3.00	10.03	0.242	0.402	120.4	0.131	7.5	39.3	D	36
G34	3910	XI	24.0	1.75	12.30	0.242	0.082	117.8	0.277	2.5	35.5	B	36
G35	3550	XI	6.00	3.00	10.15	0.242	0.397	122.4	0.097	5.0	36.6	D	48
G36	4040	XI	6.00	1.75	9.25	0.242	0.437	~70.0	0.327	3.0	39.3	B	36
G37	3210	XI	6.00	3.00	10.12	0.242	0.398	122.5	0.139	5.0	35.5	D	48
G38	3520	XI	24.0	1.85	12.30	0.242	0.082	123.0	0.327	3.0	39.3	B	36

TABLE 2

SIEVE ANALYSIS OF AGGREGATES

Percentages Retained

	Aggregate Lot	I	II	III	IV	V	VI
	Sieve						
Gravel	1/2	-	-	3.1	0.7	0.7	2.0
	3/8	1.2	3.2	24.5	12.5	12.5	23.2
	No. 4	96.2	93.2	97.8	97.2	97.2	93.4
	No. 8	97.9	99.4	98.6	98.5	98.5	97.4
	No. 16	98.2	99.6	-	98.7	98.7	98.0
Sand	No. 4	1.5	2.8	2.7	0.3	0.2	0.2
	No. 8	14.9	19.1	19.7	13.7	13.2	13.2
	No. 16	42.5	37.8	41.5	38.4	36.2	36.2
	No. 30	70.4	66.2	70.5	70.2	64.4	64.4
	No. 50	93.2	94.5	94.9	92.5	90.4	90.4
	No. 100	98.2	98.8	98.6	98.2	98.3	98.3
	Fineness Modulus	3.21	3.20	3.28	3.13	3.03	3.03

TABLE 3

PROPERTIES OF CONCRETE MIXES

Mark	Cement:Sand:Gravel by weight	Water/Cement by weight		Slump in.		Compressive Strength f'_c psi		Modulus of Rupture f_r psi		Age at Test days	Aggregate Lot
Batch	I and II	I	II	I	II	I	II	I	II		
G1	1:4.2:4.4	.94	.94	6	3.5	2950	3100	408	442	7	I
G2	1:4.2:4.4	1.02	1.02	4	5	2750	3280	342	433	9	I
G3	1:4.3:4.5	.95	.95	5	3	3160	2640	333	366	9	I
G4	1:4.2:4.5	.89	.89	3	8	3180	2840	375	342	8	I
G5	1:4.2:4.5	.93	.91	6	1.5	4460	3240	408	425	6	II
G6	1:4.2:4.5	.93	.91	1	3	3360	3010	408	425	8	II
G7	1:2.6:3.1	.70	.67	7	7	4660	4660	484	458	8	II
G8	1:4.2:4.5	.91	.87	6	2	2415	2310	410	348	8	II
G9	1:4.2:4.6	.86	.86	2	1.5	2875	3080	333	366	8	II
G10	1:4.2:4.5	.91	.95	1	1	2635	2535	366	317	8	II
G11	1:4.2:4.5	.86	.86	2	1.5	2950	3020	400	-	8	II
G12	1:4.2:4.5	.86	.86	2	1	3120	3050	358	392	8	II
G13	1:4.2:4.5	.84	.84	2	2	2870	3140	333	371	8	II
G14	1:4.1:4.5	.91	.91	1.5	1	2890	3110	342	316	7	II
G15	1:4.2:4.4	.86	.89	1	1.5	2580	2990	350	416	8	II
G16	1:4.1:4.5	.84	.84	2	2	2870	2810	338	342	8	II
G17	1:4.1:4.4	.88	.88	1	3	2910	2780	346	392	8	II
G18	1:4.1:4.4	.80	.83	1.5	1	2840	2870	333	350	7	II
G19	1:3.9:4.2	.87	.85	2.5	2.5	3050	2860	466	359	8	II
G20	1:3.9:4.2	.92	.88	4.5	2.5	2450	2400	400	367	8	II

TABLE 3 (Continued)

Mark	Cement:Sand:Gravel	Water/Cement		Slump		Compressive Strength f'_c		Modulus of Rupture f_r		Age at Test	Aggregate Lot
	by weight	by weight		in.		psi		psi		days	
Batch	I and II	I	II	I	II	I	II	I	II		
G21	1:3.8:4.1	.87	.87	1.5	2	2800	2690	375	342	7	II
G22	1:3.7:4.0	.75	.75	1	2	3280	3300	383	425	8	II
G23	1:3.7:3.9	.94	.94	2.5	4	2900	2680	416	400	8	II
G24	1:3.7:4.0	.80	.80	2	2.5	3040	3010	421	383	8	II
G25	1:3.7:3.9	.81	.78	5	3	3170	3230	466	396	7	III
G26	1:3.7:4.0	.87	.83	6	2	3260	3420	433	508	9	IV
G27	1:3.2:3.5	.67	.67	1	2	5420	5050	518	492	11	IV
G28	1:4.1:4.4	.79	.76	7	3	3190	3870	383	425	11	V
G29	1:3.9:4.2	.82	.82	1.5	1.5	3860	4330	408	433	11	V
G30	1:3.2:3.5	.65	.62	3	2.5	5520	5430	517	475	10	VI
G31	1:4.0:4.3	.88	.91	1.5	2.5	3800	3160	383	267	10	VI
G32	1:4.0:4.3	.86	.83	4.5	2.5	3290	3200	333	367	11	VI
G33	1:4.1:4.3	.80	.79	2.5	3.5	3100	2680	304	304	9	VI
G34*	1:4.1:4.3	.82	.79	3	2	3320	3910	425	362	12	VI
G34s	1:3.9:4.0	.78	-	2.5	-	3000	-	383	-	6	VI
G35	1:4.1:4.3	.75	.75	4	2	3620	3550	375	392	11	VI
G36	1:4.1:4.3	.79	.82	1	2	3910	4040	350	333	18	VI
G37	1:4.2:4.4	.87	.83	3	3.5	3300	3210	417	392	8	VI
G38*	1:4.1:4.3	.80	.79	2.5	4.5	4030	3520	433	275	15	VI
G38s	1:3.8:4.1	.75	-	1	-	3280	-	333	-	9	VI

* Mix corresponding to the cast-in-place slab. Only one batch.

TABLE 4

COMPUTED AND OBSERVED DEFLECTION IN THE "ELASTIC" RANGE

Mark	Load lb.	Midspan Deflection at Reported Load		Obs. Defl. / Comp. Defl.
		Computed in.	Observed in.	
G1	6340	0.057	0.058	1.02
G2	7110	0.065	0.070	1.08
G3	11780	0.104	0.107	1.03
G4	9380	0.085	0.081	0.95
G5	14320	0.123	0.123	1.00
G6	10000	0.088	0.093	1.06
G7	12200	0.098	0.094	0.96
G8	7430	0.082	0.072	0.88
G9	7850	0.075	0.072	0.96
G10	11650	0.112	0.112	1.00
G11	6650	0.060	0.057	0.95
G12	11650	0.097	0.095	0.98
G13	8550	0.075	0.072	0.96
G14	12750	0.106	0.103	0.97
G15	9080	0.082	0.090	1.10
G16	12750	0.109	0.112	1.03
G17	12750	0.106	0.106	1.00
G18	8880	0.074	0.074	1.00
G19	12200	0.098	0.098	1.00
G20	12750	0.126	0.120	0.95
G21	7870	0.073	0.072	0.99
G22	11650	0.091	0.116	1.27
G23	7300	0.066	0.066	1.00
G24	12220	0.101	0.110	1.09
G25	7210	0.055	0.059	1.07
G26	12200	0.098	0.120	1.22
G27	13860	0.087	0.098	1.13
G28	10540	0.080	0.088	1.10
G29	17200	0.107	0.114	1.07
G30	13320	0.086	0.098	1.14

TABLE 4 (Continued)

Mark	Load lb.	Midspan Deflection at Reported Load: Computed in.	Midspan Deflection at Reported Load: Observed in.	Obs. Defl. / Comp. Defl.
G31	8330	0.072	0.075	1.04
G32	16090	0.108	0.121	1.12
G33	11650	0.091	0.098	1.08
G34	12850	0.038	0.046	1.21
G35	8930	0.076	0.088	1.16
G36*	-	-	-	-
G37	9430	0.084	0.093	1.11
G38	17200	0.051	0.059	1.16
			Ave.	1.05

* The deflections were not recorded since this was a defective specimen.

TABLE 5

COMPUTED AND OBSERVED VALUES OF INCLINED TENSION CRACKING LOAD

Mark	Tensile Strength f_t psi	Effective Prestress Force F_{se} kips	$\frac{F_{se}}{A_c f_t}$	Cracking Load P_c kips	$\frac{M_c}{f_t\ bd^2\sqrt{b'/b}}$ Obs.	Comp.	Obs./Comp.
G1	248	15.2	1.29	13.0	2.67	2.29	1.17
G2	239	15.2	1.33	12.5	2.66	2.33	1.14
G3	257	28.9	2.36	17.8	3.86	3.36	1.15
G4	257	28.2	2.30	18.5	3.98	3.30	1.21
G5	299	29.2	2.05	18.8	3.48	3.05	1.14
G6	264	28.9	2.30	18.2	3.73	3.30	1.13
G7	304	29.4	2.03	18.9	3.39	3.03	1.12
G8	223	15.3	1.44	12.9	2.94	2.44	1.20
G9	245	15.2	1.30	13.9	2.84	2.30	1.23
G10	234	28.7	2.58	17.7	4.15	3.58	1.16
G11	248	15.4	1.30	12.9	2.65	2.30	1.15
G12	255	28.2	2.07	21.0	3.49	3.07	1.14
G13	244	15.2	1.31	12.4	2.56	2.31	1.11
G14	245	29.0	2.22	20.8	3.54	3.22	1.10
G15	231	15.2	1.38	12.1	2.68	2.38	1.12
G16	244	29.3	2.25	19.7	3.34	3.25	1.03
G17	246	29.1	2.21	21.4	3.62	3.21	1.13
G18*	243	15.3	1.18	-	-	2.18	-
G19	252	29.5	2.19	20.0	3.30	3.19	1.03
G20	225	29.4	2.74	16.3	3.89	3.74	1.04
G21	241	15.2	1.32	14.4	3.02	2.32	1.30
G22	261	27.2	2.19	17.3	3.55	3.19	1.11
G23	246	15.2	1.30	12.4	2.53	2.30	1.10
G24	253	29.1	2.42	18.3	3.90	3.42	1.14
G25	257	15.4	1.26	13.5	2.66	2.26	1.18
G26	260	28.7	2.32	13.3	2.78	3.32	0.84
G27	322	29.4	1.92	22.1	3.64	2.92	1.25
G28	258	28.3	2.05	20.4	3.34	3.05	1.09
G29	281	28.7	2.14	19.8	3.02	3.14	0.96
G30	325	29.0	1.67	25.2	3.22	2.67	1.21

* This beam failed before any inclined tension crack formed.

TABLE 5 (Continued)

Mark	Tensile Strength f_t psi	Effective Prestress Force F_{se} kips	$\frac{F_{se}}{A_c f_t}$	Cracking Load P_c kips	$\frac{M_c}{f_t bd^2\sqrt{b'/b}}$ Obs.	Comp.	$\frac{\text{Obs.}}{\text{Comp.}}$
G31	279	29.5	1.98	13.4	3.04	2.98	1.02
G32	260	28.8	1.92	17.8	2.88	2.92	0.99
G33	254	29.2	2.15	24.3	4.03	3.15	1.28
G34	262	28.5	2.28	20.9	4.49	3.28	1.37
G35	273	29.6	2.03	17.2	3.51	3.03	1.16
G36*	283	17.0	1.26	-	-	3.26	-
G37	262	29.7	2.12	18.8	3.95	3.12	1.27
G38	286	29.8	2.19	19.4	3.58	3.19	1.12
						Ave.	1.13

* The inclined cracking load for this beam was not recorded because this was a defective specimen.

TABLE 6

COMPUTED AND MEASURED CAPACITIES

Mark	Steel Stress at Ultimate Comp. $(f_{su})_c$ ksi	Steel Stress at Ultimate Meas. $(f_{su})_m$ ksi	Total Ultimate Bending Moment Computed for Flexure M_f k-in.	Total Ultimate Bending Moment Computed for Shear M_s k-in.	Total Ultimate Bending Moment Measured from Tests M_t k-in.	$\frac{M_t}{M_f}$	$\frac{M_t}{M_s}$**	Observed Failure Mode***	Predicted Failure Mode
(1)	(2)	(3)	(4)	(5)	(6)	(7)	(8)	(9)	(10)
G1	248	238	294	566	296	1.01	-	F	F
G2	249	-	296	476	294	0.99	-	F	F
G3	232	190	462*	548	420	0.91	-	F	F
G4	233	220	477*	497	466	0.98	-	F	F
G5	235	208	503	431	464	0.92	1.08	S	S
G6	234	180	498*	400	394	0.79	0.99	S	S
G7	239	221	528	479	498	0.94	1.04	S	S
G8	244	240	286	333	296	1.03	-	F	F
G9	248	237	294	317	297	1.01	-	F	F
G10	232	200	453*	451	430	0.95	0.95	S	S
G11	248	-	294	316	295	1.00	-	F	F
G12	234	221	480*	509	477	0.99	-	F	F
G13	248	228	294	259	284	0.97	1.10	S	S
G14	235	218	489*	450	477	0.98	1.06	S	S
G15	248	236	295	264	289	0.98	1.09	T	S
G16	233	200	465*	480	438	0.94	-	F	F
G17	233	213	464*	552	452	0.97	-	F	F
G18	247	225	291	302	297	1.02	-	F	F
G19	233	202	470*	484	438	0.93	-	F	F
G20	231	185	437*	502	437	1.00	0.87	S	F
G21	246	240	290	269	287	0.99	1.07	S	S
G22	235	226	504	561	484	0.96	-	F	F
G23	246	238	290	323	289	1.00	-	F	F
G24	226	215	485	684	473	0.98	-	F	F
G25	241	219	287	284	288	1.00	1.01	F	S
G26	227	213	489	547	464	0.95	0.85	T	F
G27	232	223	518	589	512	0.99	-	F	F
G28	228	212	494	483	479	0.97	0.99	S	S
G29	230	218	502	496	495	0.99	1.00	S	S
G30	233	226	520	511	510	0.98	1.00	F	S

* Value compensated for non-rectangular compression zone
**Tabulated for shear and transition failures only
*** F: Flexural failure, S: Shear failure, T: Transition failure

TABLE 6 (Continued)

Mark	Steel Stress at Ultimate: Comp. $(f_{su})_c$	Steel Stress at Ultimate: Meas. $(f_{su})_m$	Total Ultimate Bending Moment: Computed for Flexure M_f	Total Ultimate Bending Moment: Computed for Shear M_s	Total Ultimate Bending Moment: Measured from Tests M_t	$\frac{M_t}{M_f}$	$\frac{M_t}{M_s}$**	Observed Failure Mode***	Predicted Failure Mode
	ksi	ksi	k-in.	k-in.	k-in.				
(1)	(2)	(3)	(4)	(5)	(6)	(7)	(8)	(9)	(10)
G31	226	205	480*	501	469	0.98	-	F	F
G32	226	208	482	522	466	0.97	-	F	F
G33	225	193	446*	482	447	1.00	0.93	T	F
G34	256	223	743	602	655	0.88	1.09	S	S
G35	227	213	495	492	477	0.96	0.97	T	S
G36[t]	-	-	-	-	386	-	-	F	-
G37	226	-	485*	536	472	0.97	-	F	F
G38	256	256	743	741	711	0.96	0.96	F	S

[t] Defective specimen. Load measurements only.

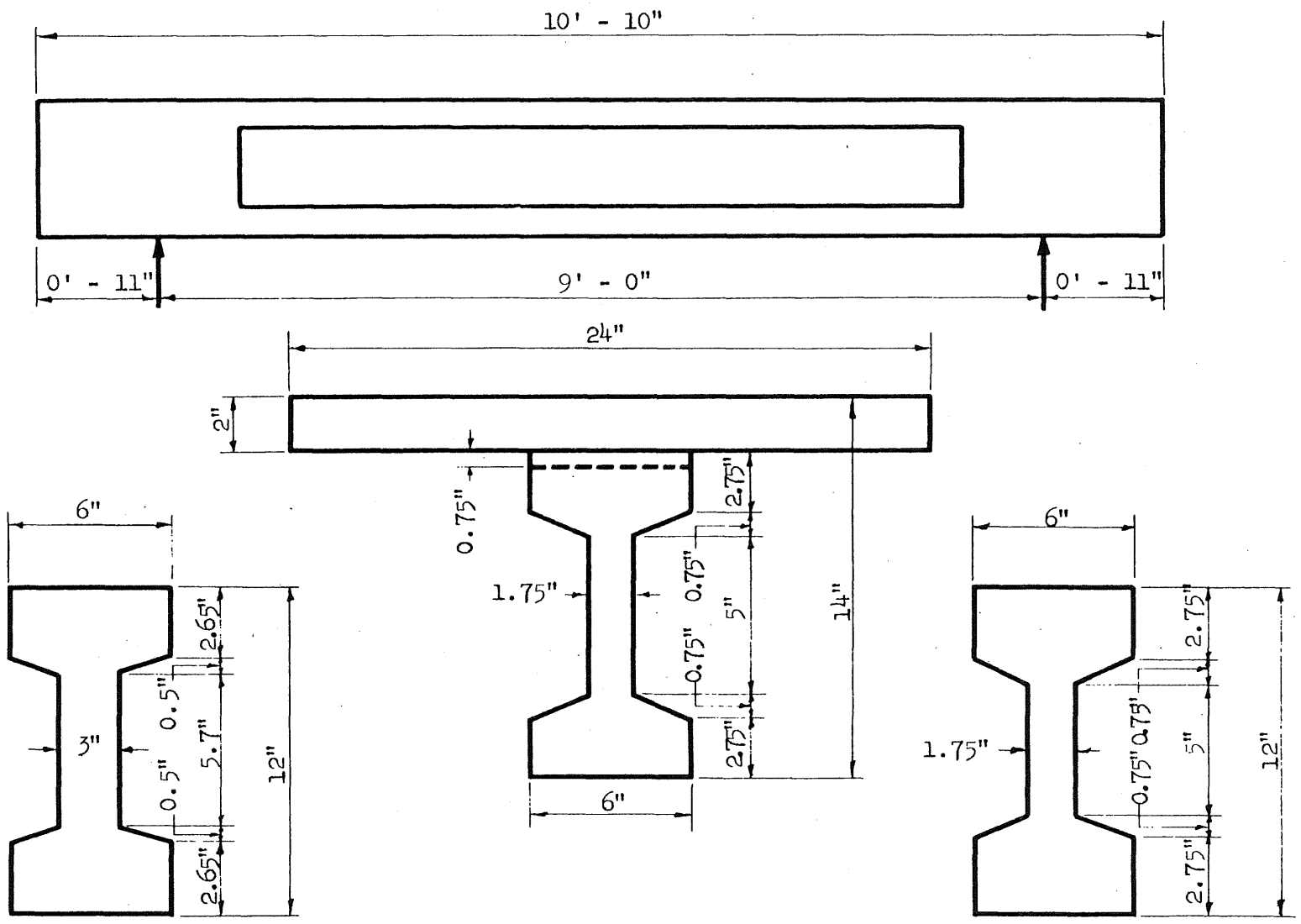

FIG. 1 NOMINAL DIMENSIONS OF BEAMS

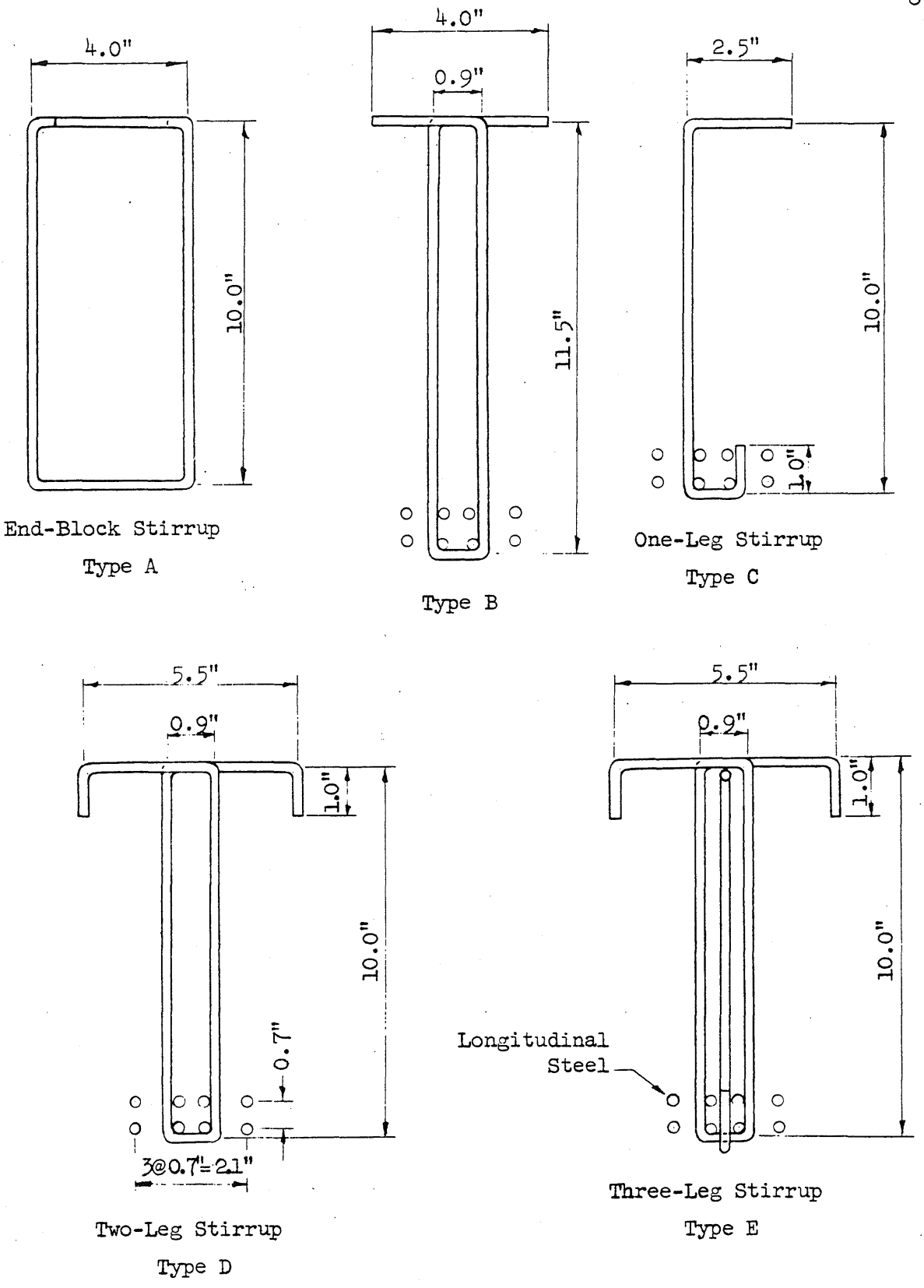

FIG. 2 NOMINAL DIMENSIONS OF STIRRUPS

Spacing

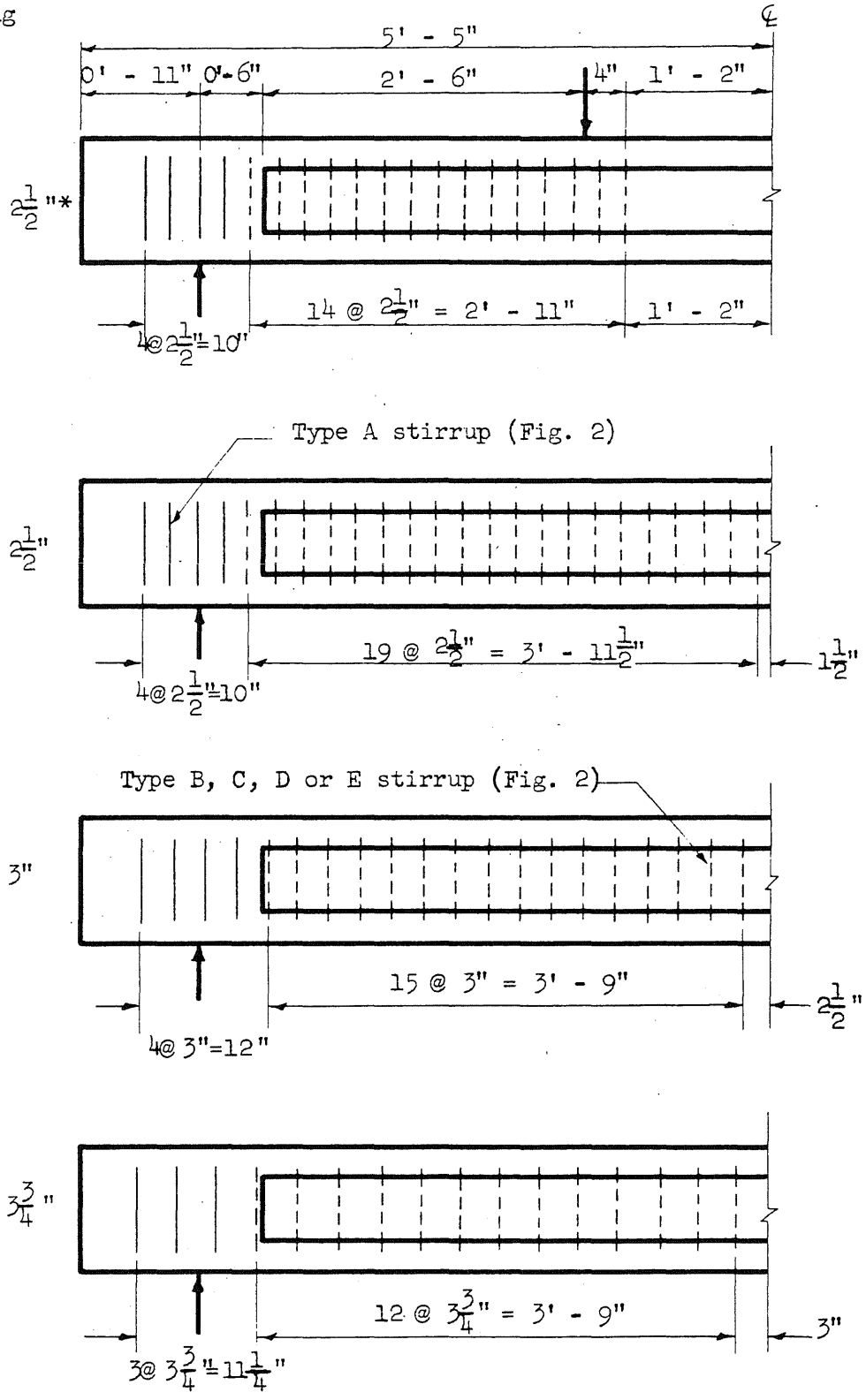

* Beams G1, G2, G3 only

FIG. 3a ARRANGEMENT OF STIRRUPS. SPACINGS $2\frac{1}{2}$ TO $3\frac{3}{4}$ IN.

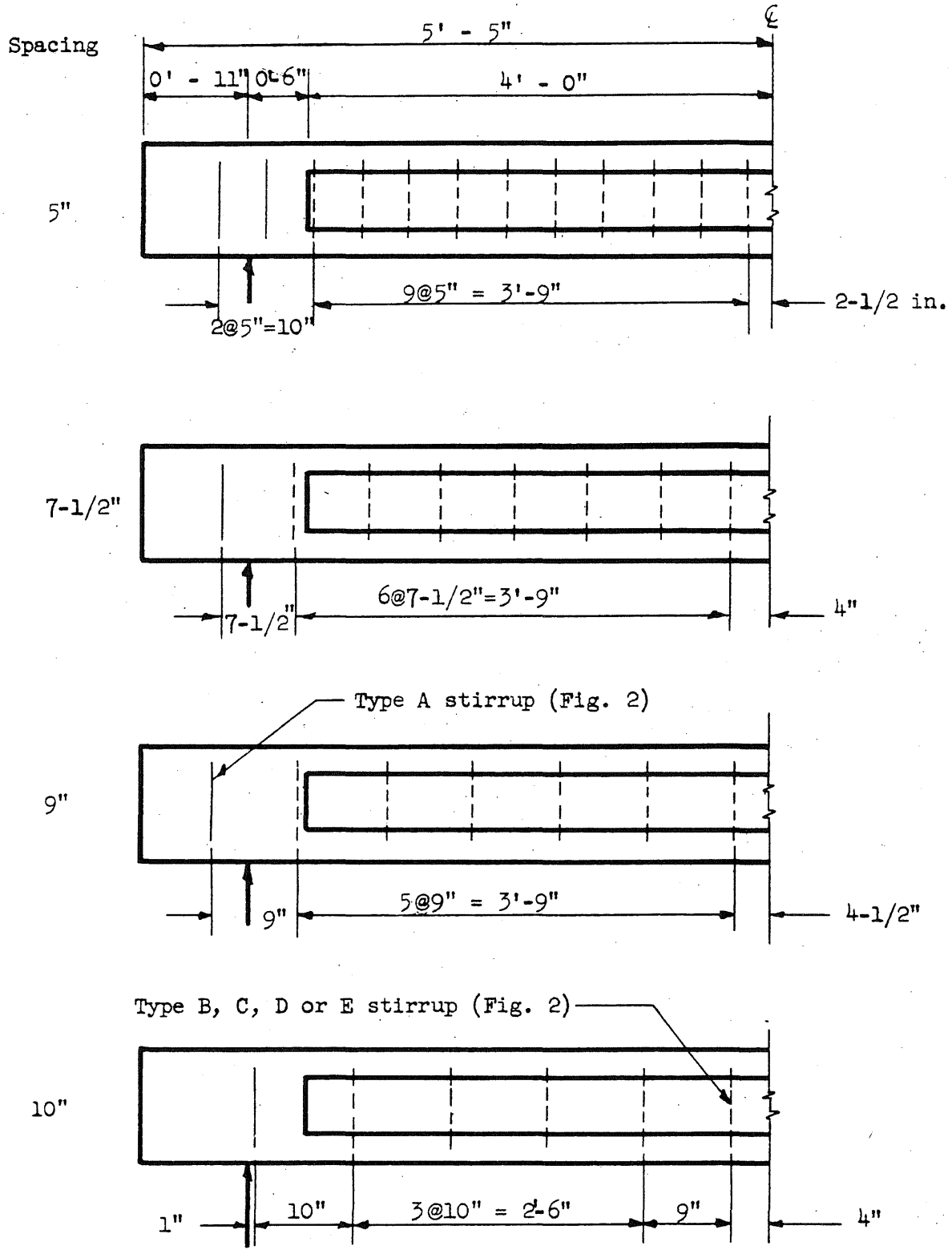

FIG. 3b ARRANGEMENT OF STIRRUPS. SPACINGS 5 TO 10 IN.

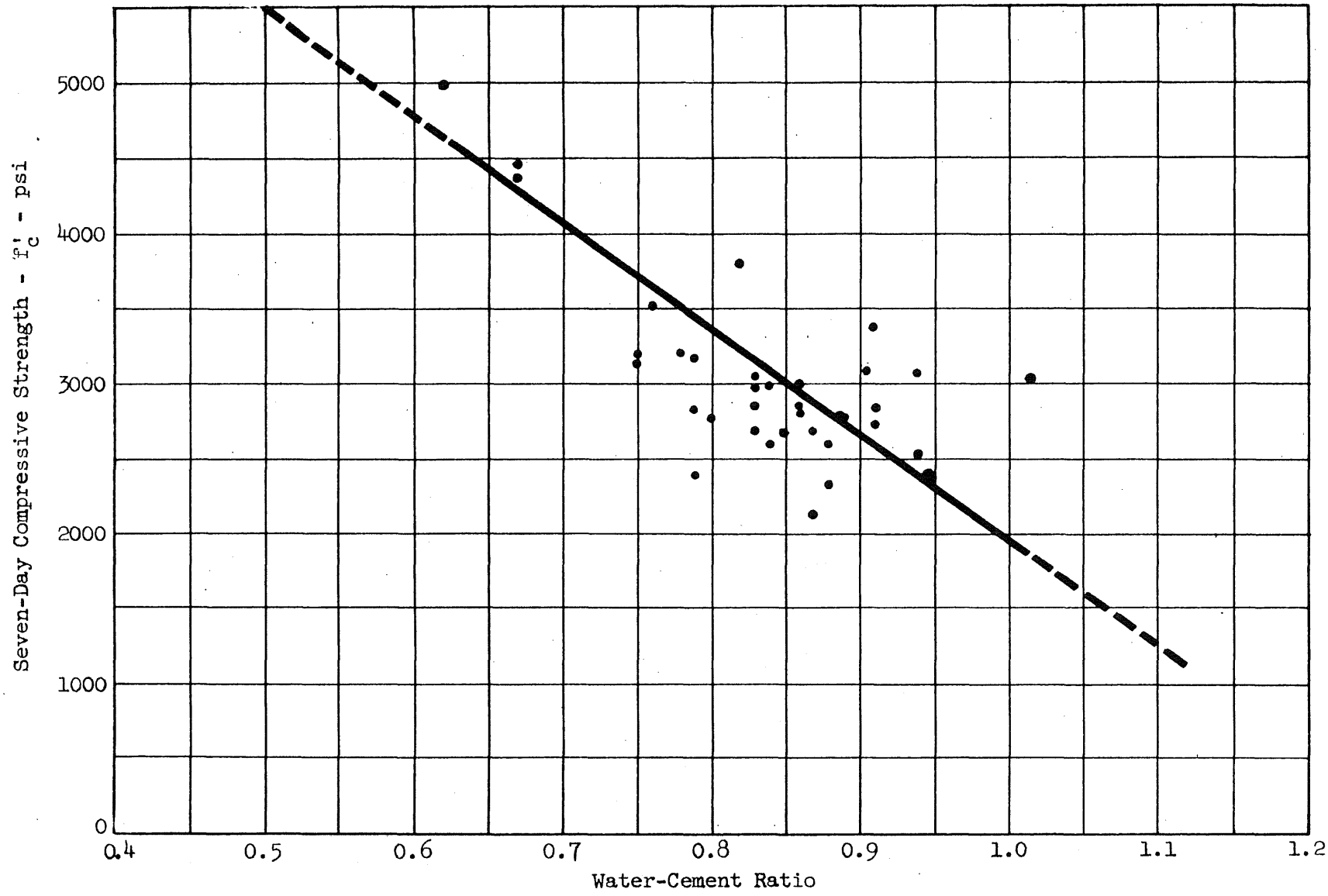

FIG. 4 SEVEN-DAY COMPRESSIVE STRENGTH OF CONCRETE VERSUS WATER-CEMENT RATIO

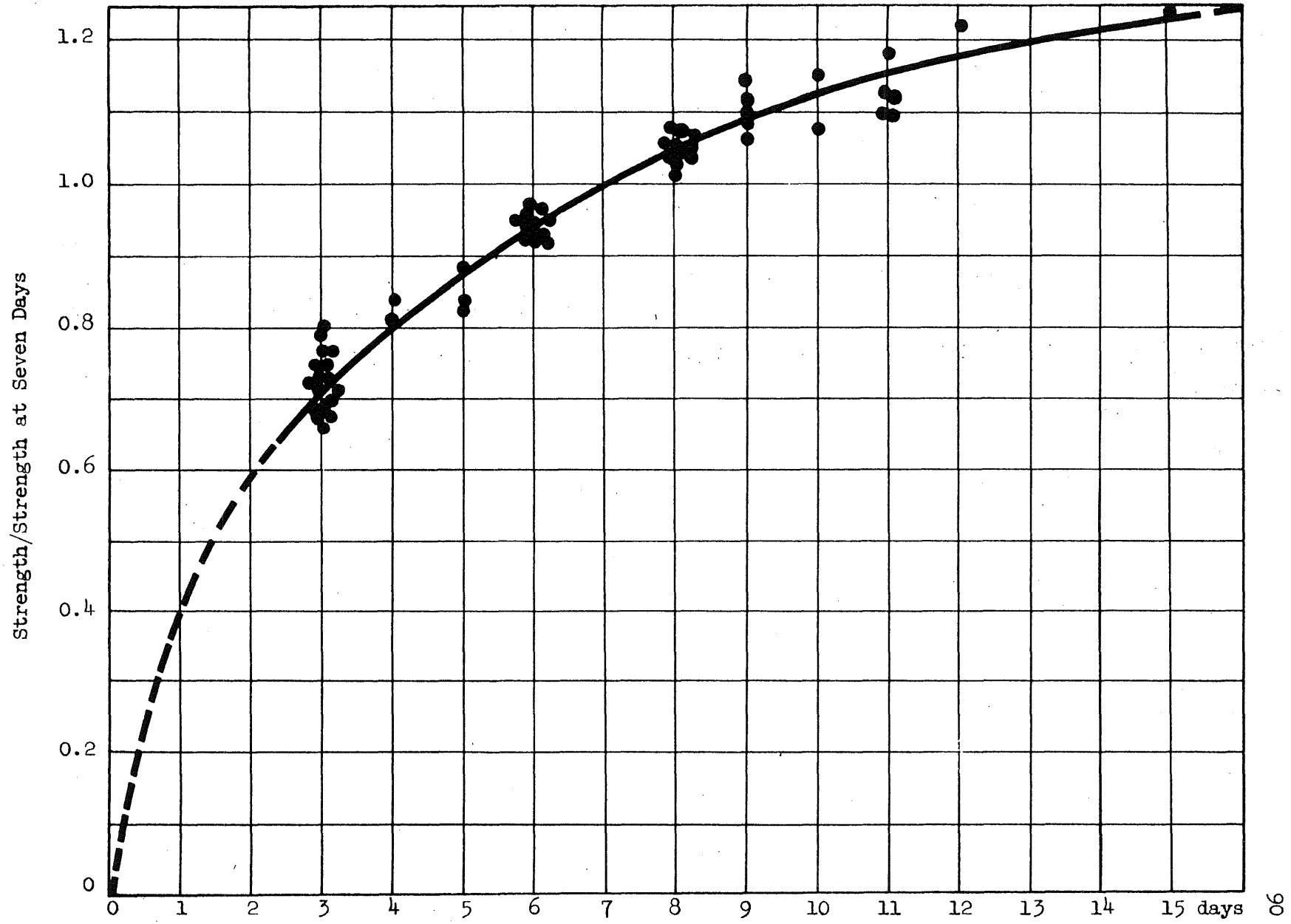

FIG. 5 INCREASE IN CONCRETE COMPRESSIVE STRENGTH WITH TIME

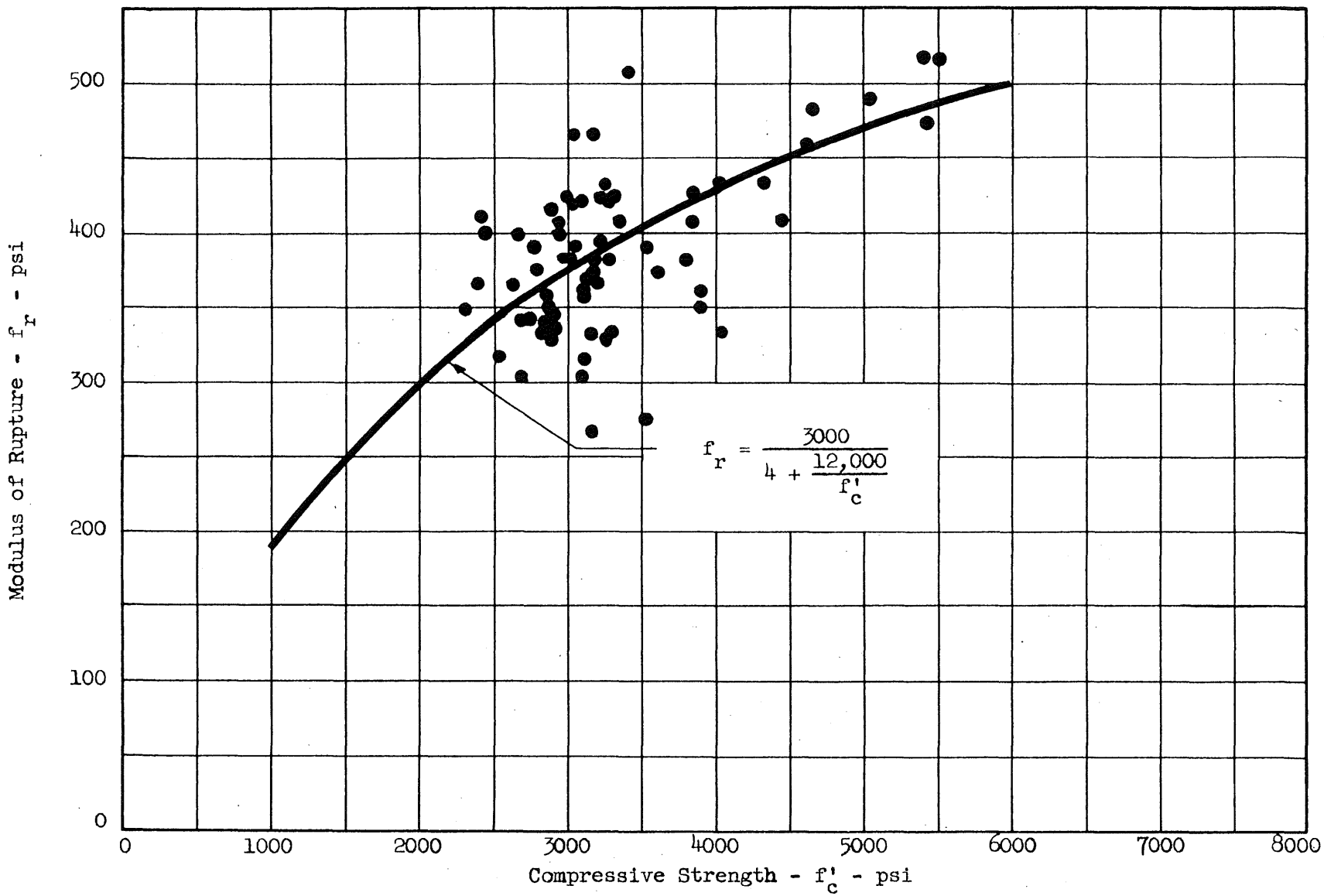

FIG. 6 COMPARISON OF MODULUS OF RUPTURE WITH COMPRESSIVE STRENGTH OF CONCRETE

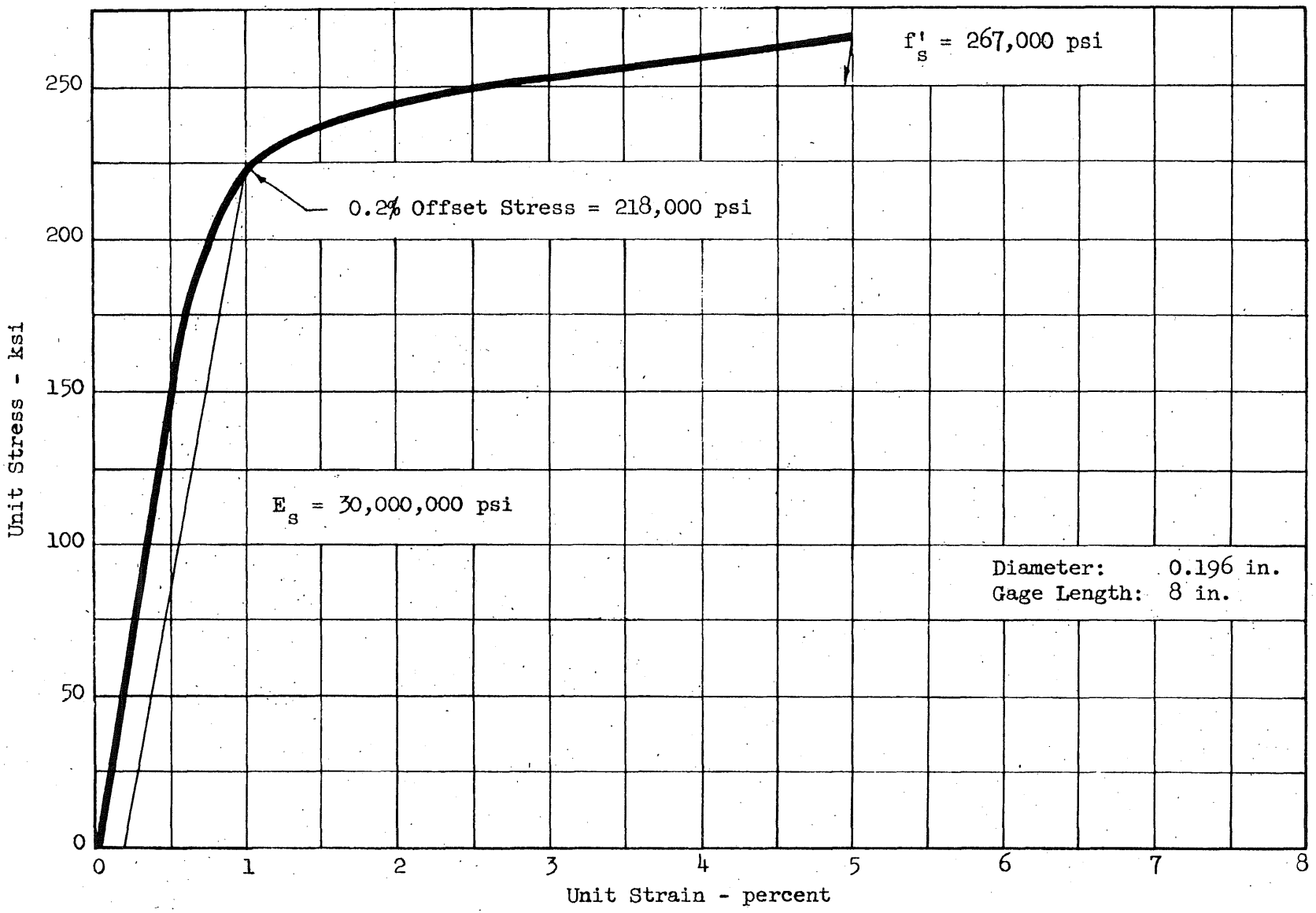

FIG. 7 STRESS-STRAIN RELATIONSHIP FOR TYPE X WIRE

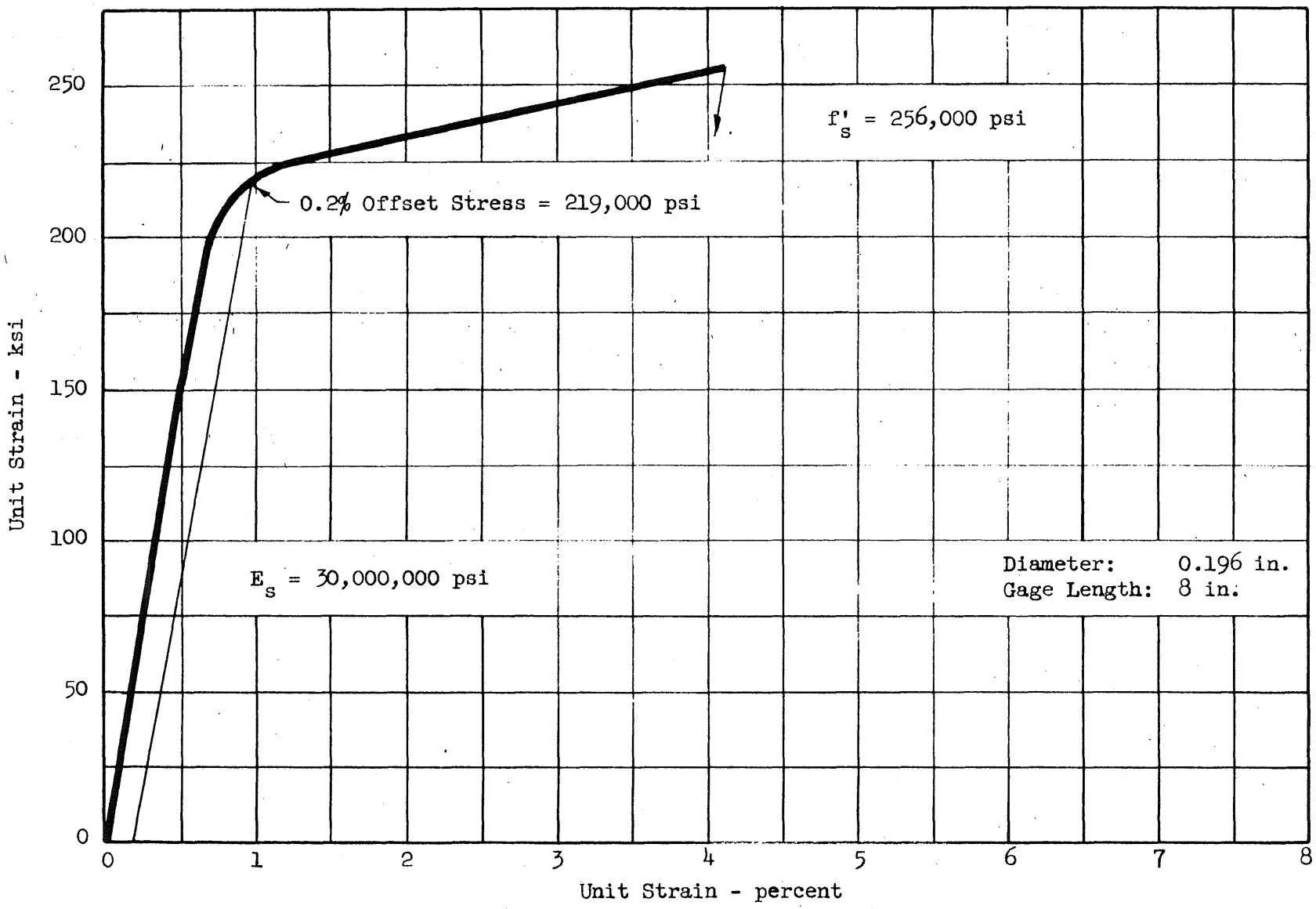

FIG. 8 STRESS-STRAIN RELATIONSHIP FOR TYPE XI WIRE

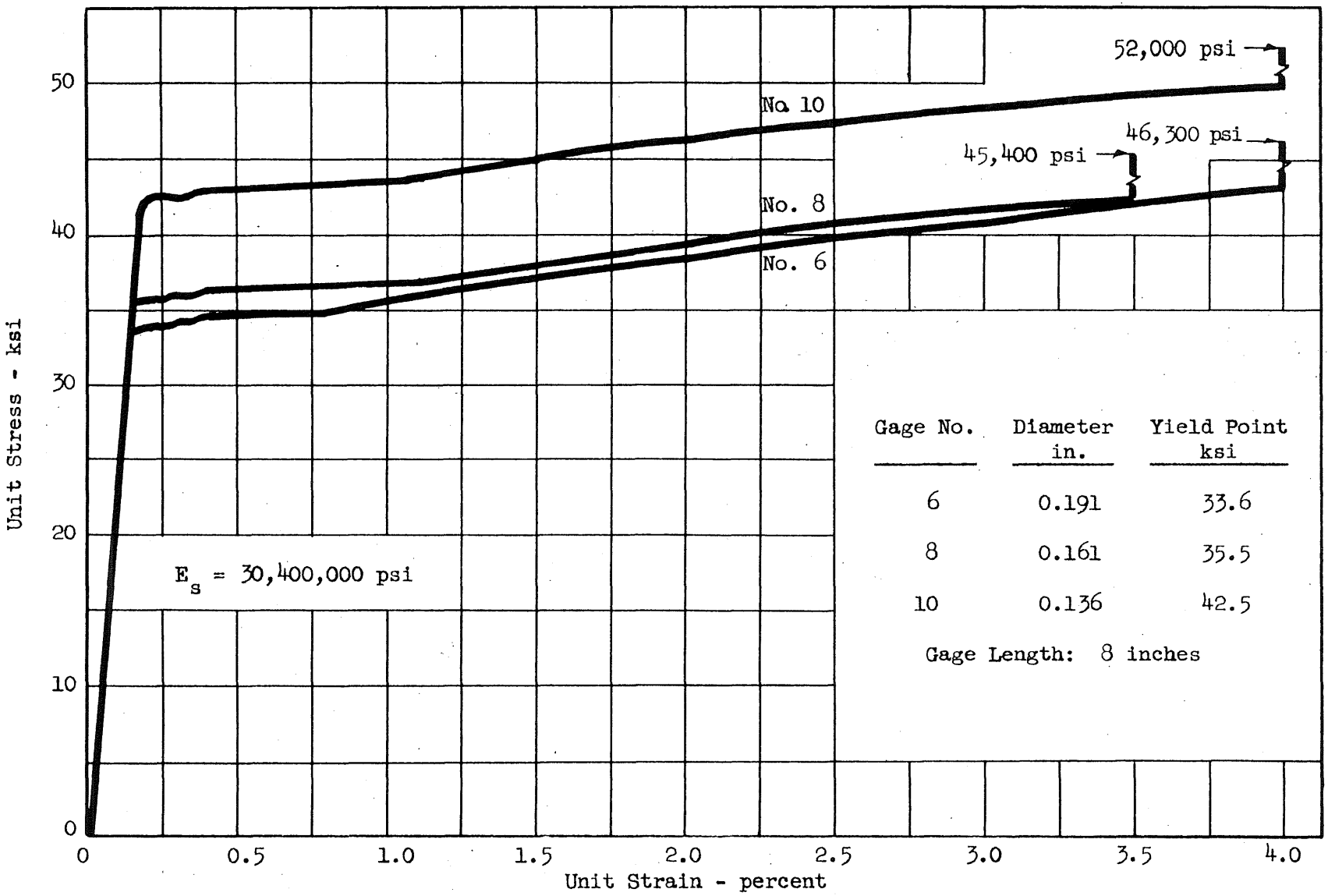

FIG. 9 STRESS-STRAIN RELATIONSHIP FOR BLACK ANNEALED WIRE, LOT A

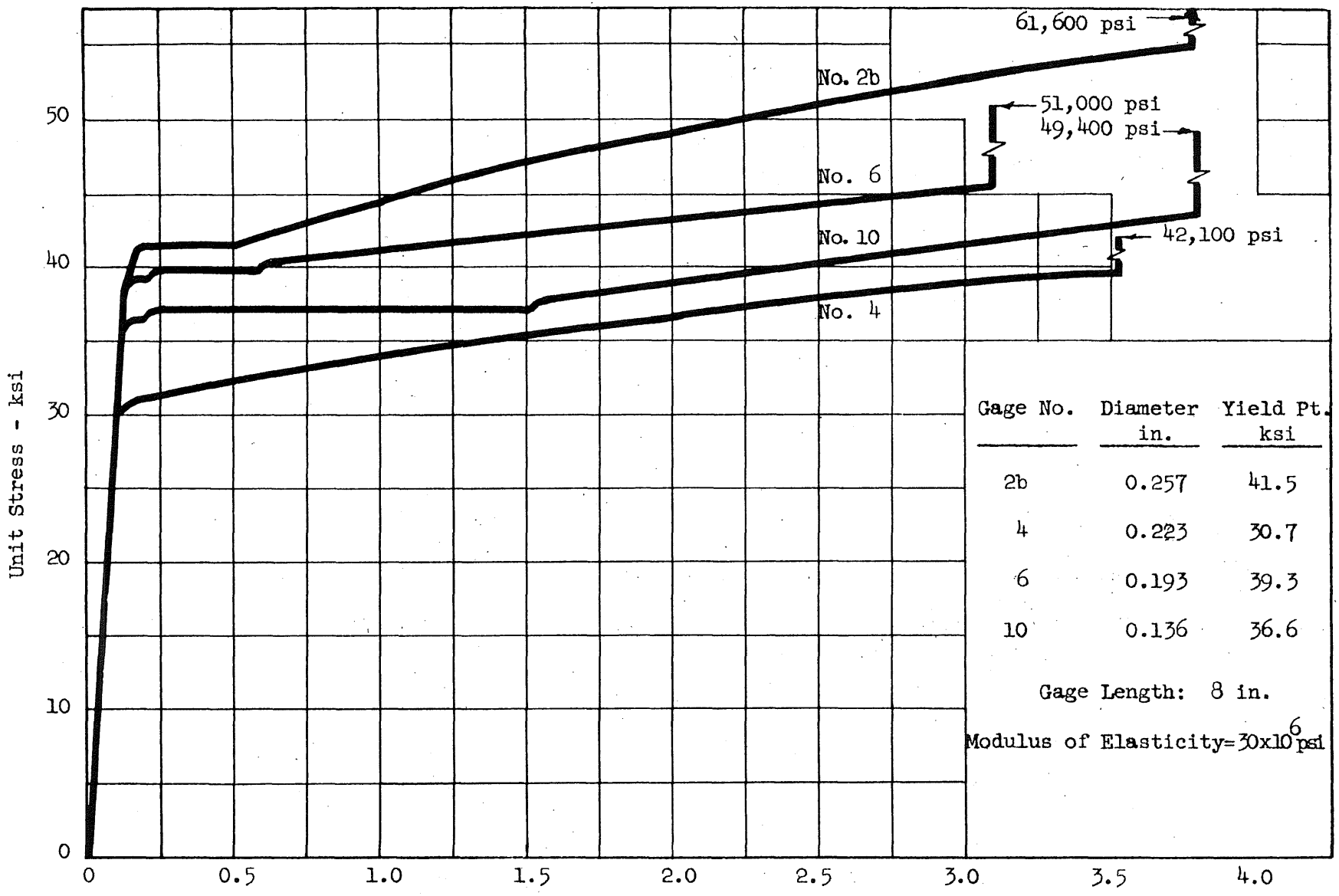

Gage No.	Diameter in.	Yield Pt. ksi
2b	0.257	41.5
4	0.223	30.7
6	0.193	39.3
10	0.136	36.6

Gage Length: 8 in.

Modulus of Elasticity=30×10^6 psi

FIG. 10 STRESS-STRAIN RELATIONSHIP FOR BLACK ANNEALED WIRE, LOT B

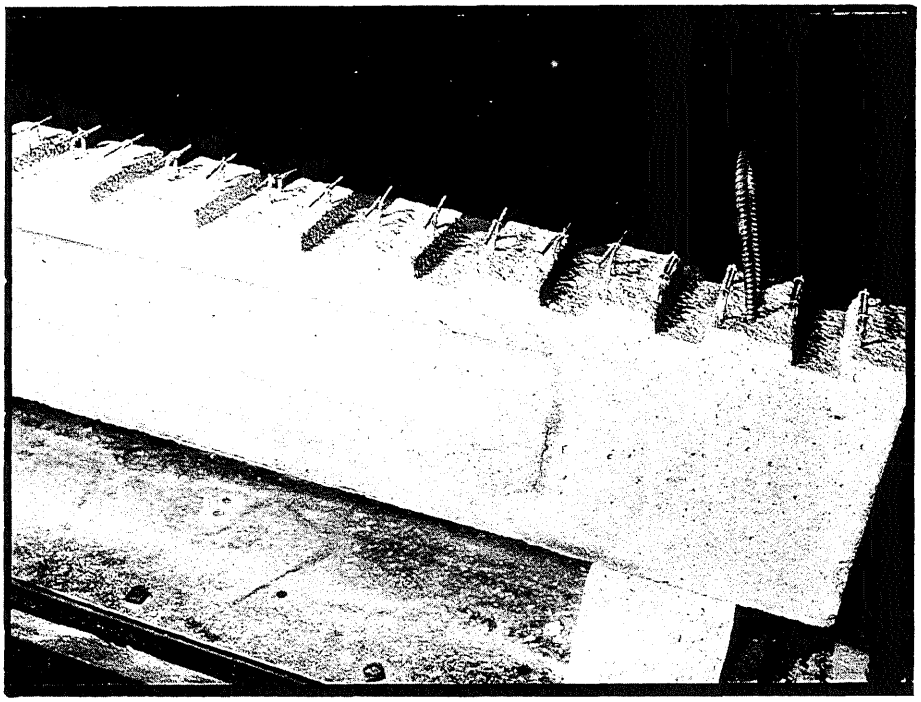

FIG. 11 VIEW OF SHEAR KEYS AND PROTRUDING ENDS OF STIRRUPS IN BEAM G34

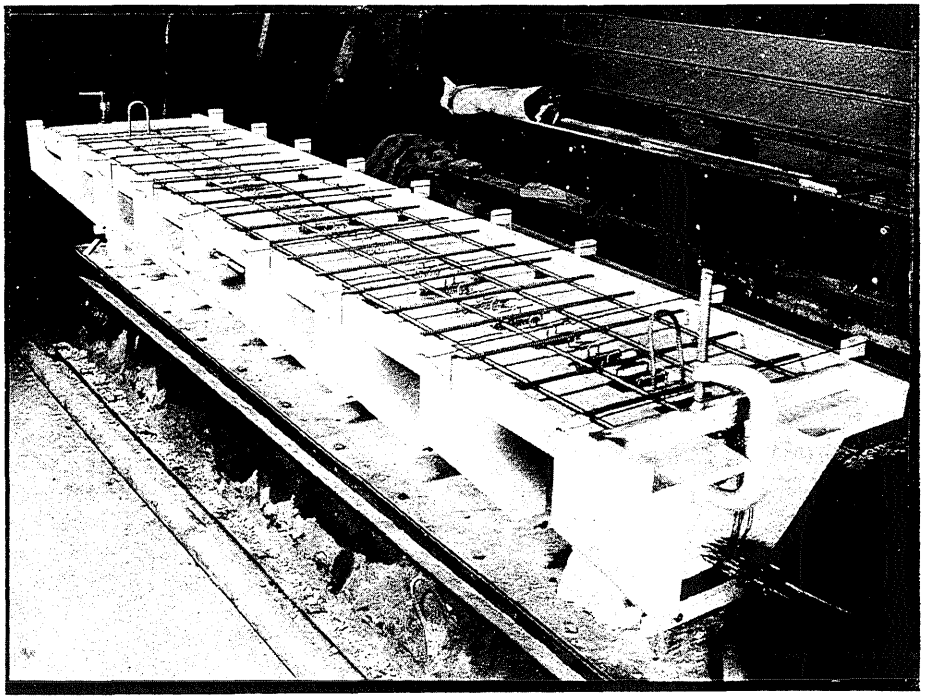

FIG. 12 BEAM G34 BEFORE CASTING THE SLAB

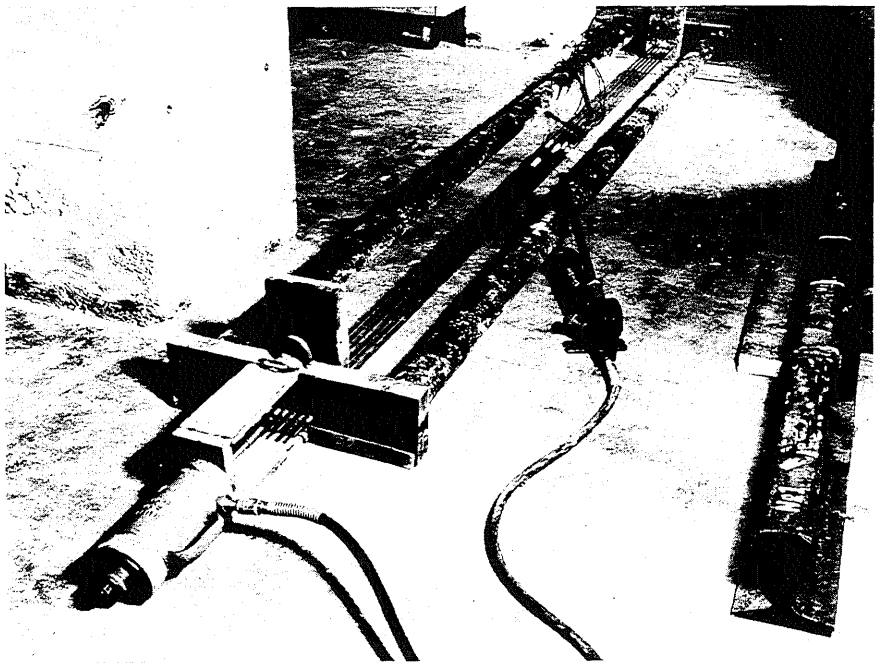

FIG. 13 PRESTRESSING FRAME

FIG. 14 SHIMS, NUT, AND DYNAMOMETER

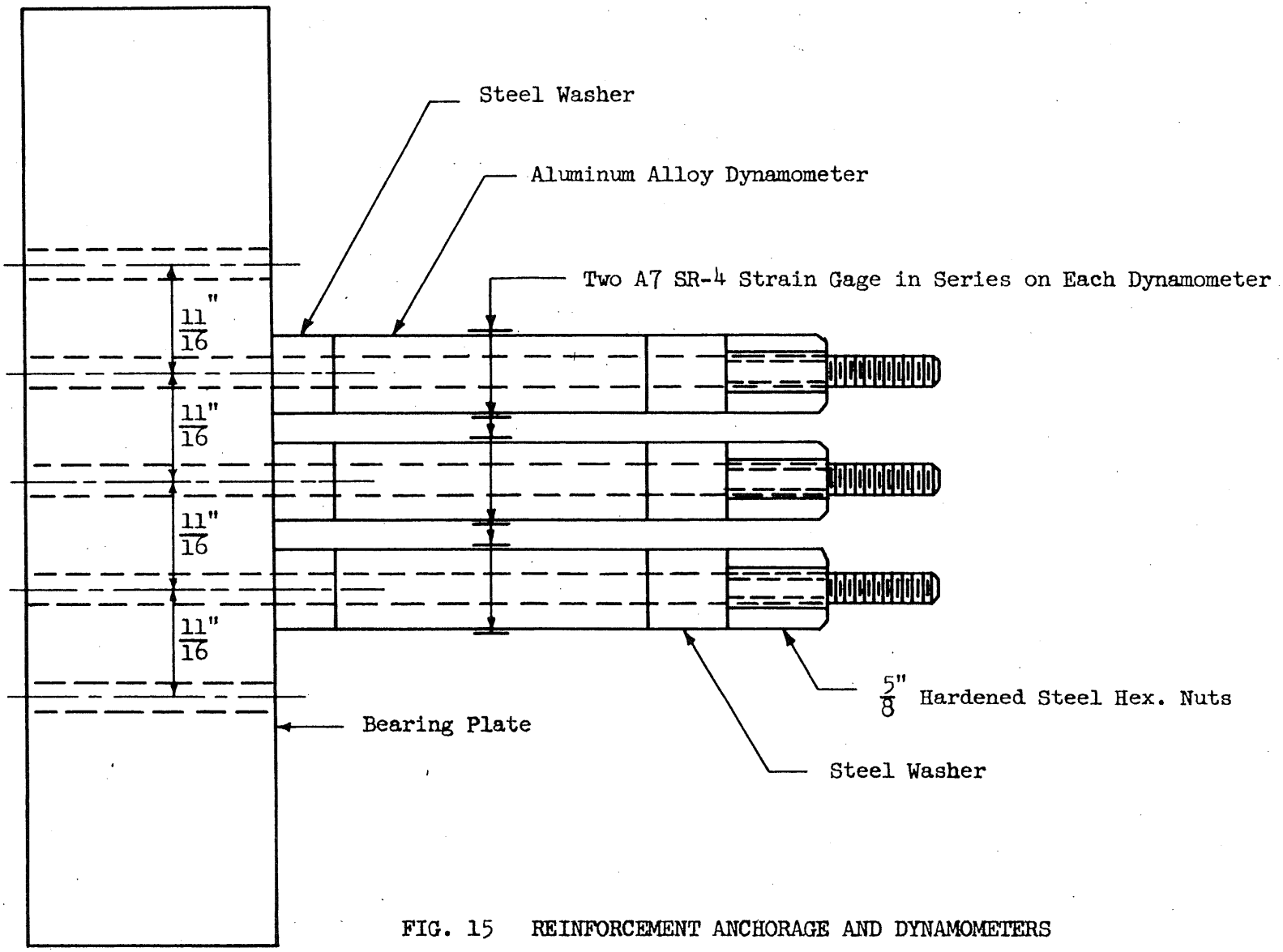

FIG. 15 REINFORCEMENT ANCHORAGE AND DYNAMOMETERS

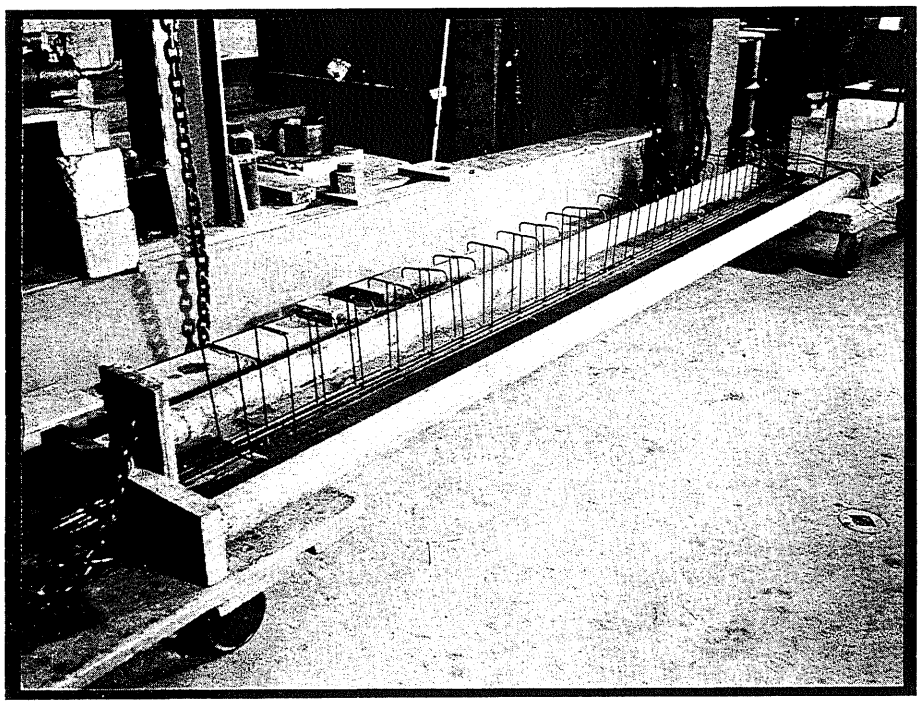

(a)

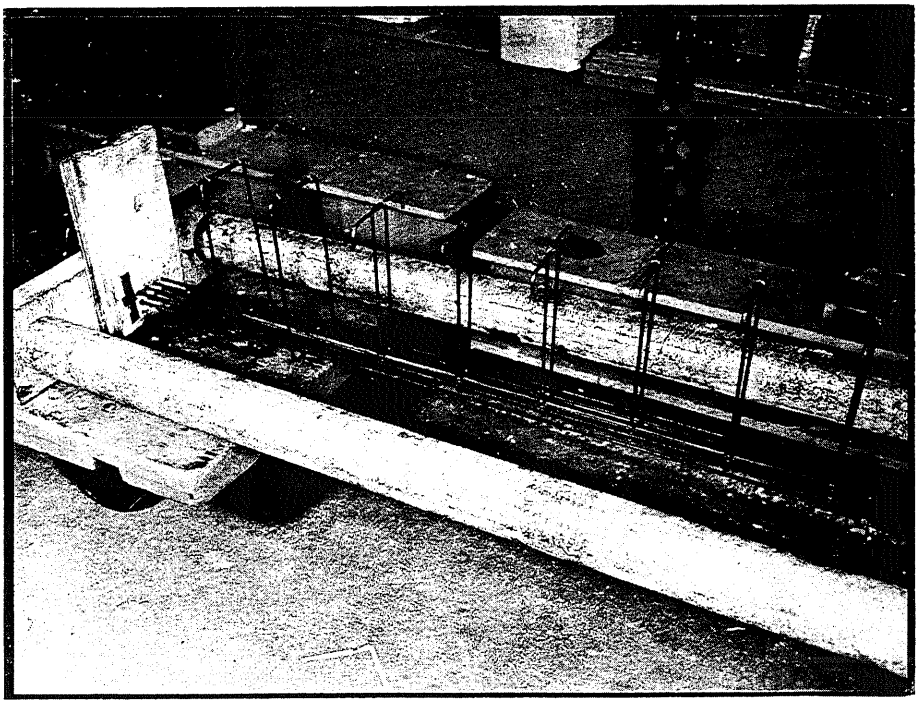

(b)

FIG. 16 TYPICAL STIRRUP ARRANGEMENT

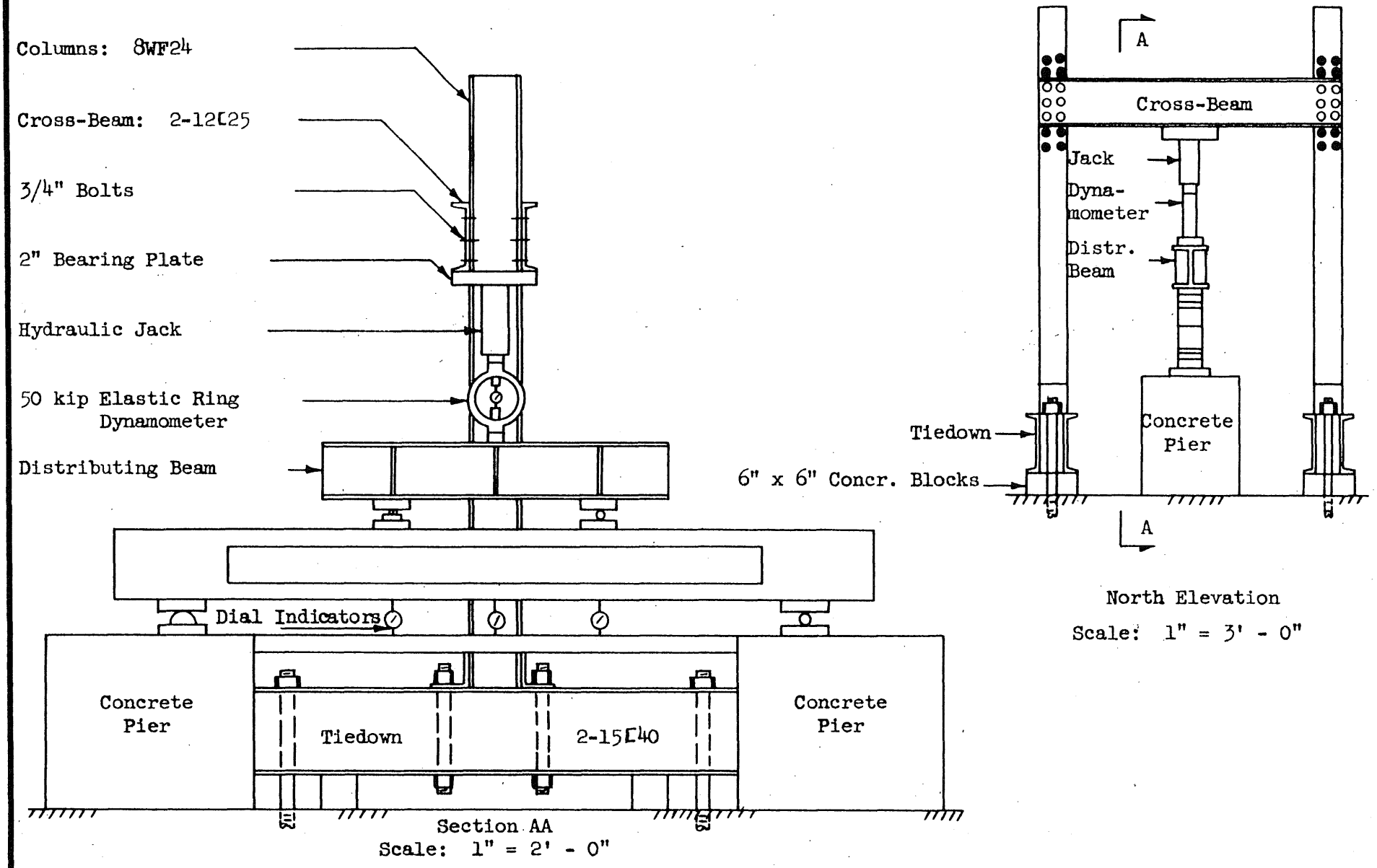

FIG. 17 SET-UP OF SPECIMEN IN LOADING FRAME

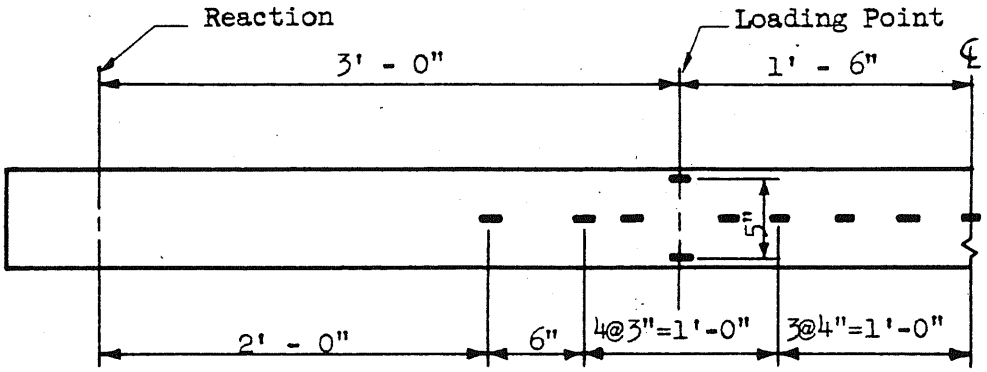

Beams G1 through G7

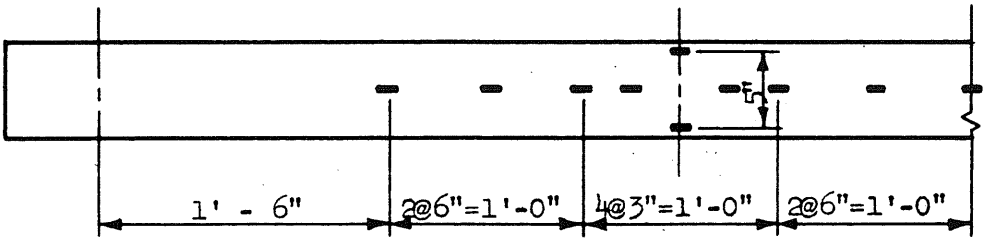

Beams G8 through G15

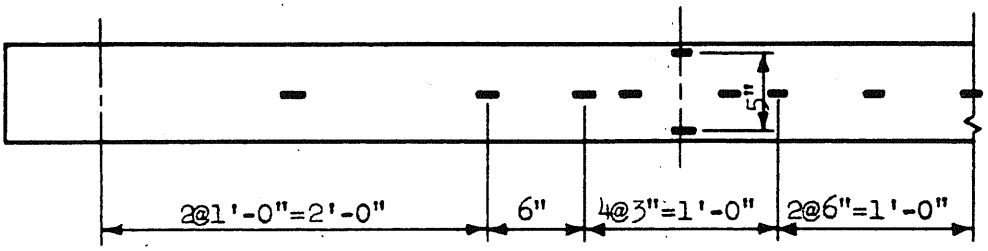

Beams with a=36" from G16 through G38

FIG. 18a POSITION OF THE STRAIN GAGES ON THE TOP SURFACE OF THE I-BEAMS

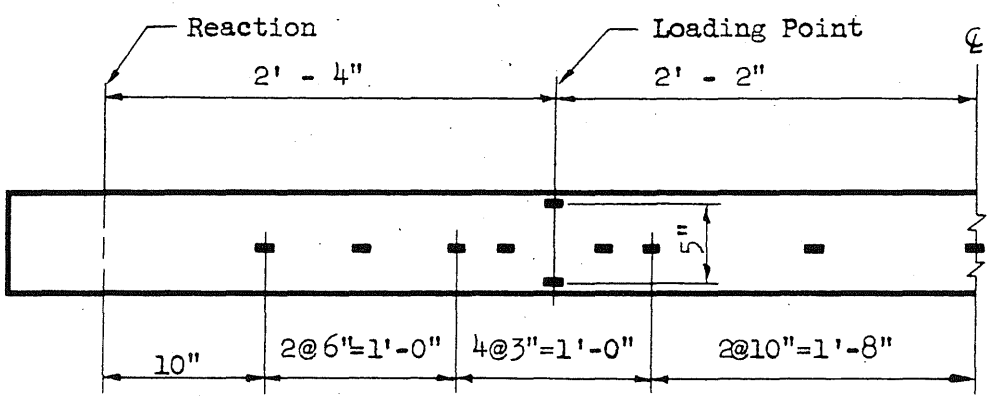

Beams with a=28"

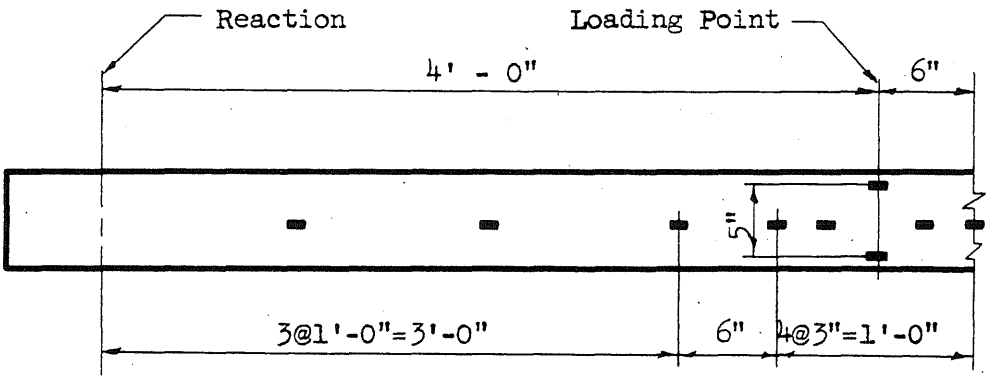

Beams with a=48"

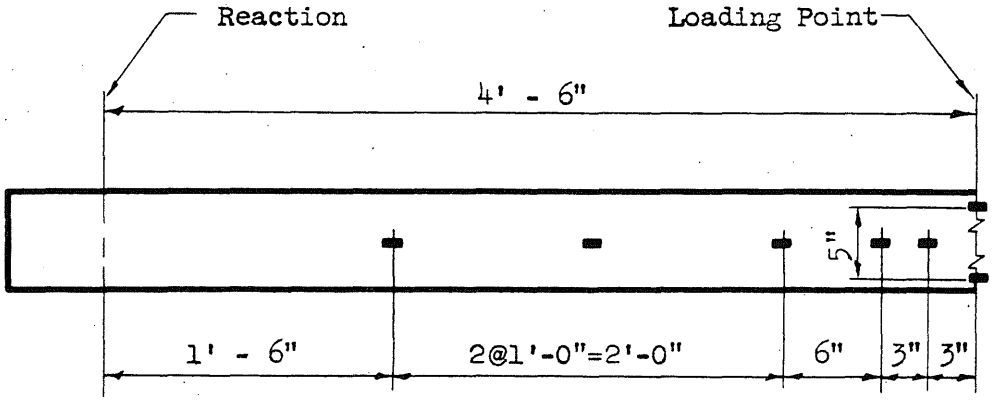

Beams with Midspan Load

FIG. 18b POSITION OF THE STRAIN GAGES ON THE TOP SURFACE OF THE I-BEAMS

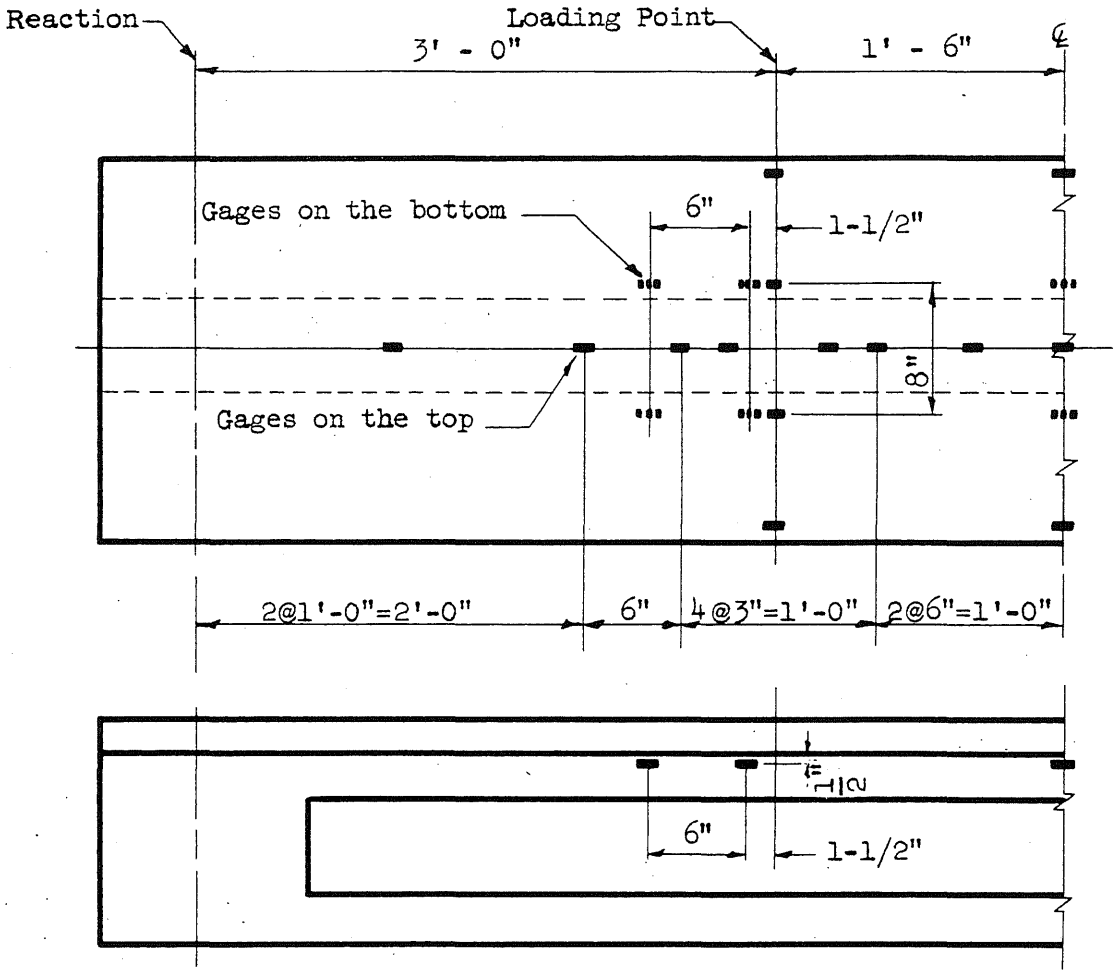

Electric Strain Gages

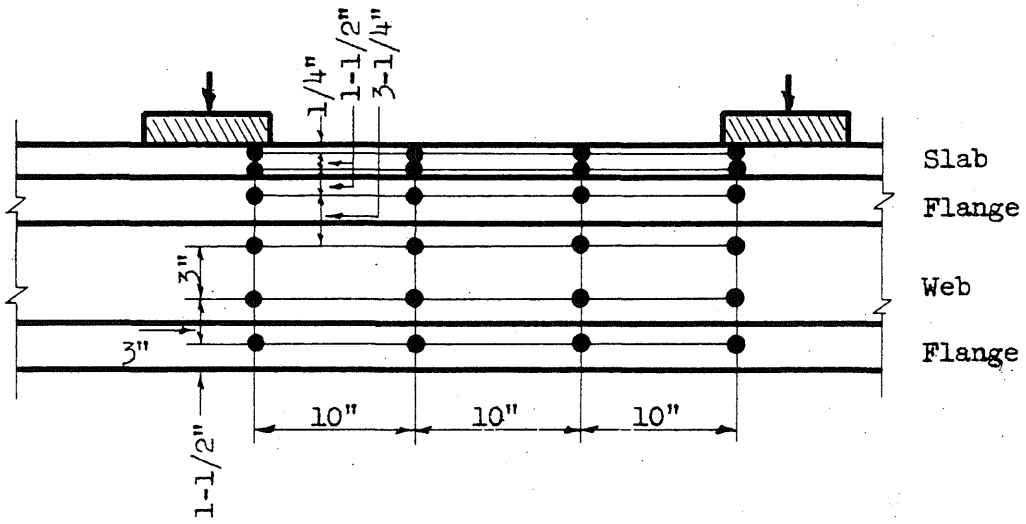

FIG. 19 POSITION OF STRAIN GAGES ON COMPOSITE BEAMS

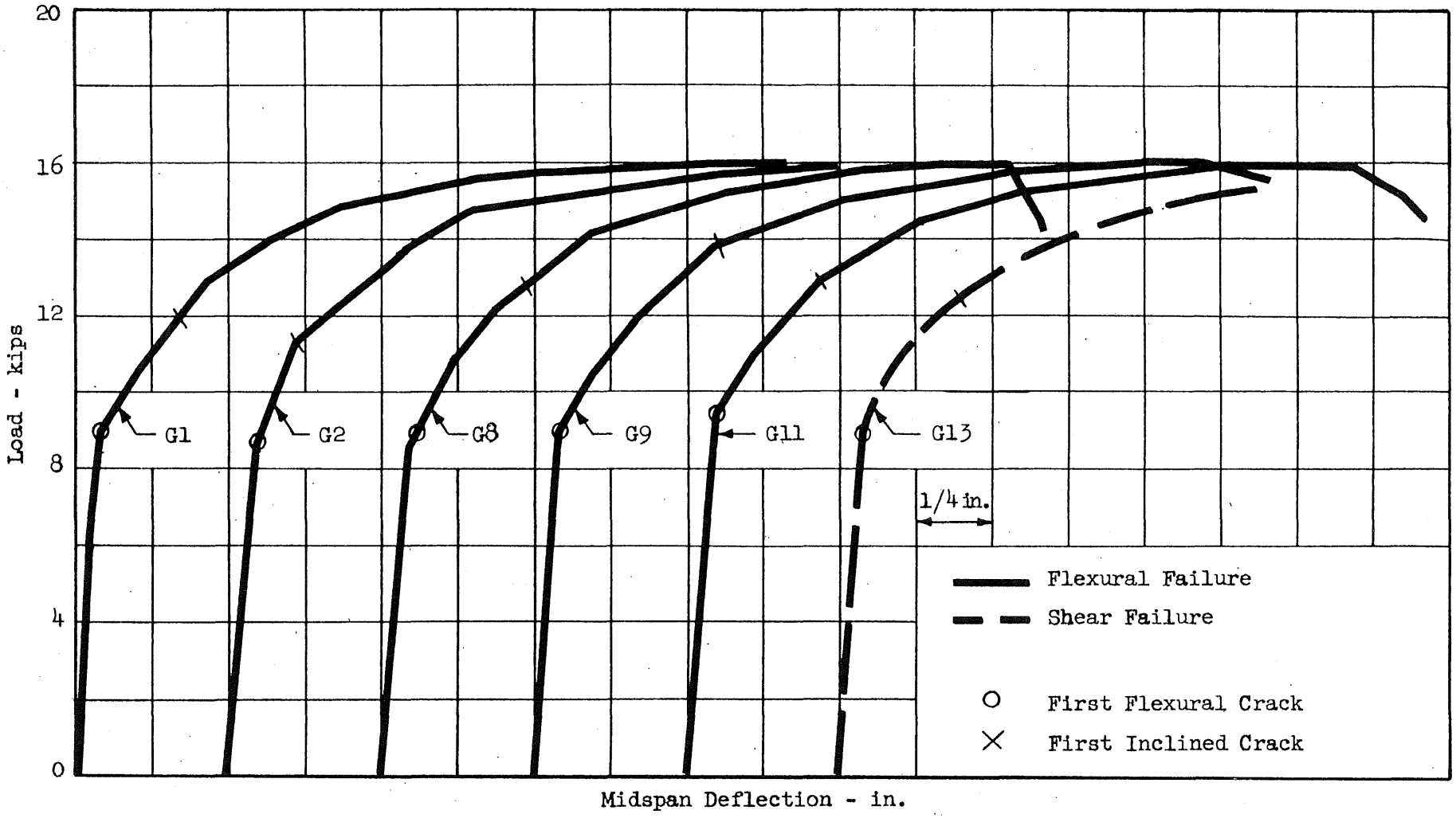

FIG. 20 LOAD-DEFLECTION CURVES FOR BEAMS WITH FOUR WIRES

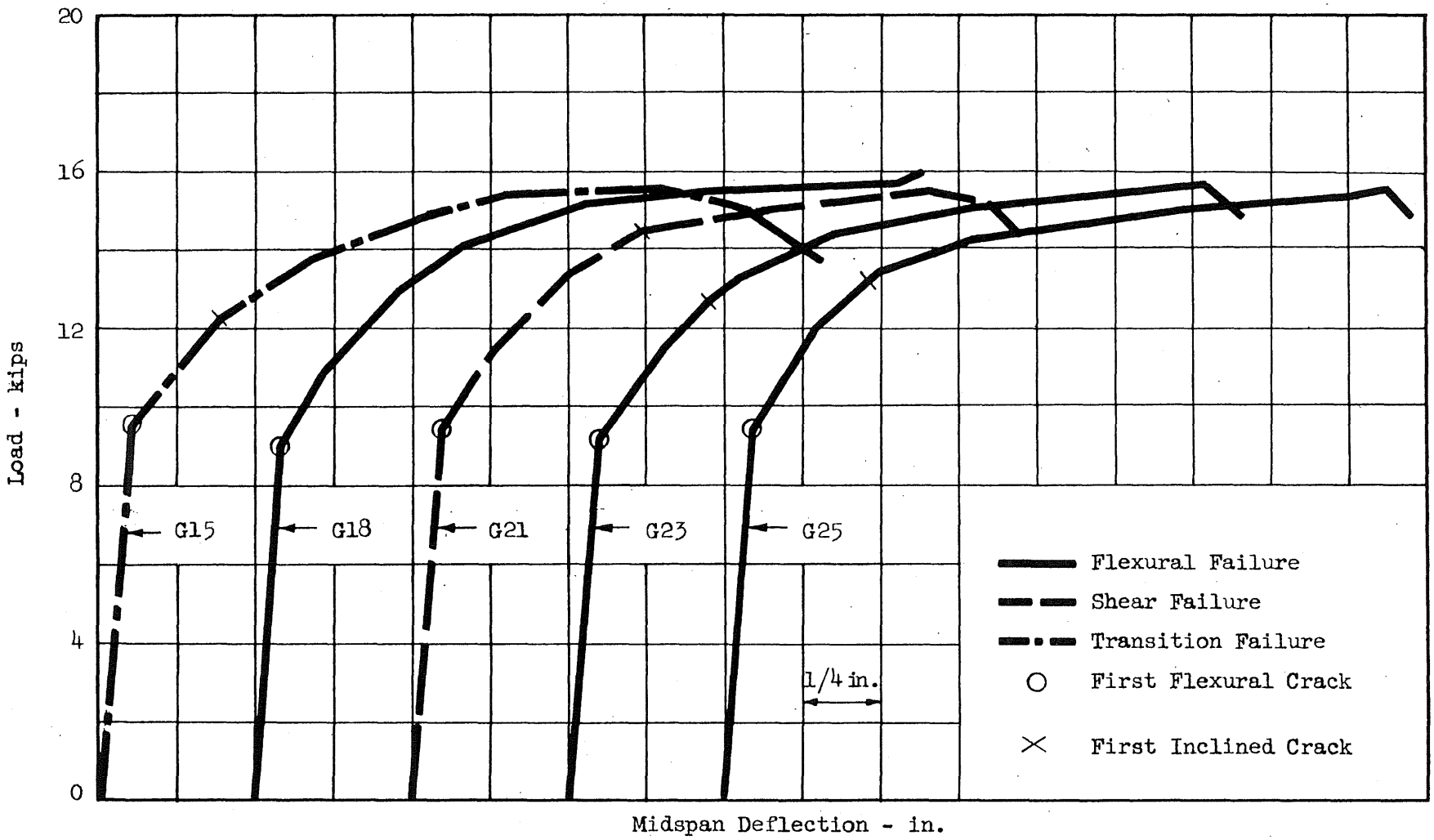

FIG. 21 LOAD-DEFLECTION CURVES FOR BEAMS WITH FOUR WIRES

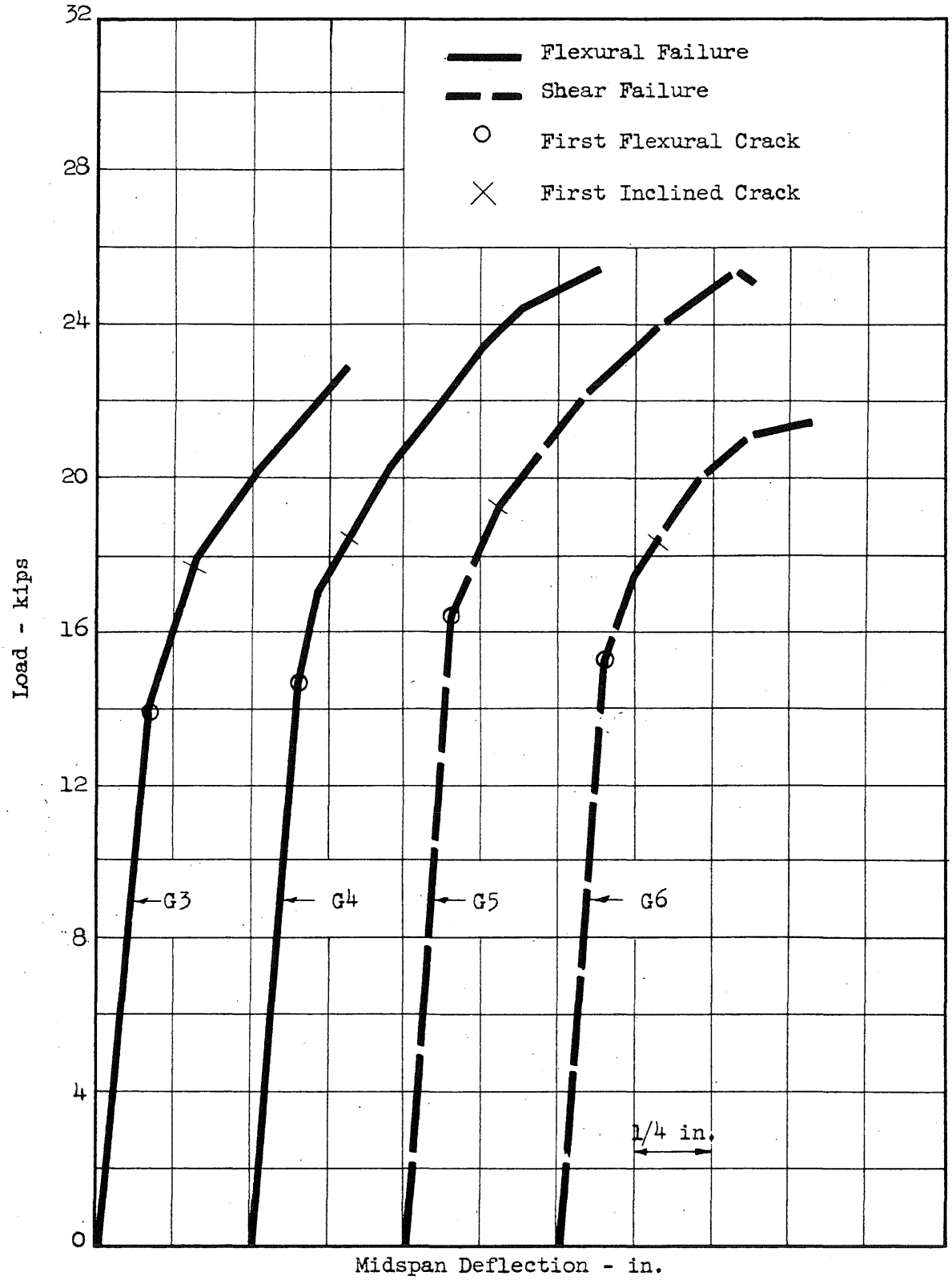

FIG. 22 LOAD-DEFLECTION CURVES FOR BEAMS WITH EIGHT WIRES AND 36-IN. SHEAR SPANS

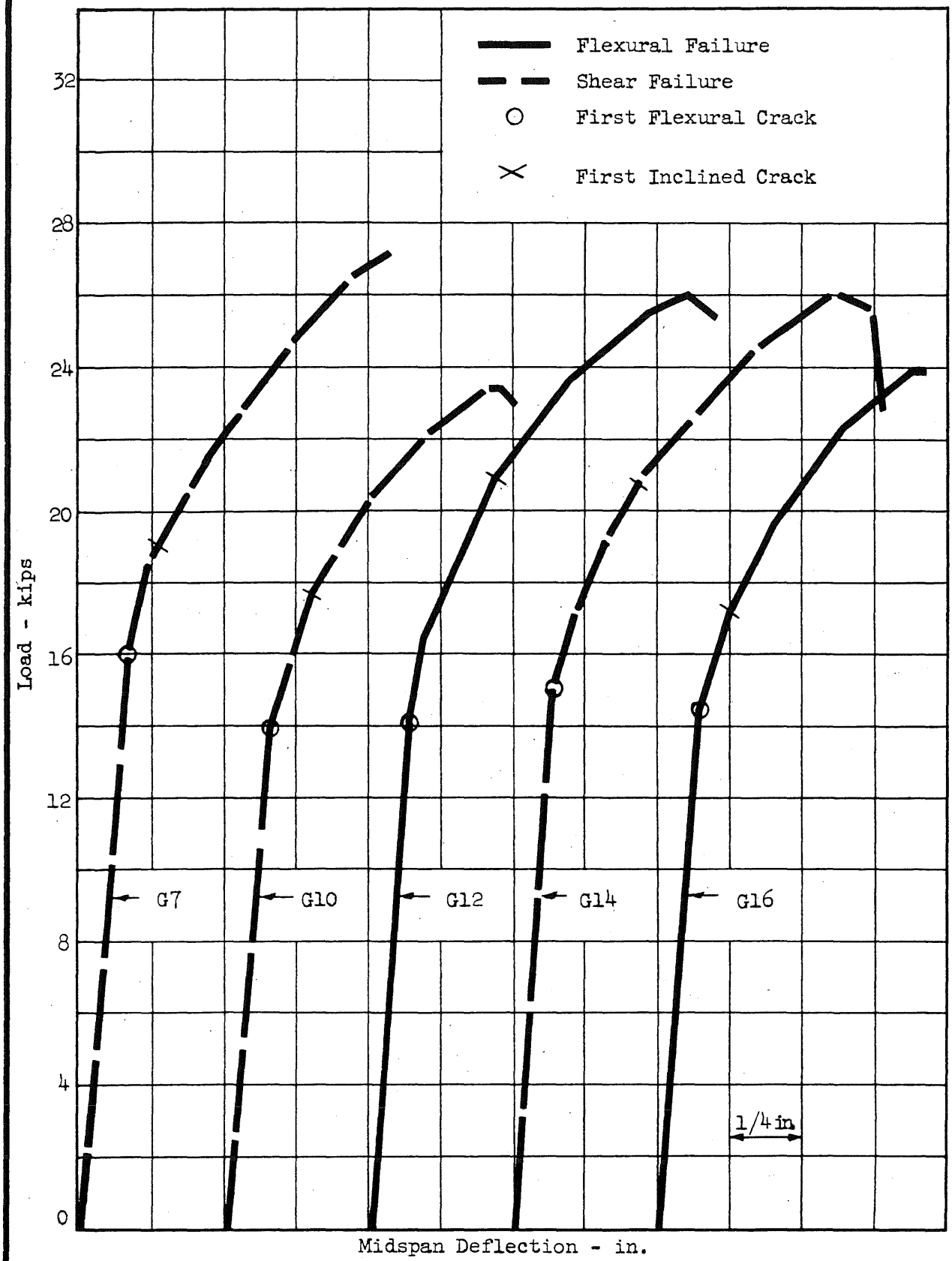

FIG. 23 LOAD-DEFLECTION CURVES FOR BEAMS WITH EIGHT WIRES AND 36-IN. SHEAR SPANS

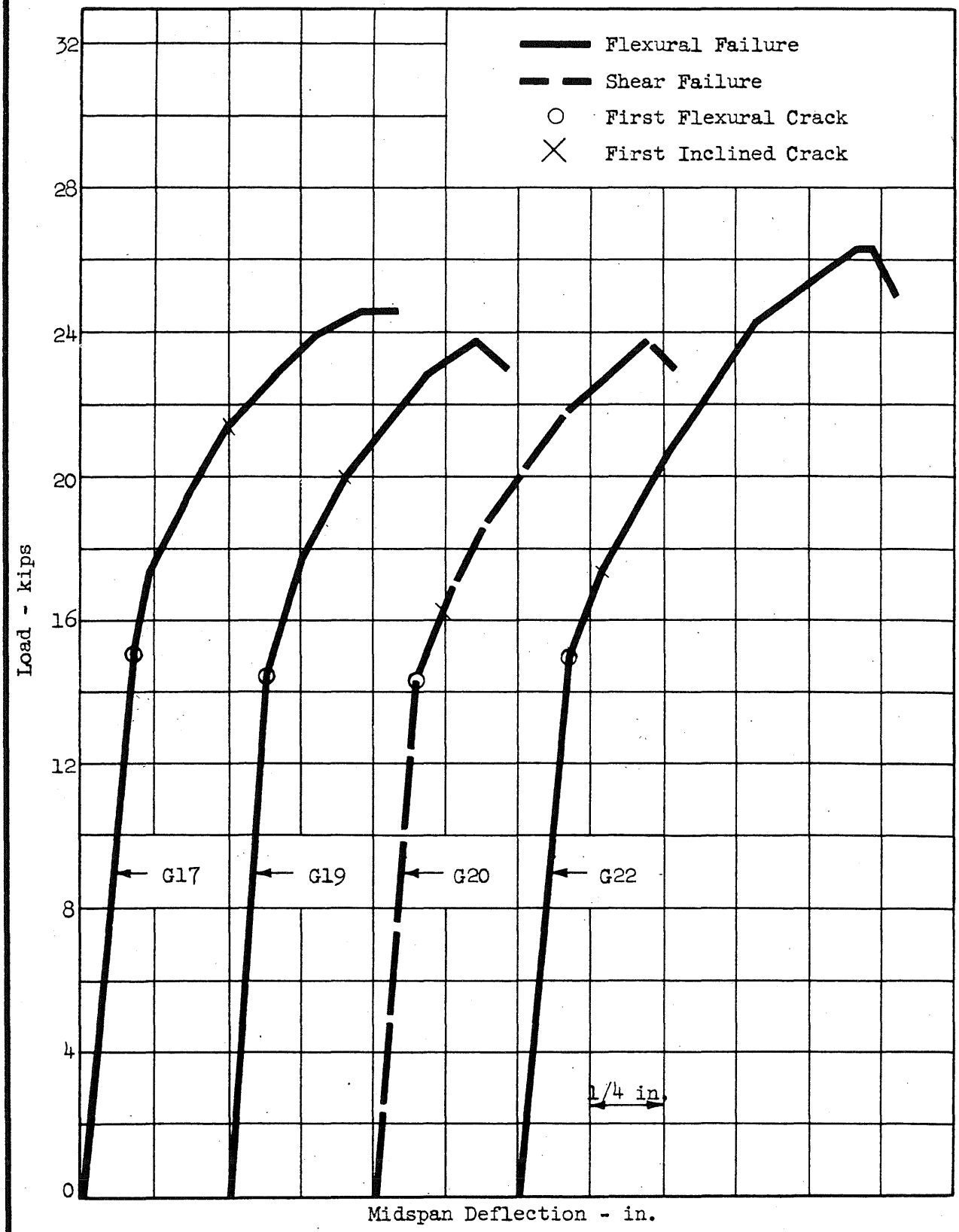

FIG. 24 LOAD-DEFLECTION CURVES FOR BEAMS WITH EIGHT WIRES AND 36-IN. SHEAR SPANS

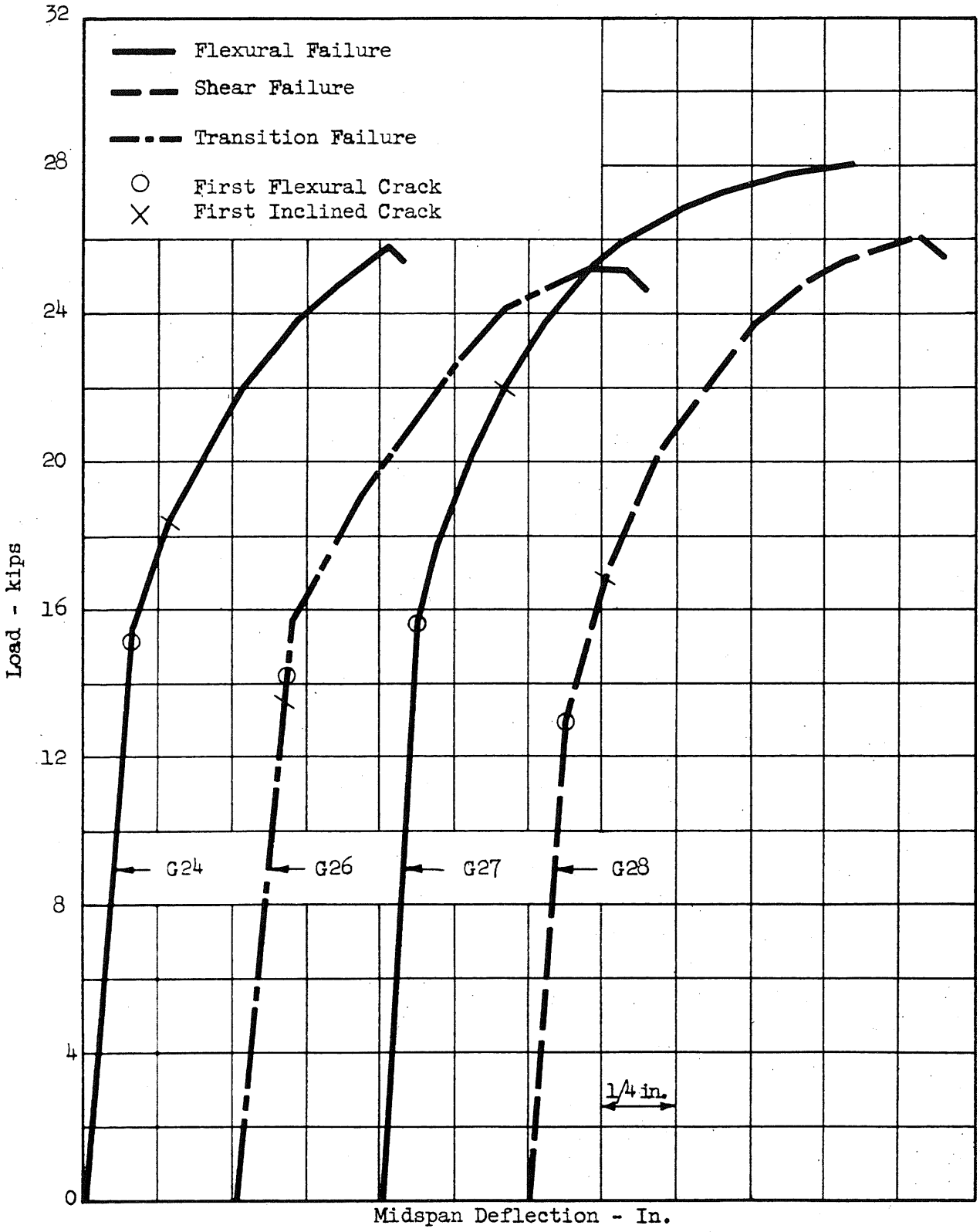

FIG. 25 LOAD-DEFLECTION CURVES FOR BEAMS WITH EIGHT WIRES AND 36-IN. SHEAR SPANS

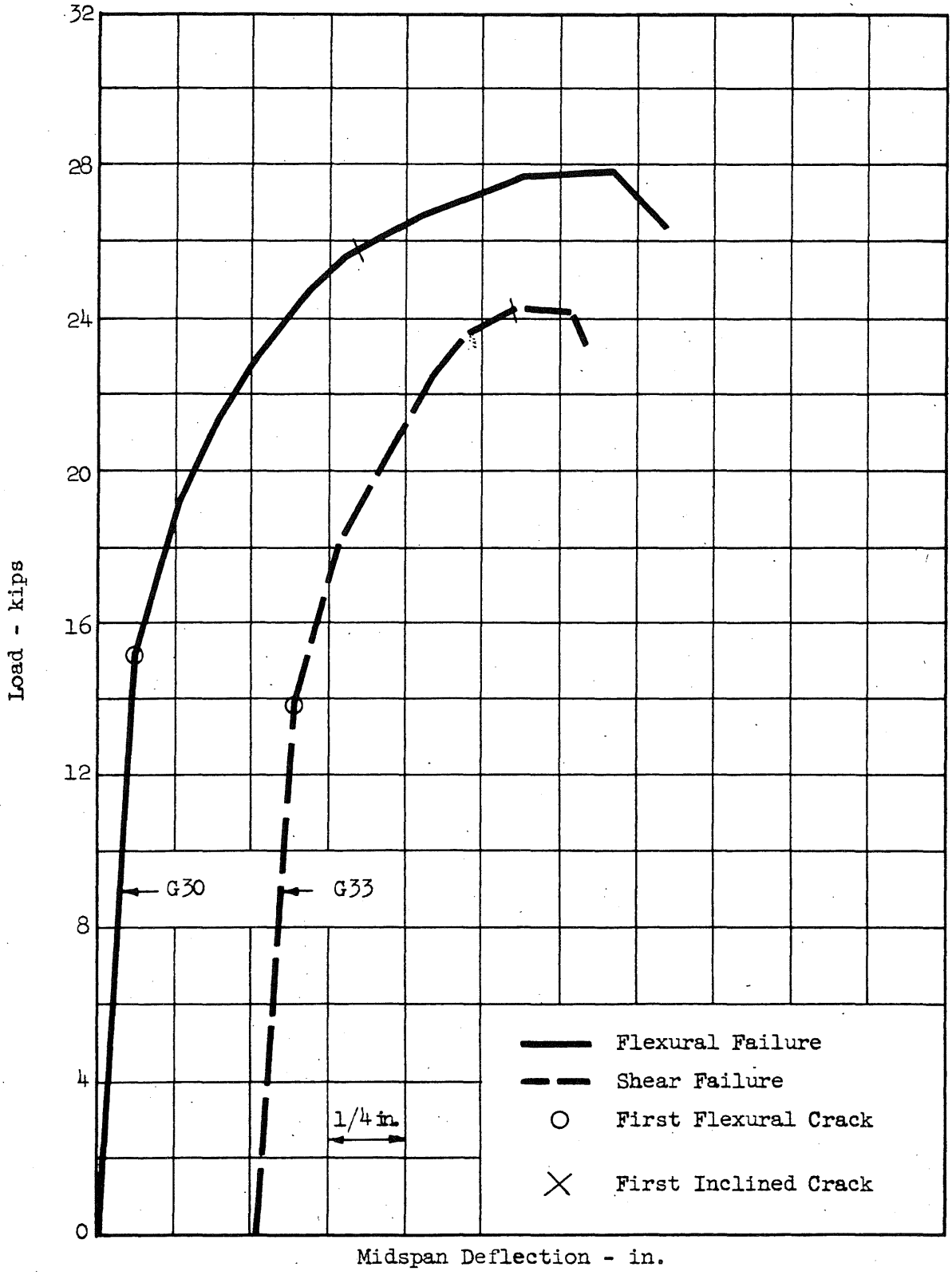

FIG. 26 LOAD-DEFLECTION CURVES FOR BEAMS WITH EIGHT WIRES AND 36-IN. SHEAR SPANS

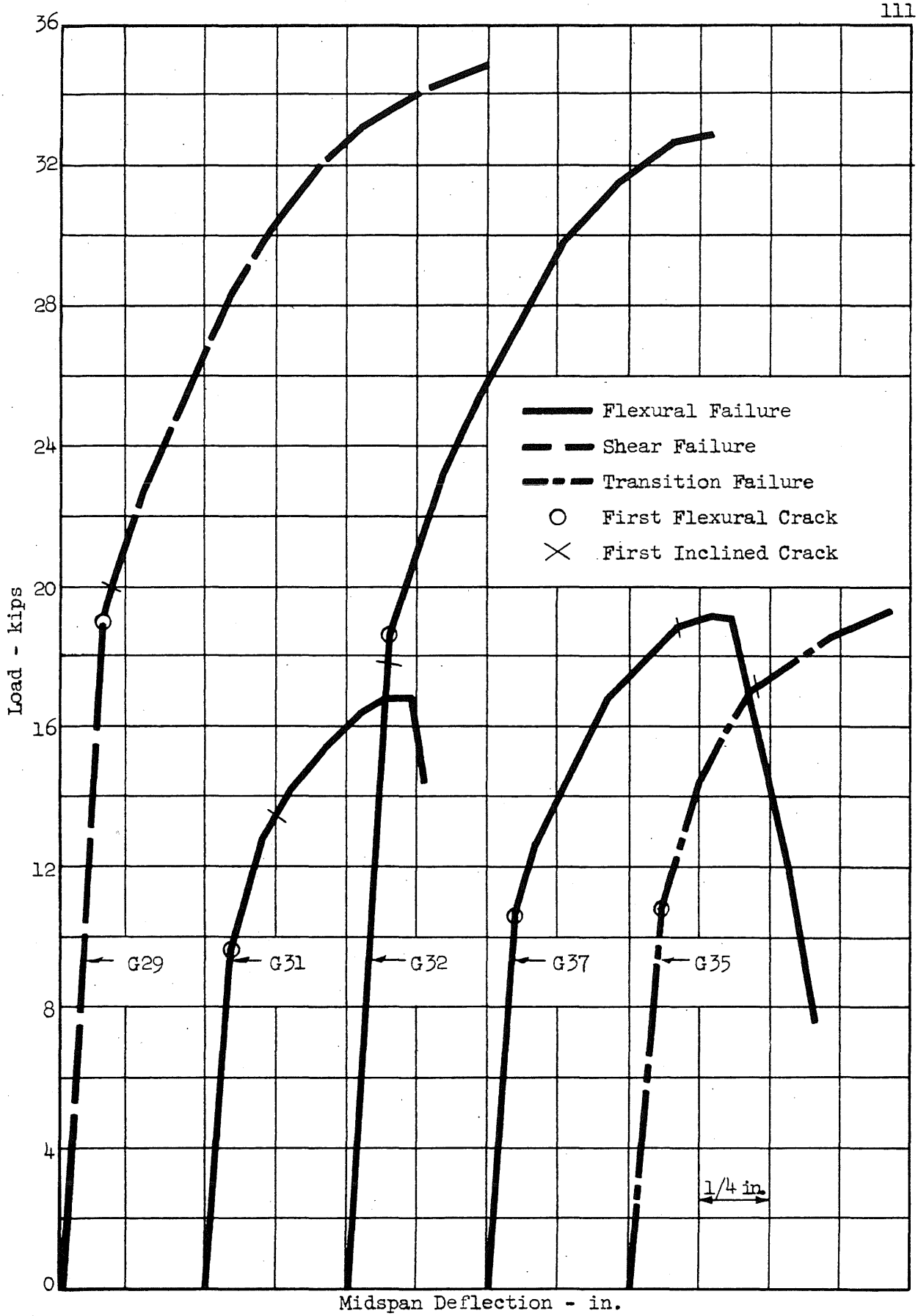

FIG. 27 LOAD-DEFLECTION CURVES FOR BEAMS WITH EIGHT WIRES AND VARIOUS SHEAR SPANS

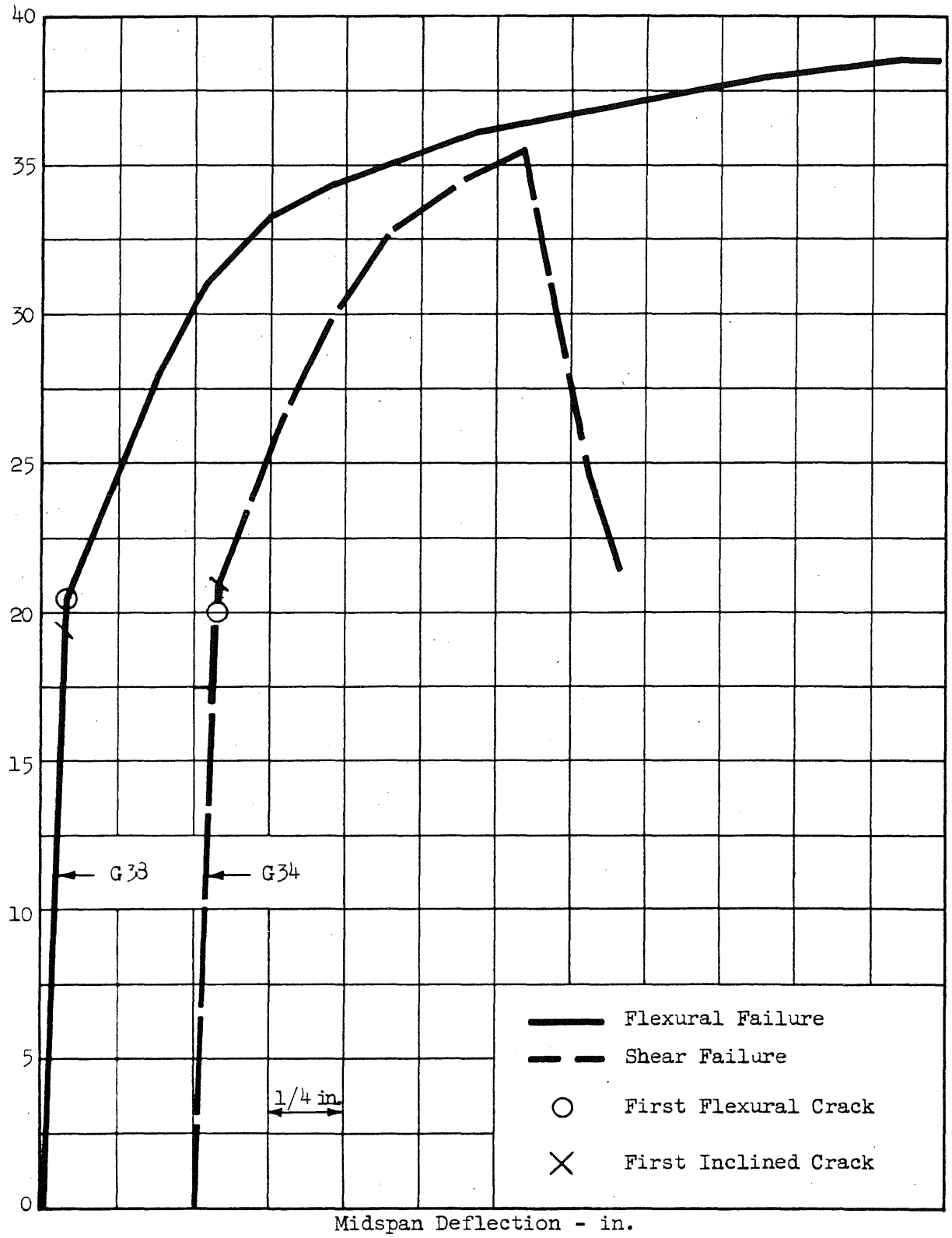

FIG. 28 LOAD-DEFLECTION CURVES FOR BEAMS WITH CAST-IN-PLACE SLABS

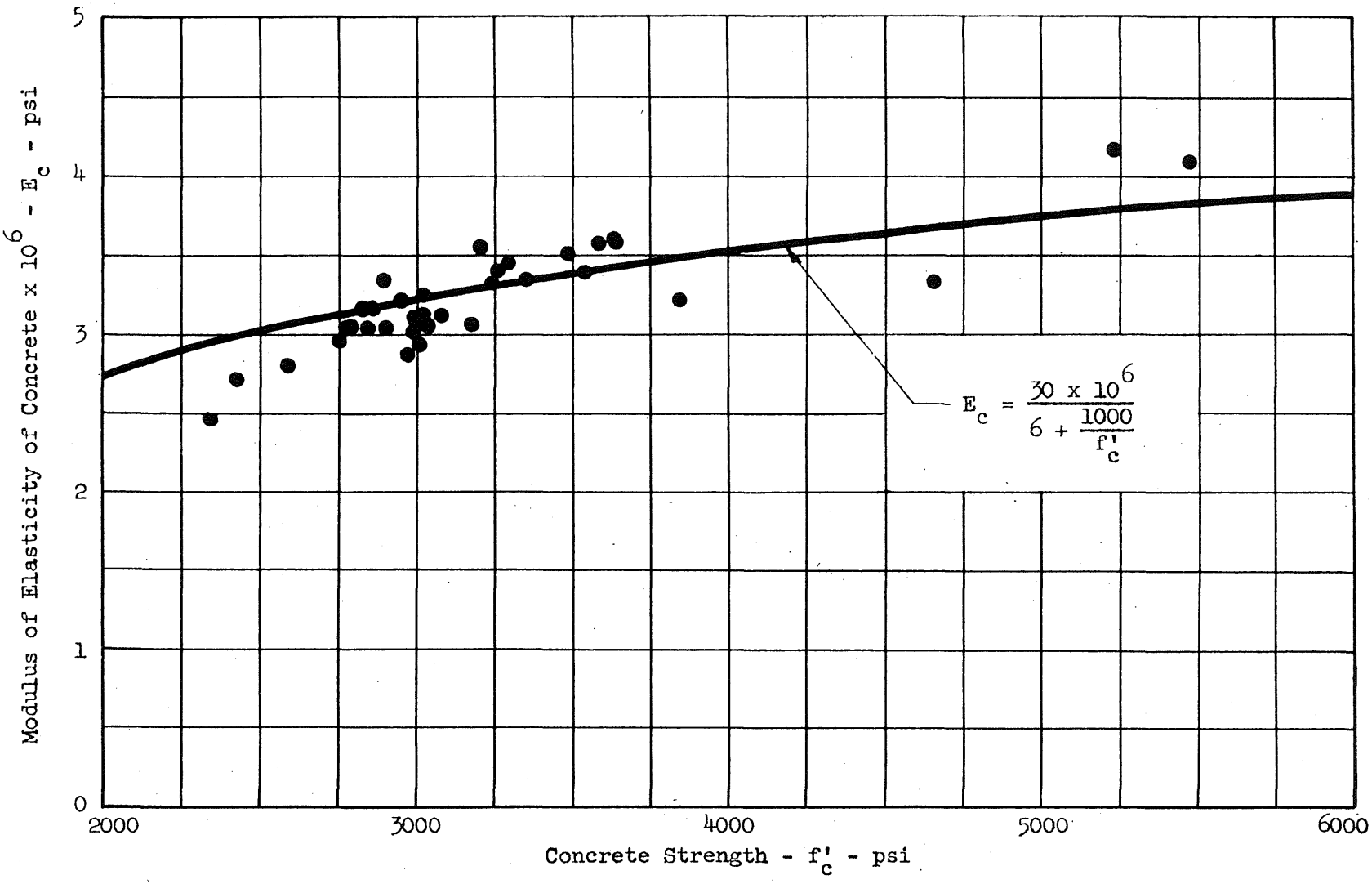

FIG. 29 RELATIONSHIP BETWEEN MODULUS OF ELASTICITY AND CONCRETE STRENGTH

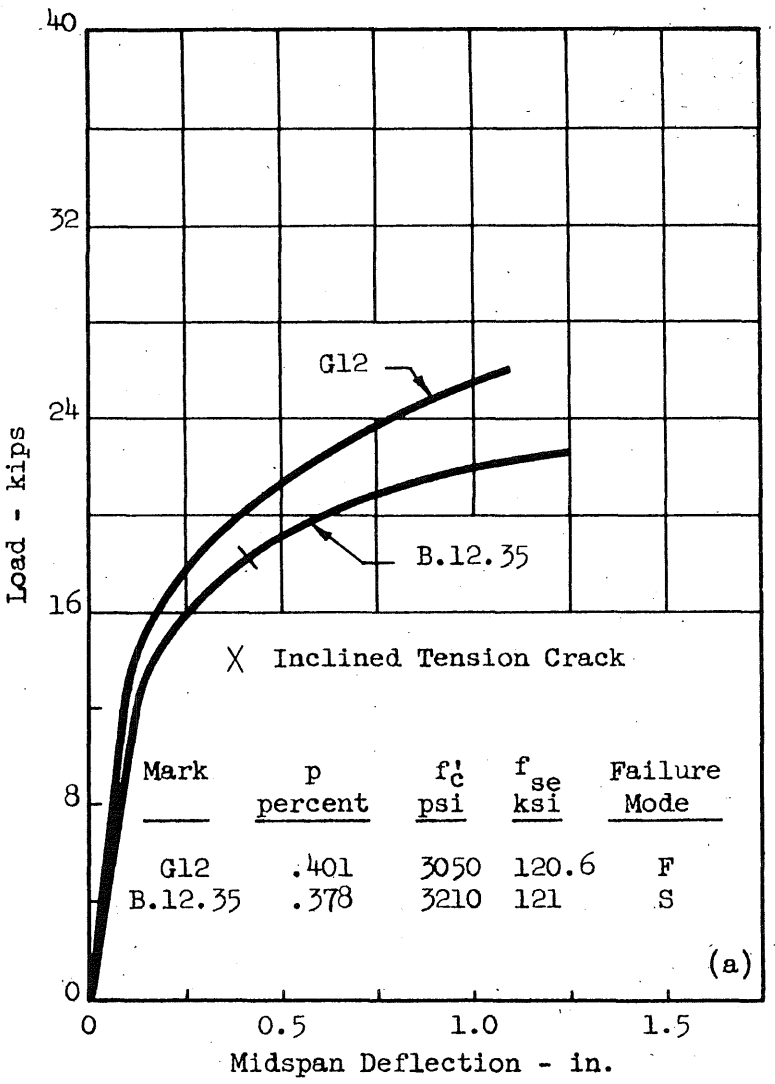

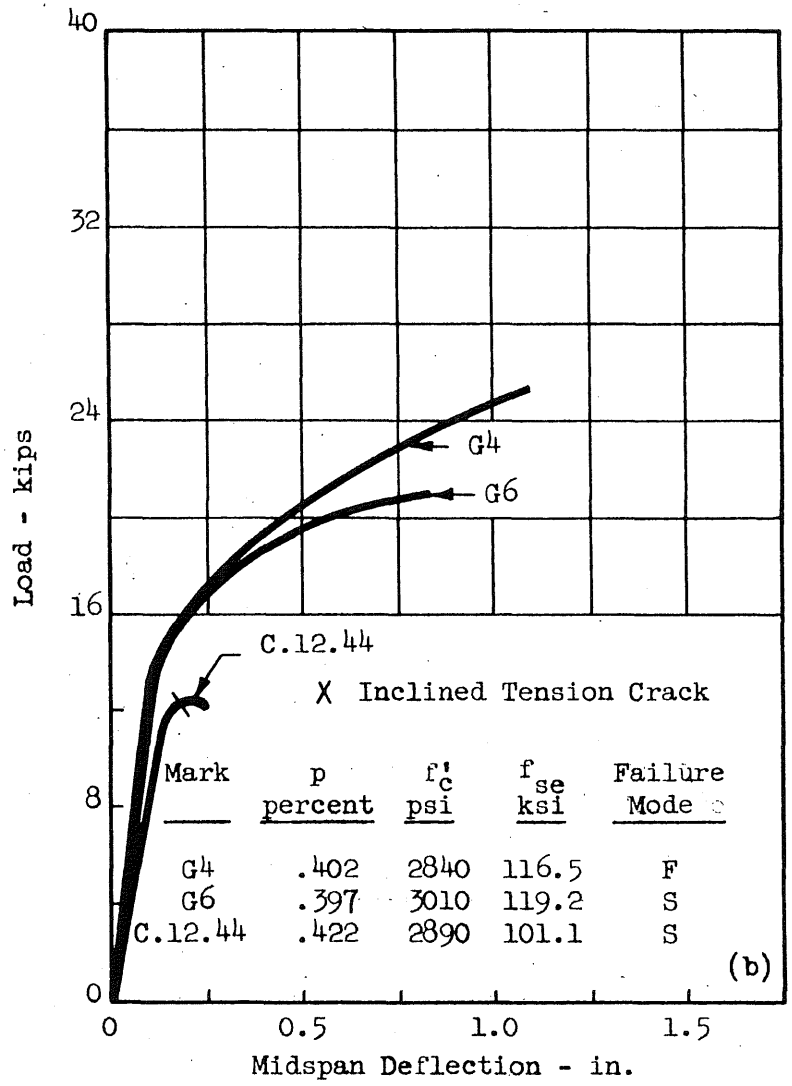

FIG. 30 COMPARISON OF LOAD DEFLECTION CURVES FOR BEAMS WITH AND WITHOUT WEB REINFORCEMENT

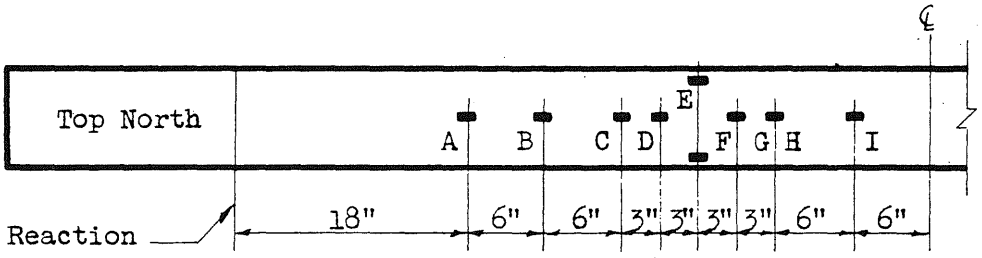

Beam G15

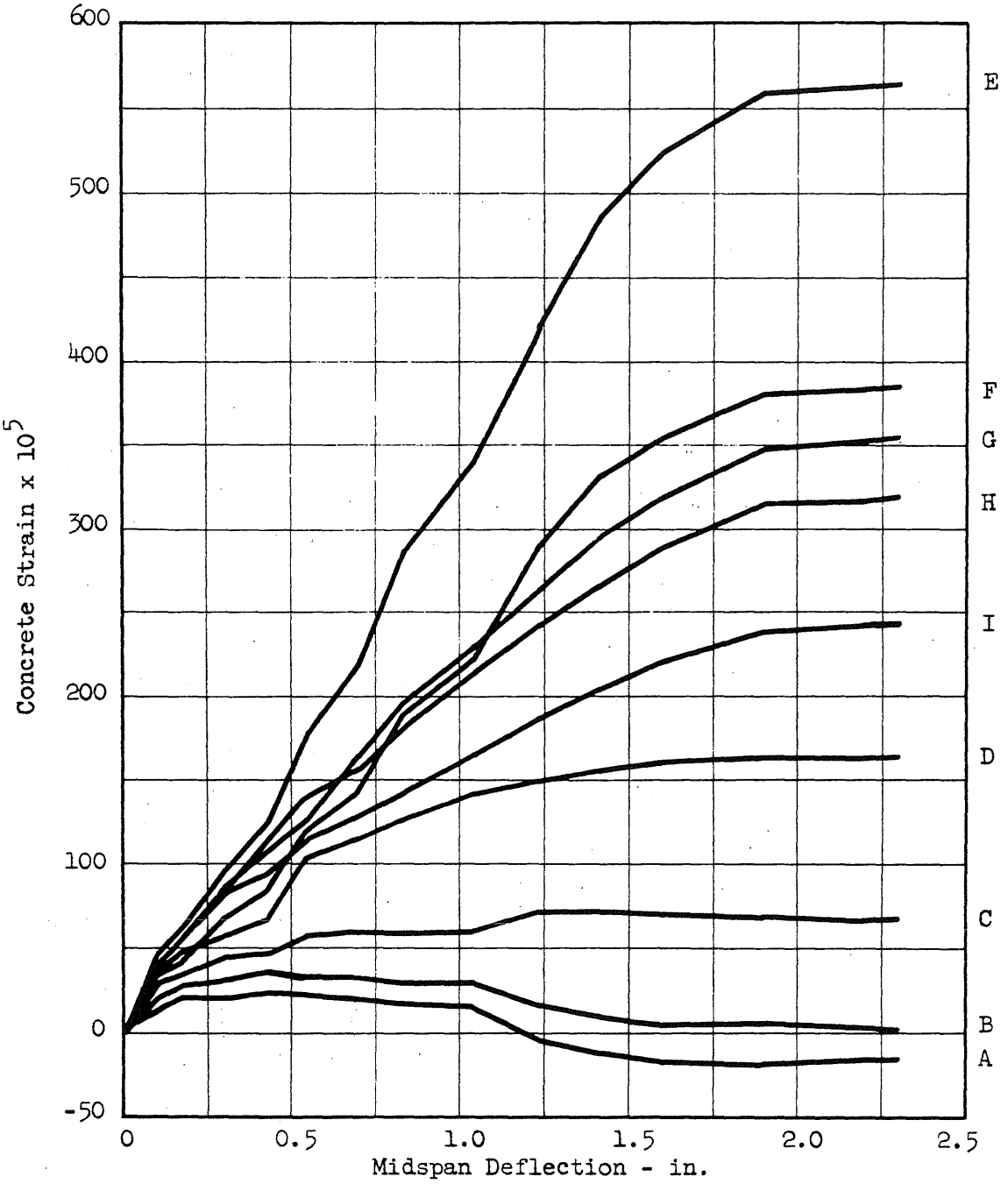

FIG. 31 RELATIONSHIP BETWEEN CONCRETE STRAINS AND DEFLECTIONS

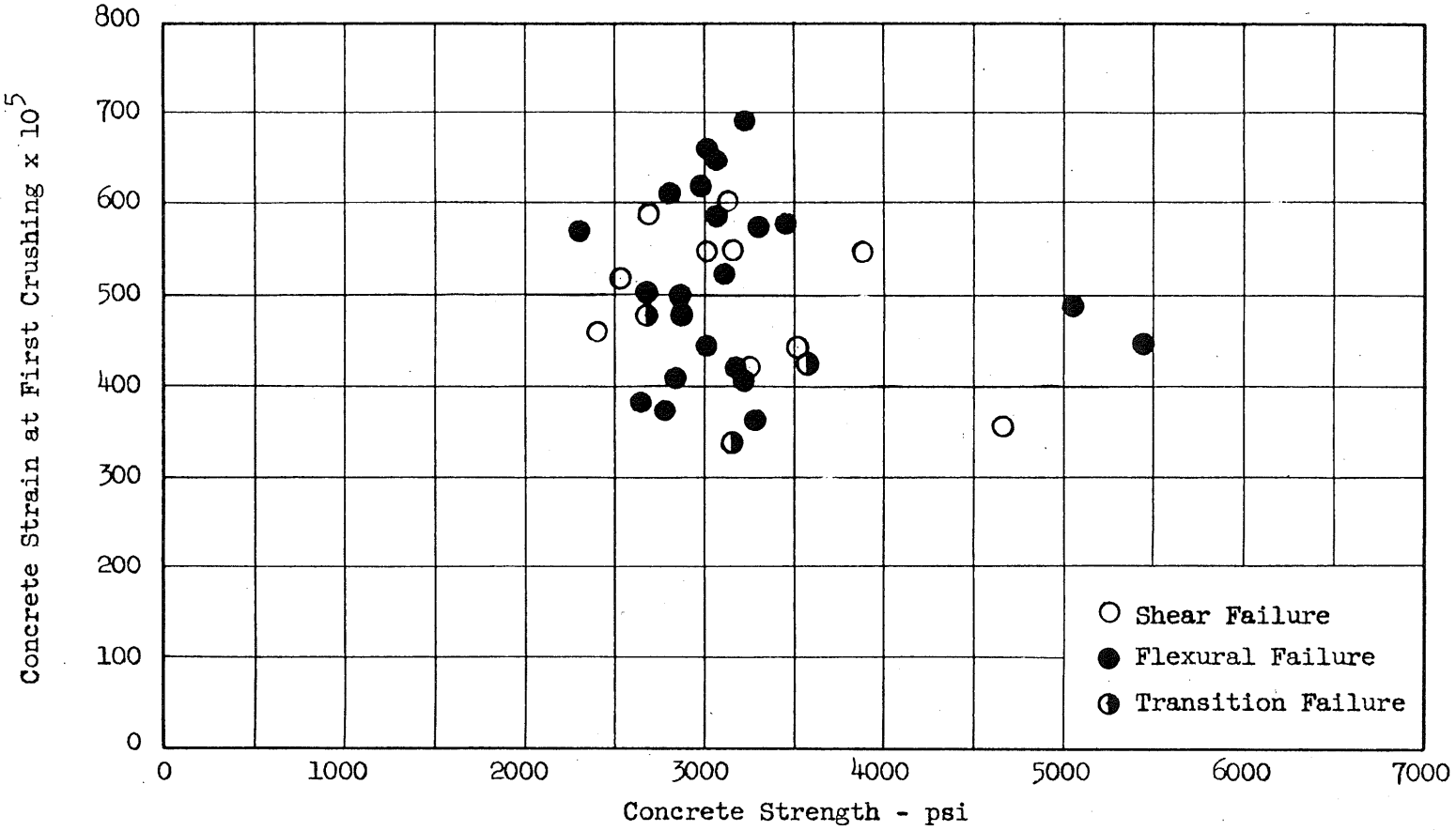

FIG. 32 MEASURED VALUES OF CONCRETE STRAIN AT FIRST CRUSHING

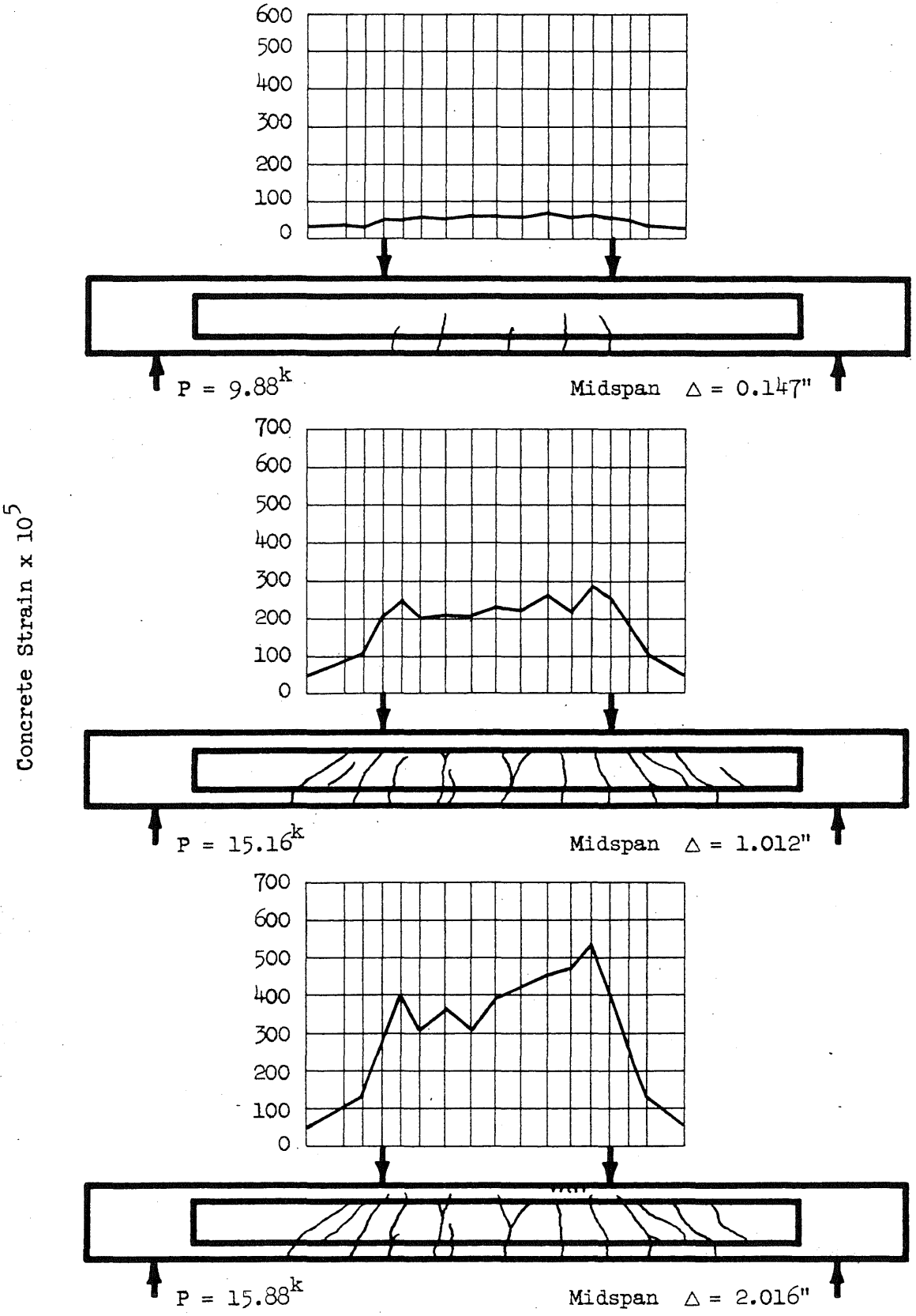

FIG. 33 CRACK PATTERNS AND CORRESPONDING DISTRIBUTIONS OF STRAIN ON TOP SURFACE OF BEAM G2

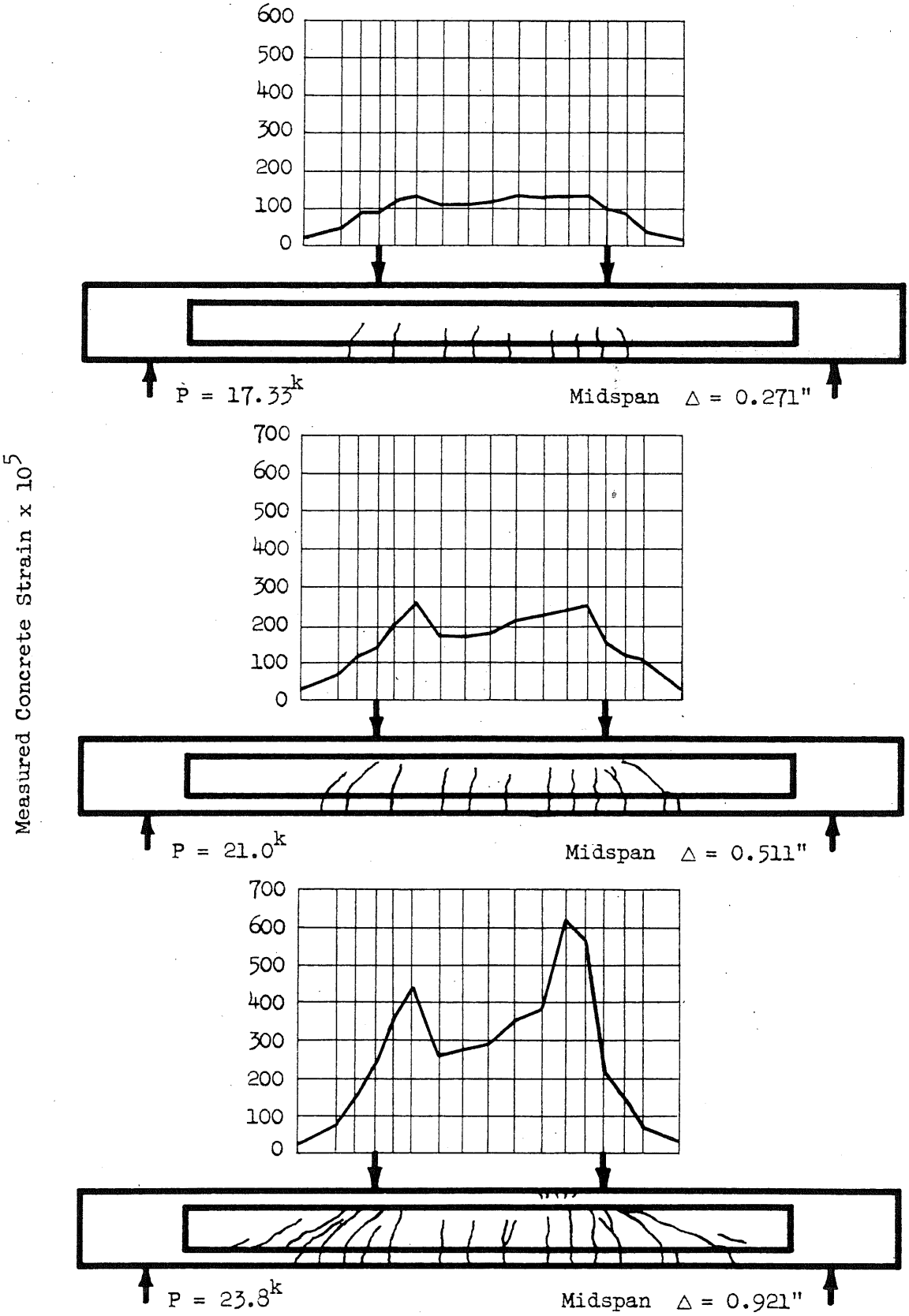

FIG. 34 CRACK PATTERNS AND CORRESPONDING DISTRIBUTIONS OF STRAINS ON TOP SURFACE OF BEAM G16

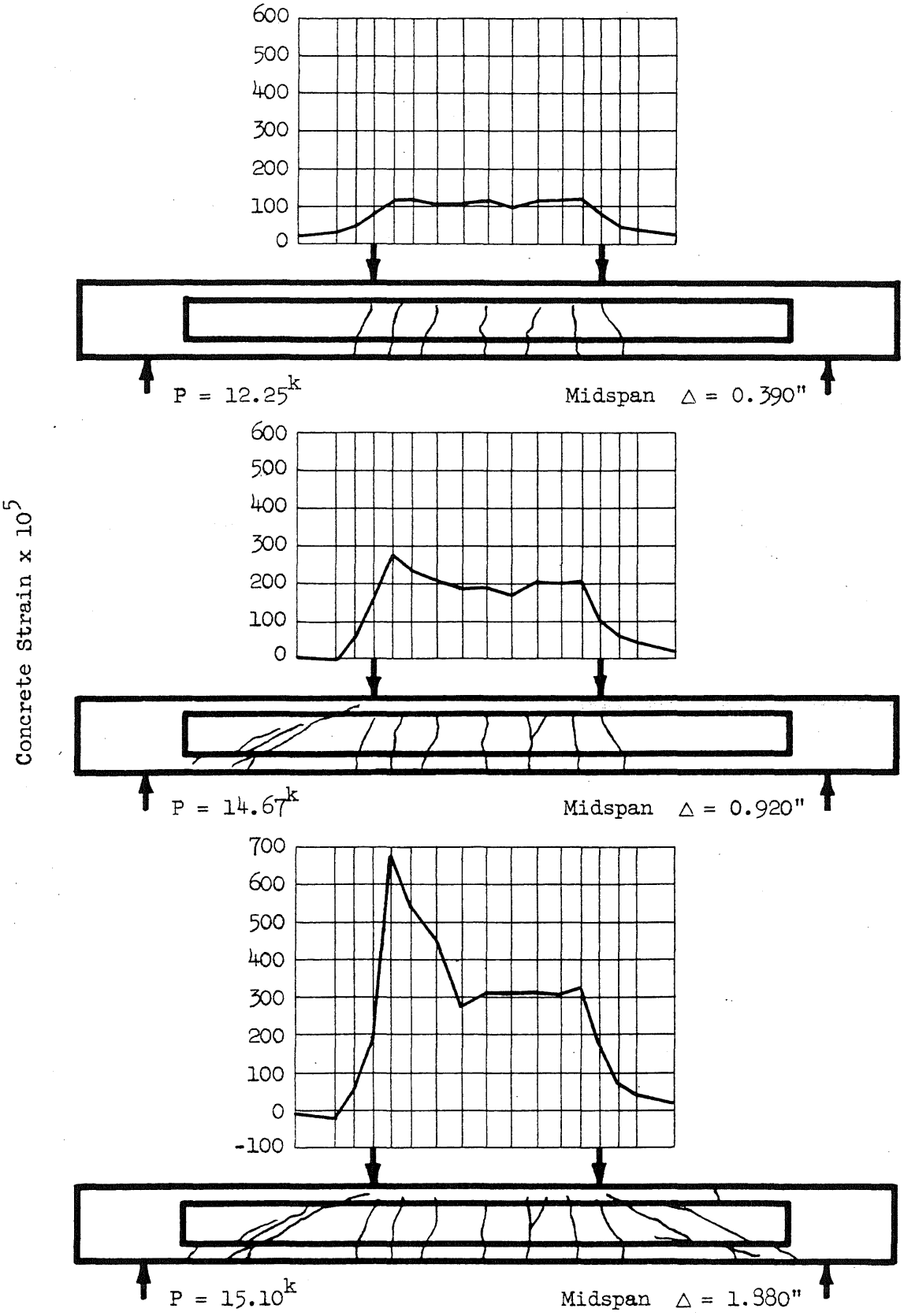

FIG. 35 CRACK PATTERNS AND CORRESPONDING DISTRIBUTIONS OF STRAINS ON TOP SURFACE OF BEAM G21

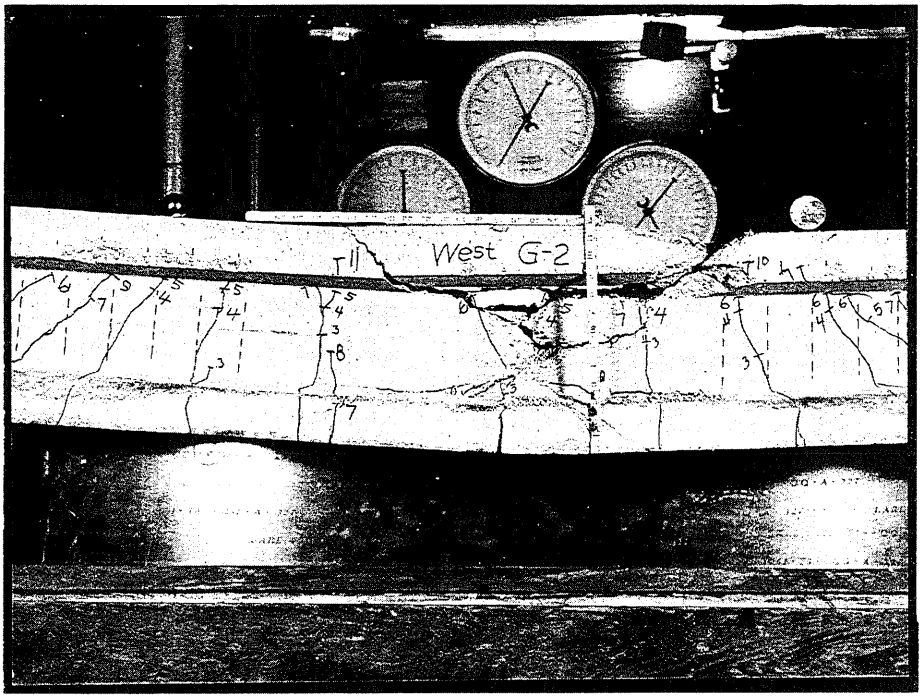

FIG. 36 FLEXURAL FAILURE IN A BEAM WITH FOUR WIRES AND WITHOUT STIRRUPS BETWEEN THE LOADS

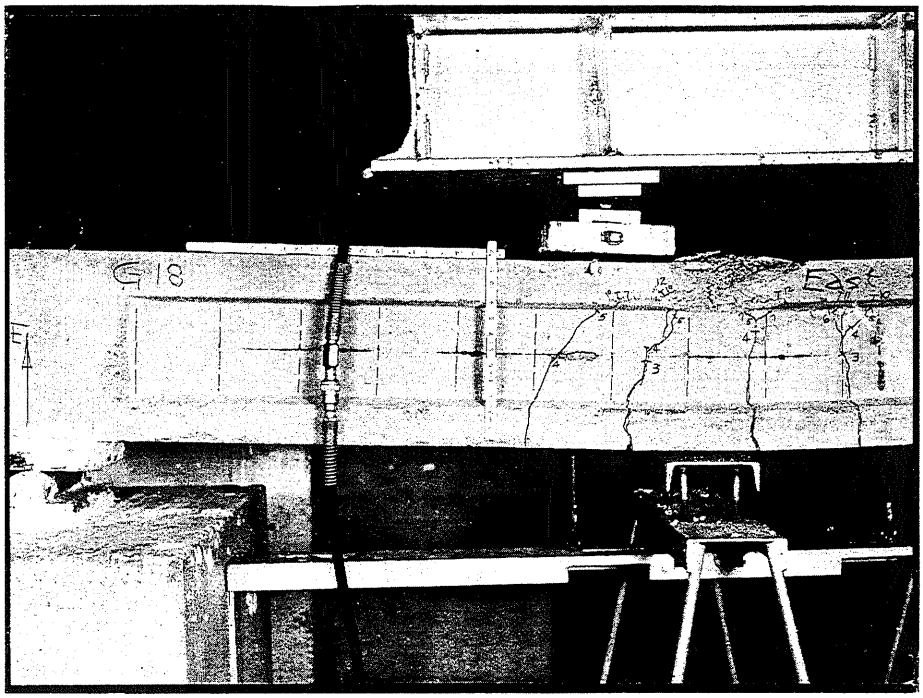

FIG. 37 FLEXURAL FAILURE IN A BEAM WITH FOUR WIRES AND STIRRUPS THROUGHOUT THE SPAN

FIG. 38 FLEXURAL FAILURE IN A BEAM WITH EIGHT WIRES

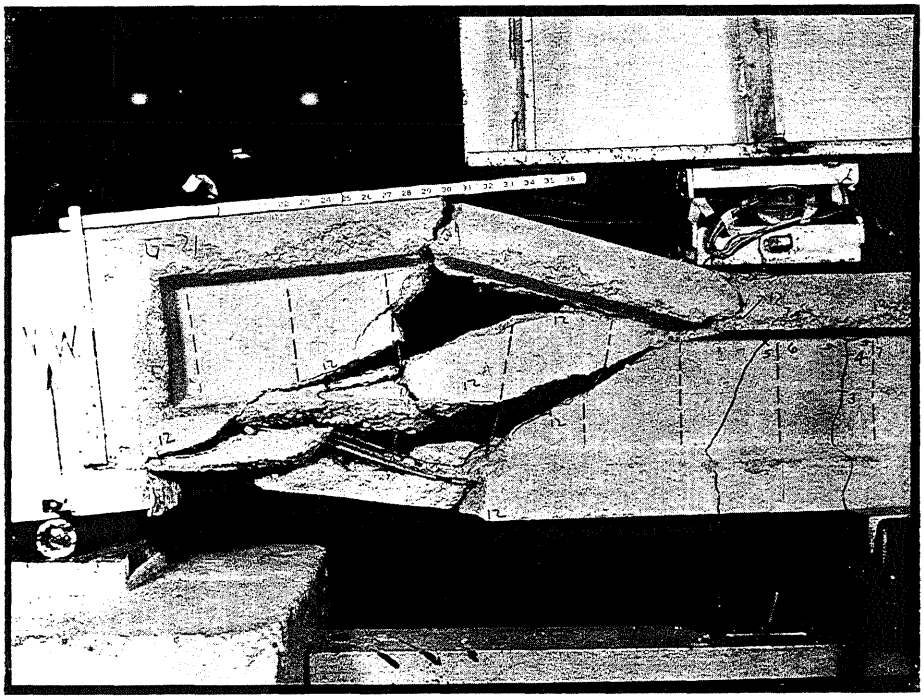

FIG. 39 FAILURE BY SEVERE DISTORTION OF THE WEB

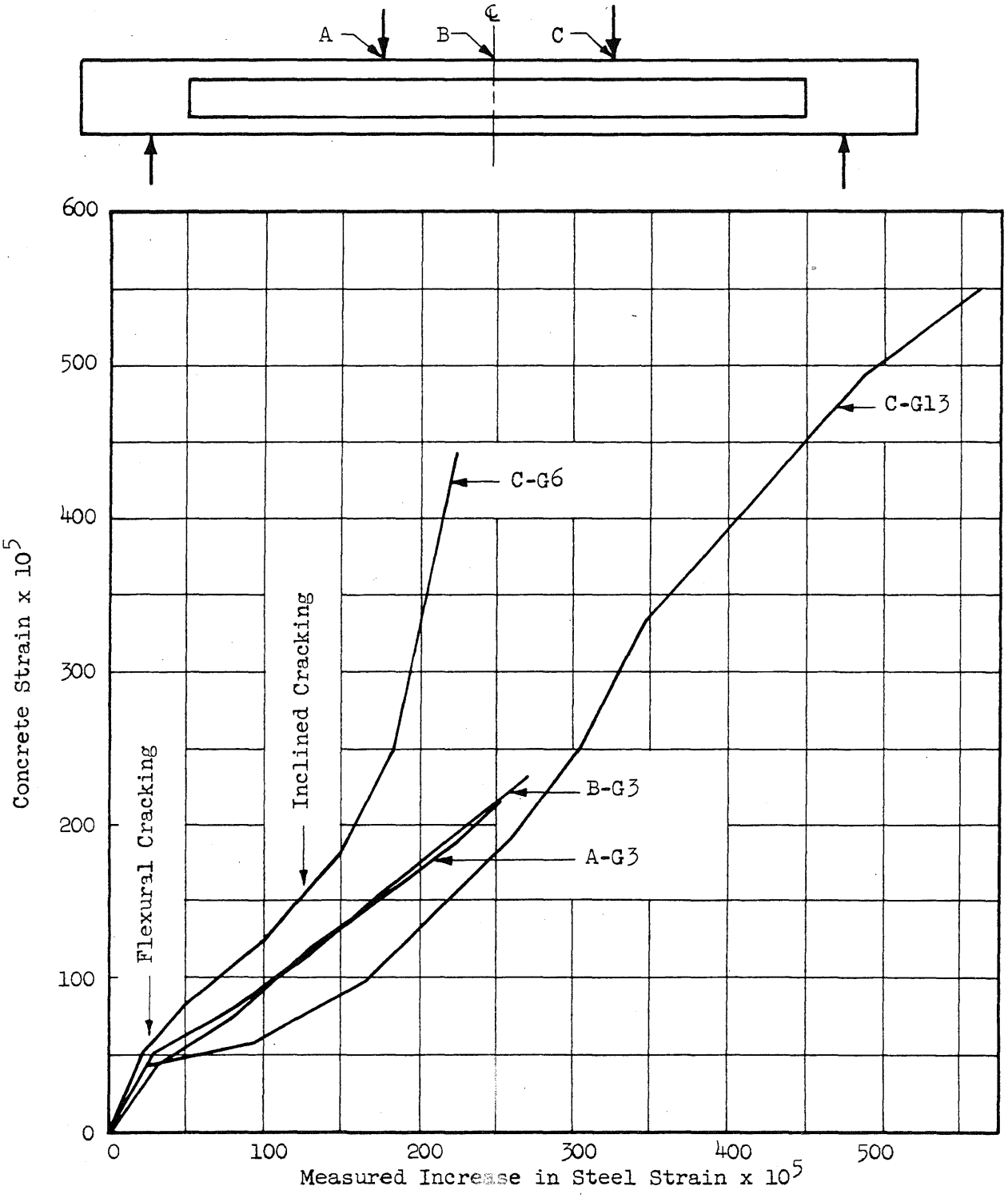

FIG. 40 RELATION BETWEEN CONCRETE AND STEEL STRAINS FOR SHEAR AND FLEXURAL FAILURES

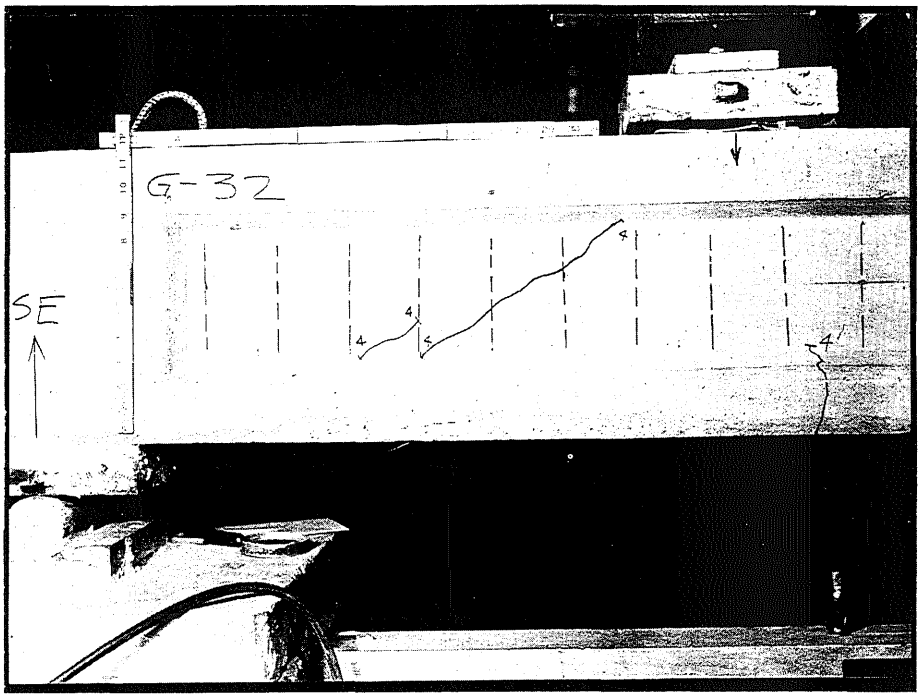

FIG. 41 FORMATION OF INCLINED CRACK IN THE WEB

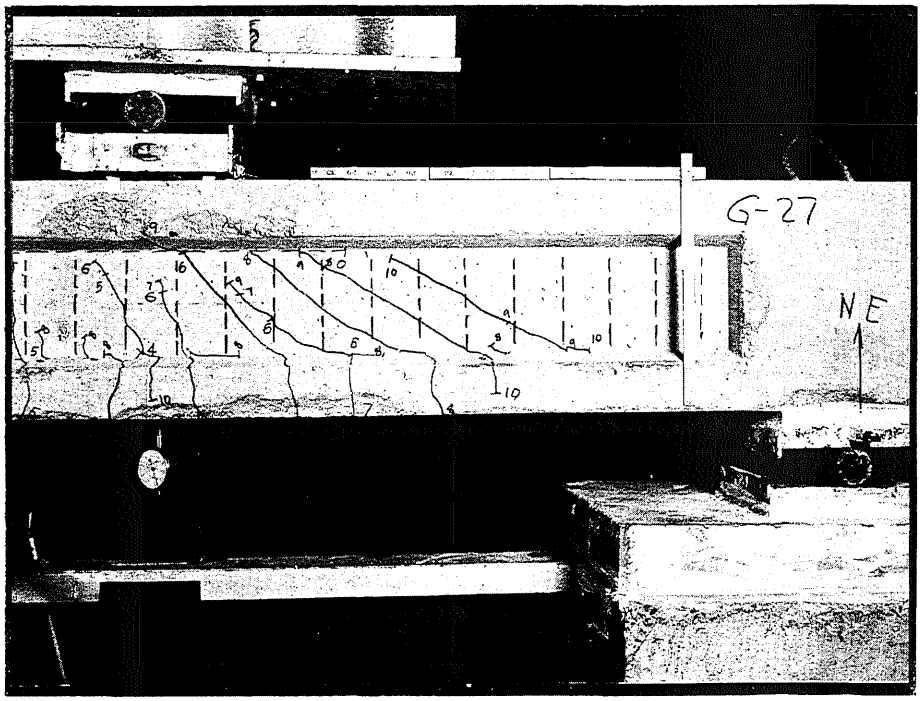

FIG. 42 SUCCESSIVE FORMATION OF INCLINED CRACKS IN A BEAM WITH VERTICAL STIRRUPS

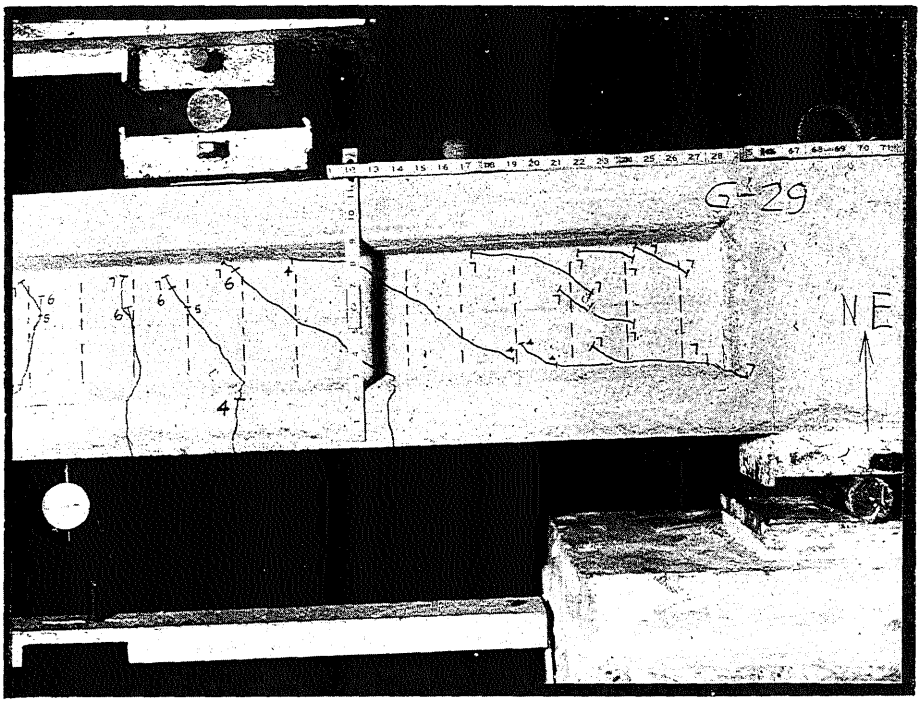

FIG. 43 SECONDARY INCLINED TENSION CRACKING

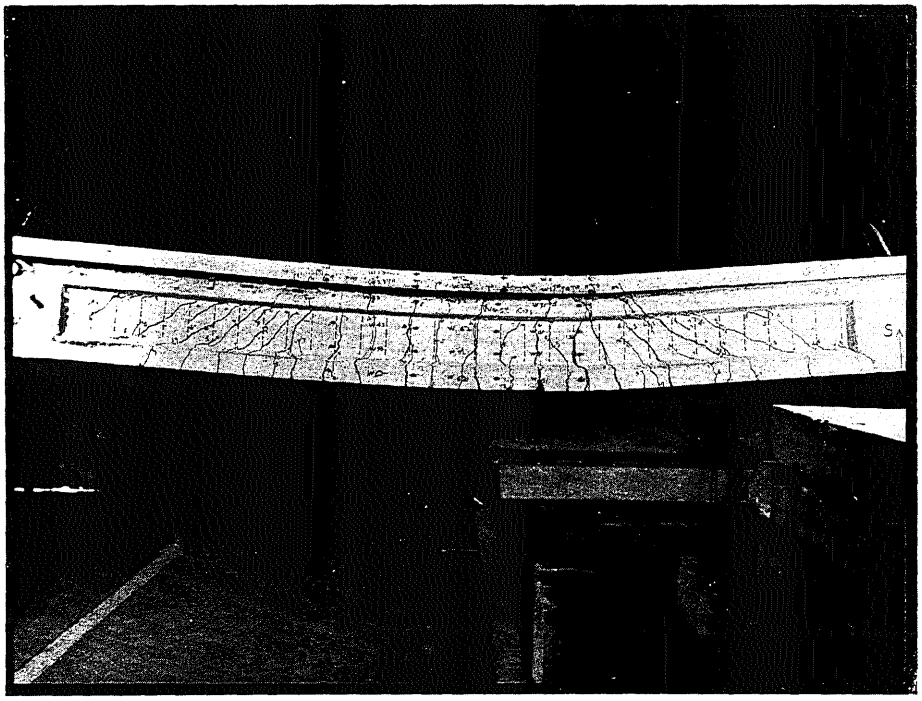

FIG. 44 FLEXURAL FAILURE OF A GREATLY UNDER-REINFORCED BEAM

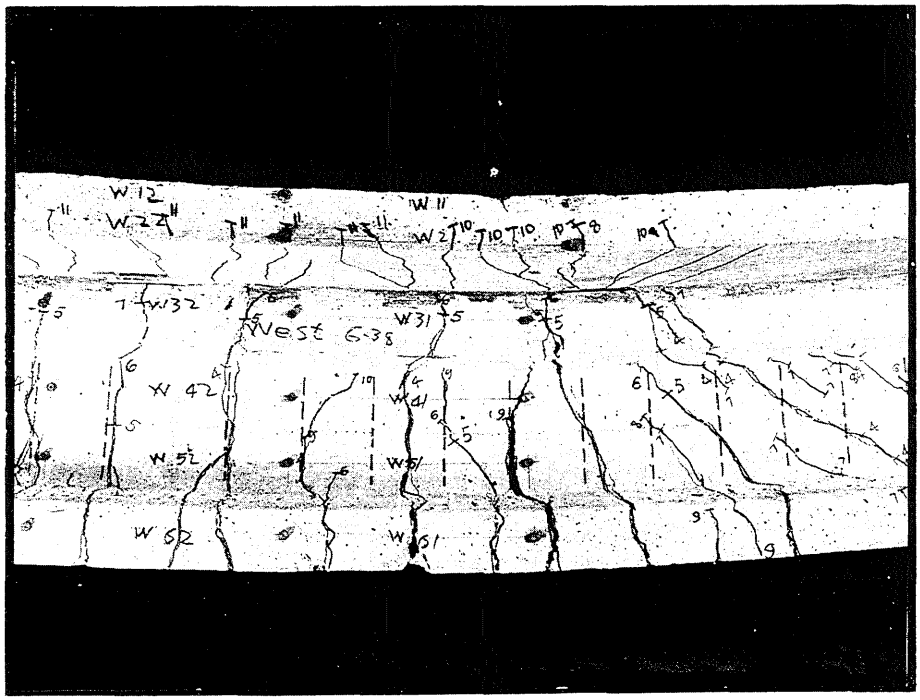

FIG. 45 WELL-DEVELOPED FLEXURAL CRACKS, BEAM G38

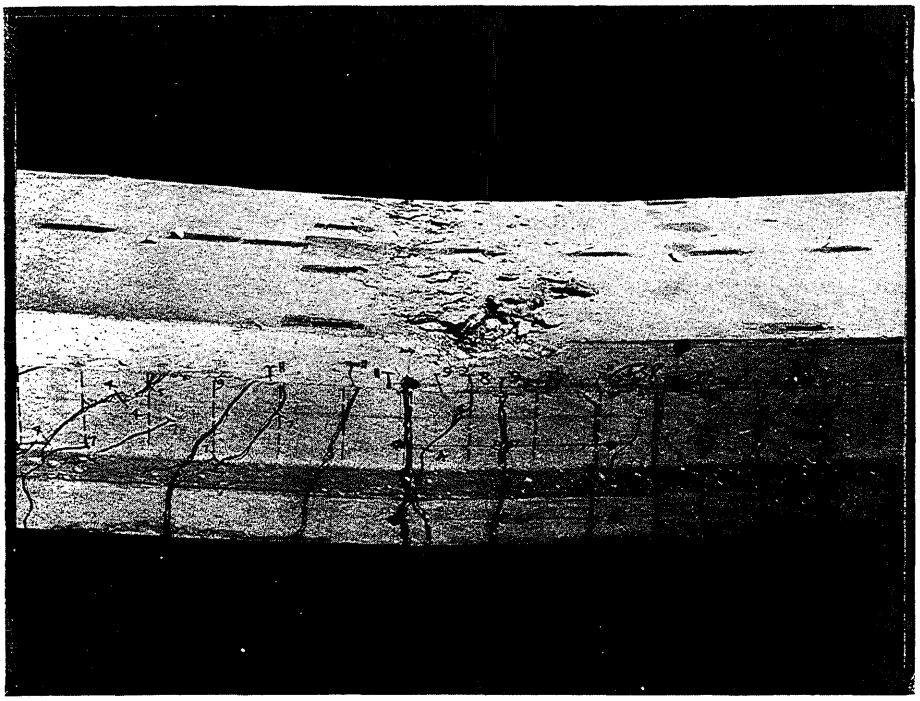

FIG. 46 CRUSHING OF CONCRETE IN THE SLAB, BEAM G38

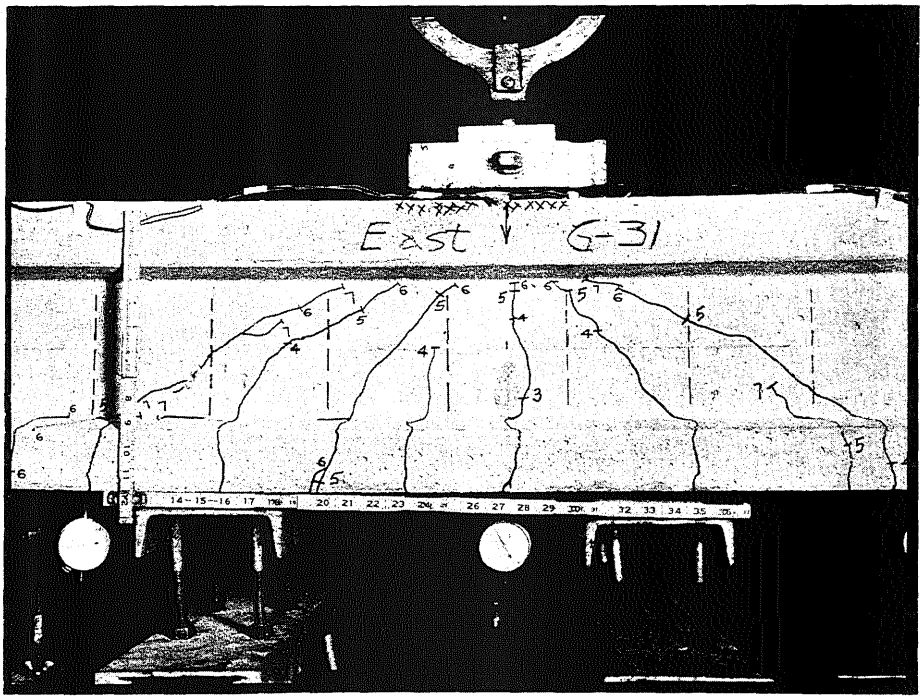

FIG. 47 BEAM G31 AFTER THE INITIATION OF CRUSHING IN THE TOP FLANGE

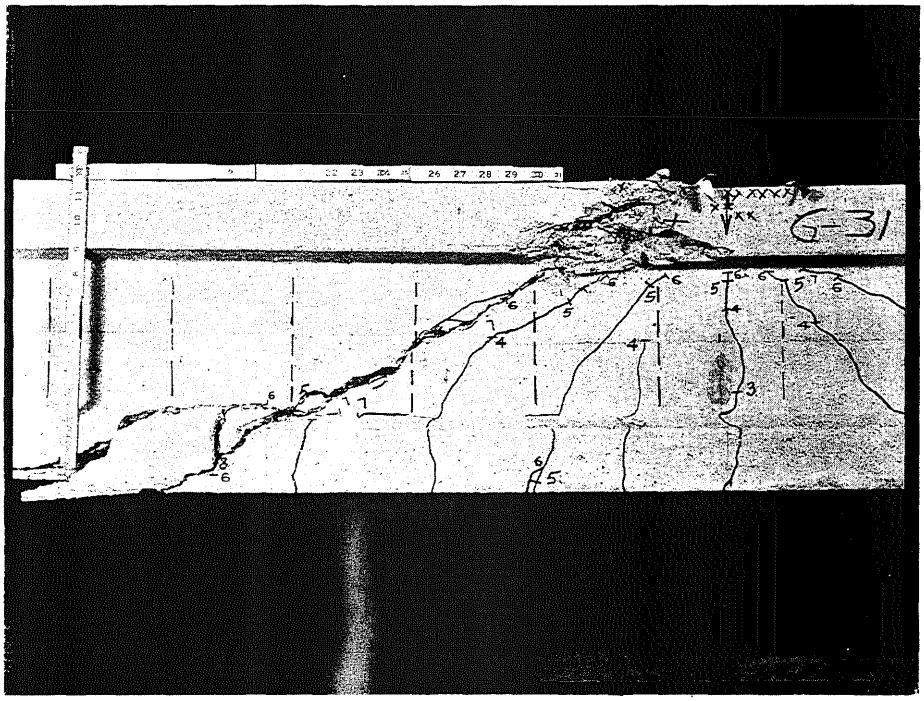

FIG. 48 BEAM G31 AFTER COLLAPSE

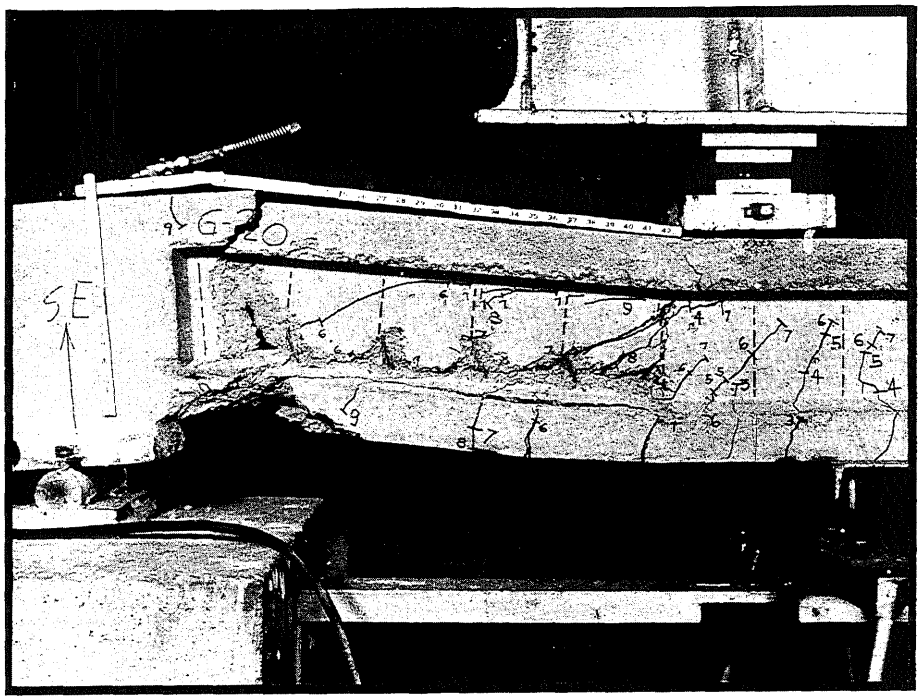

FIG. 49 TYPICAL FAILURE BY CRUSHING OF THE WEB

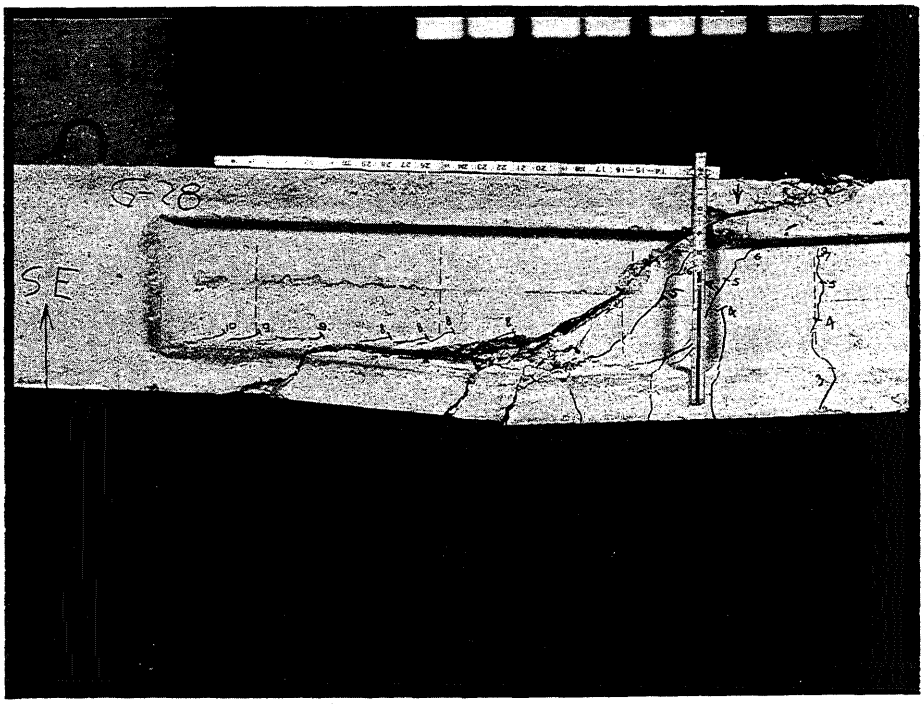

FIG. 50 SHEAR-COMPRESSION FAILURE

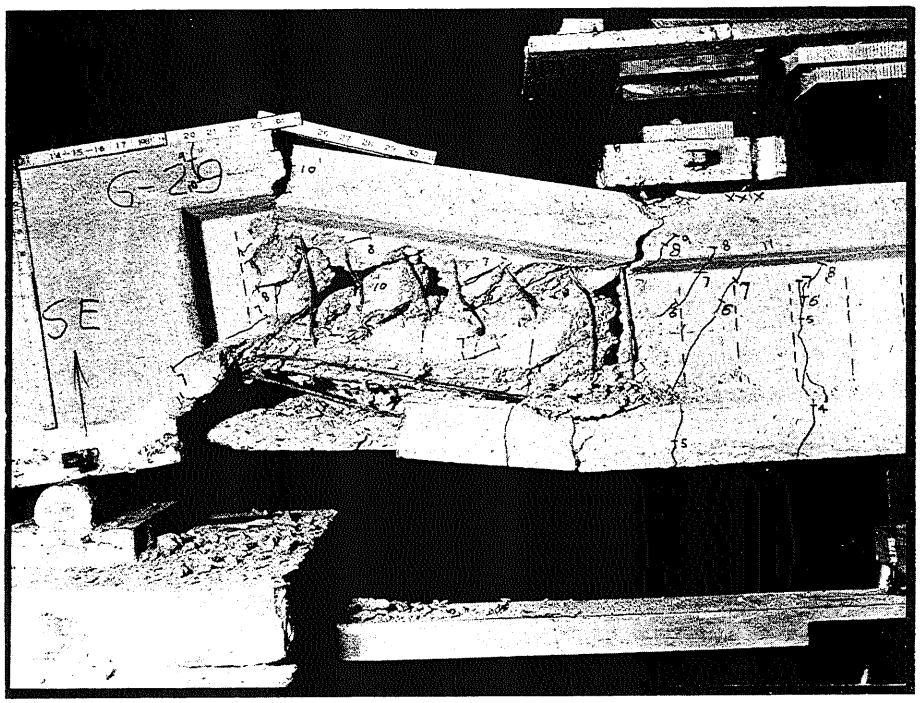

FIG. 51 SHEAR FAILURE OF A BEAM WITH EIGHT WIRES AND A SHORT SHEAR SPAN

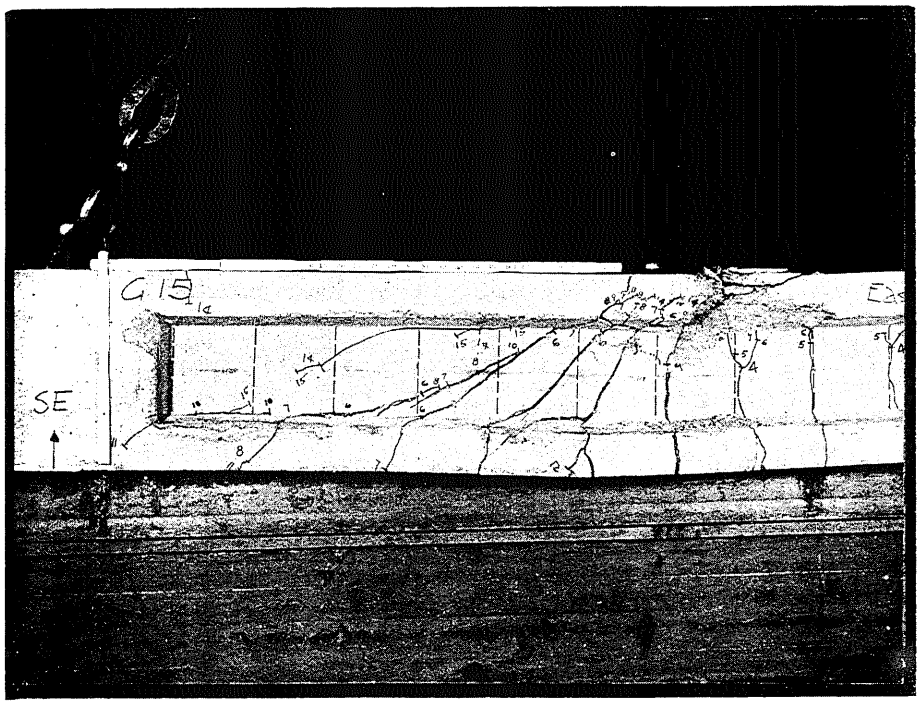

FIG. 52 TRANSITION FAILURE, BEAM G15

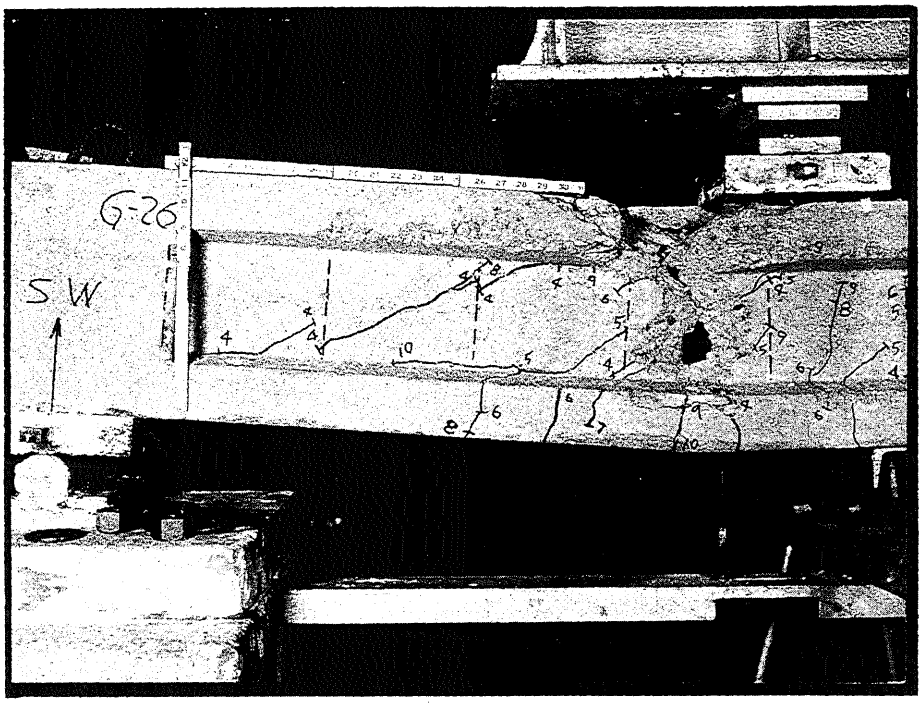

FIG. 53 TRANSITION FAILURE, BEAM G26

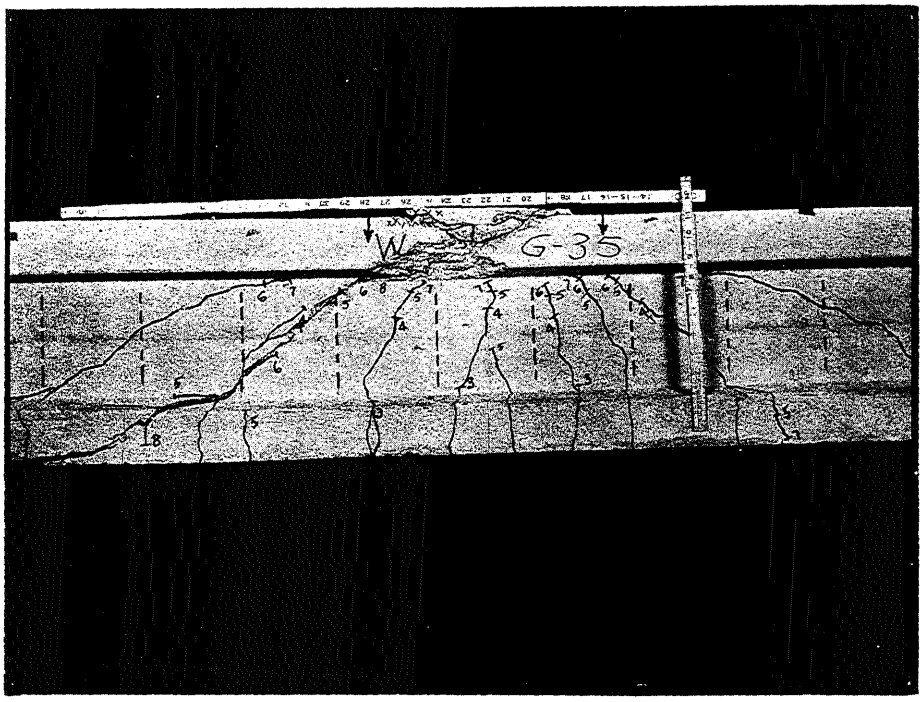

FIG. 54 TRANSITION FAILURE, BEAM G35

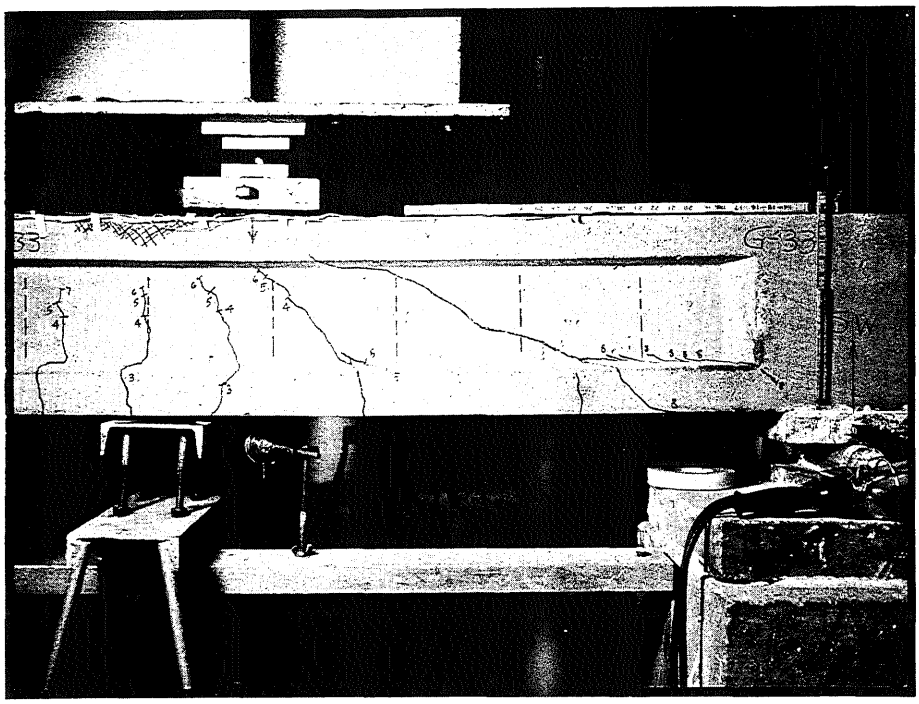

FIG. 55 INITIATION OF CRUSHING IN THE TOP FLANGE OF BEAM G33

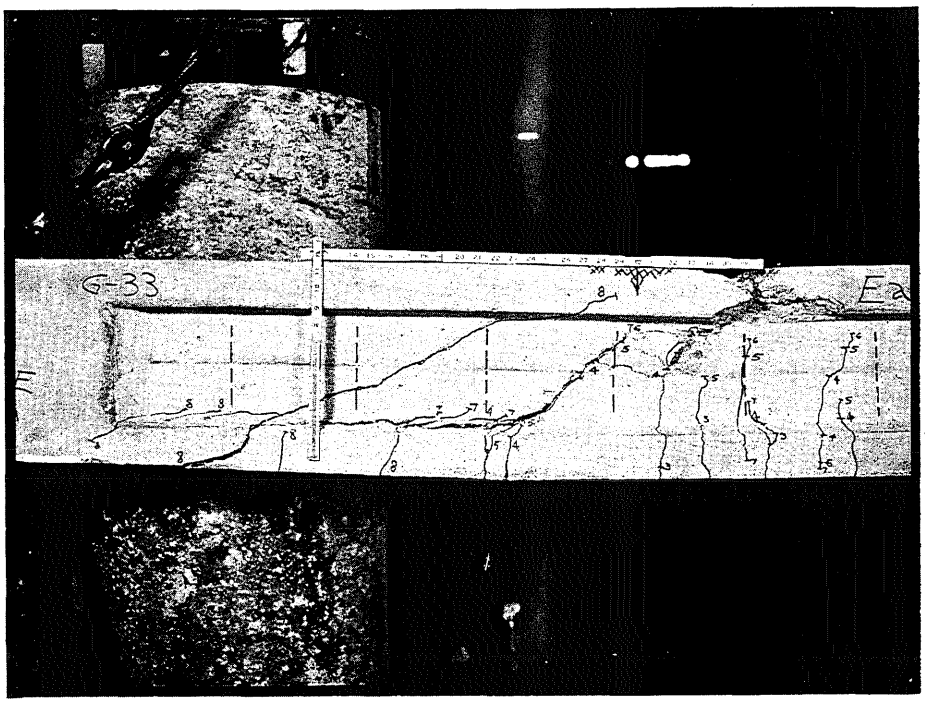

FIG. 56 BEAM G33 AFTER FAILURE

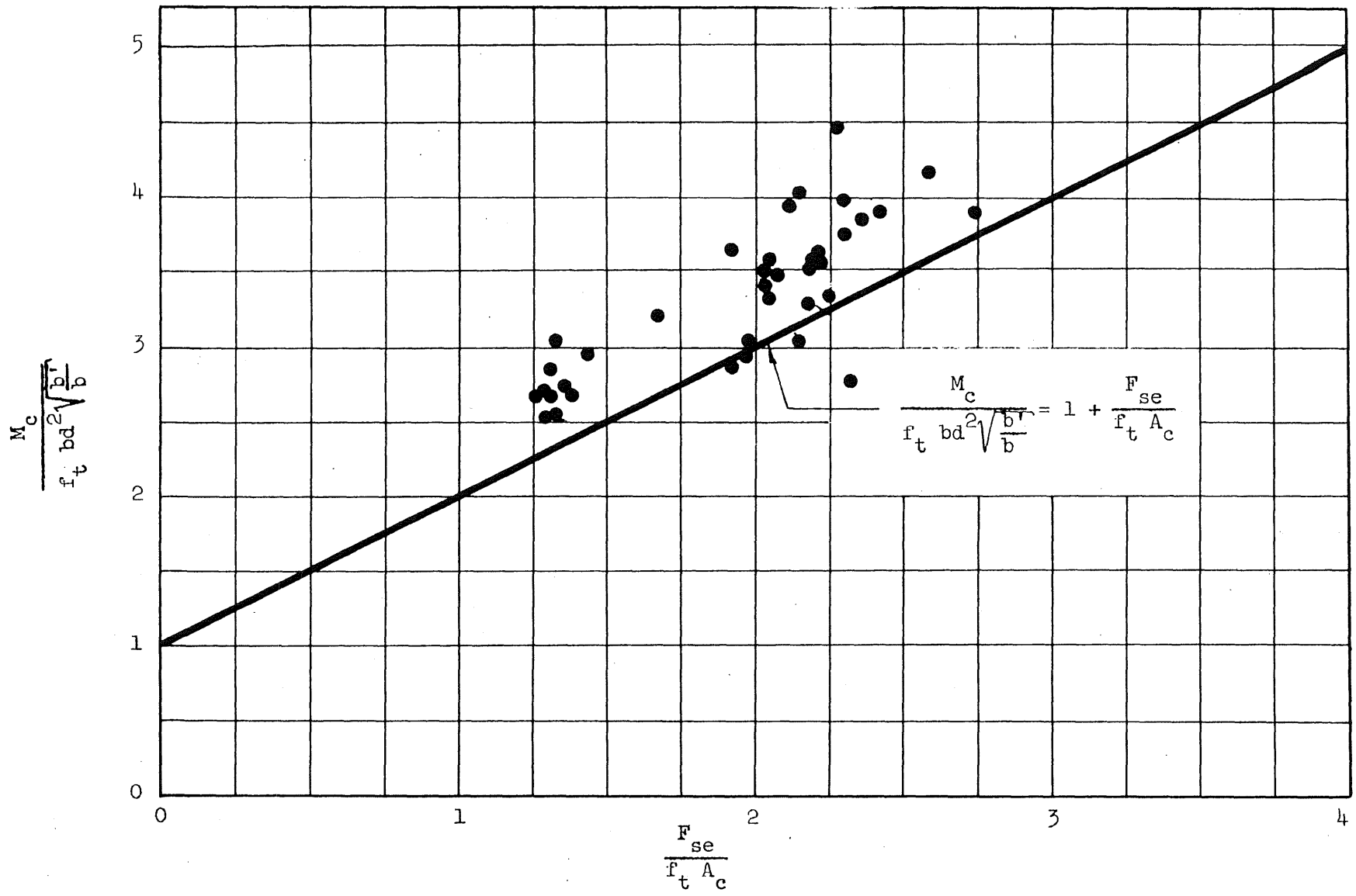

FIG. 57 RELATION BETWEEN INCLINED CRACKING MOMENT AND MEAN COMPRESSIVE PRESTRESS

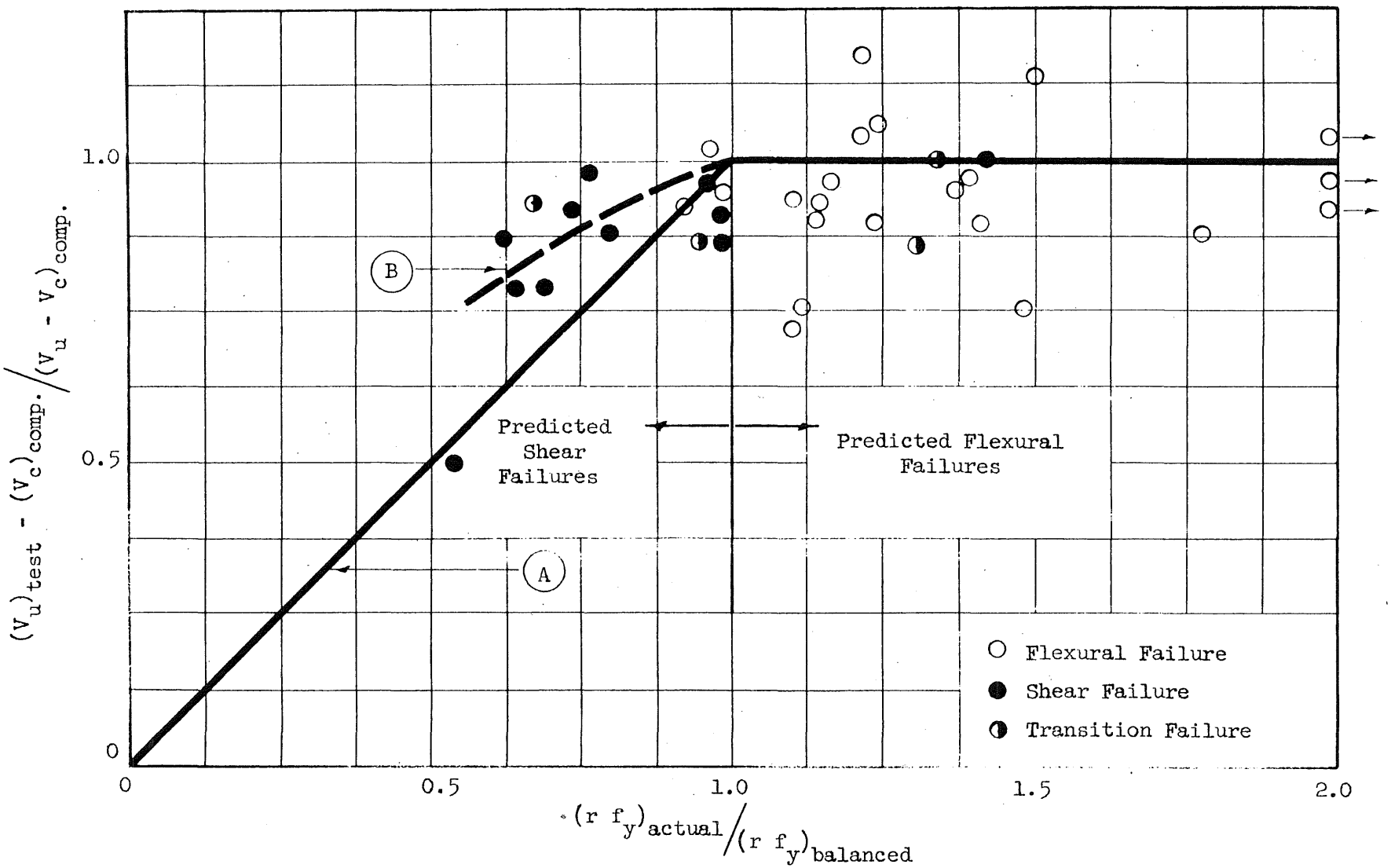

FIG. 58 RELATION BETWEEN THE AMOUNT OF WEB REINFORCEMENT AND THE INCREASE IN SHEAR BEYOND INCLINED CRACKING

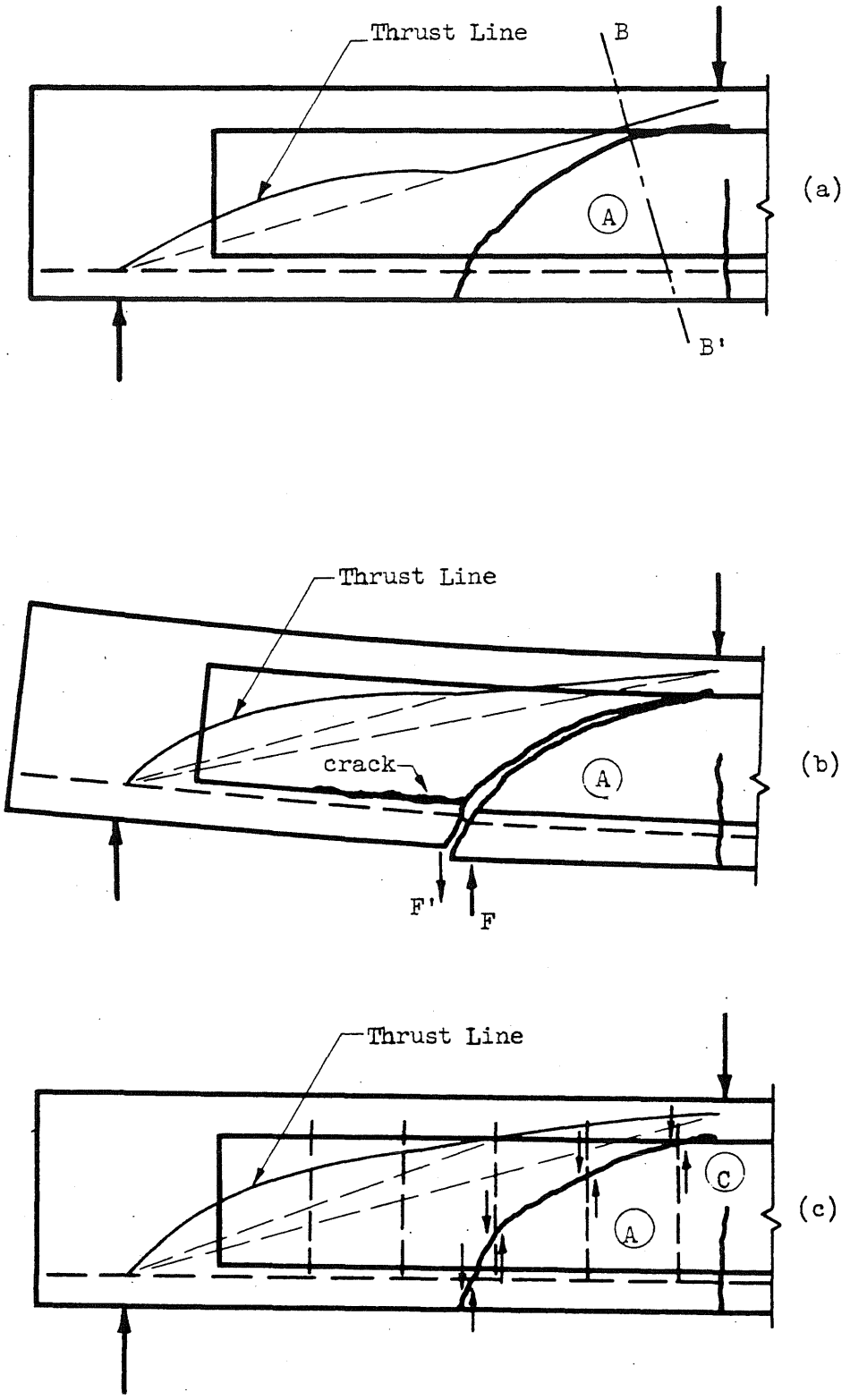

FIG. 59 IDEALIZED CONDITIONS AFTER INCLINED CRACKING

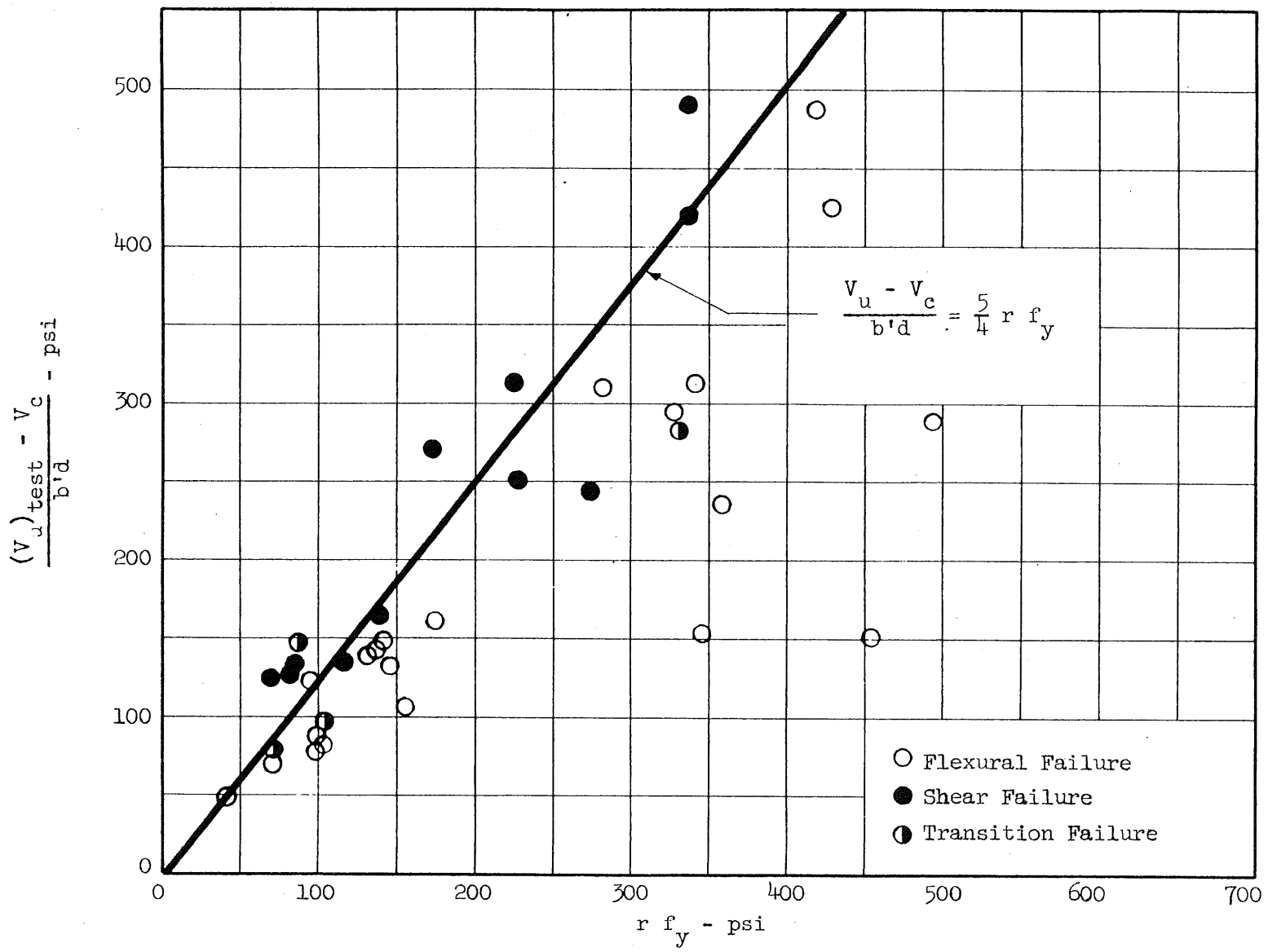

FIG. 60 EFFECT OF WEB REINFORCEMENT ON THE INCREASE IN SHEAR BEYOND INCLINED CRACKING

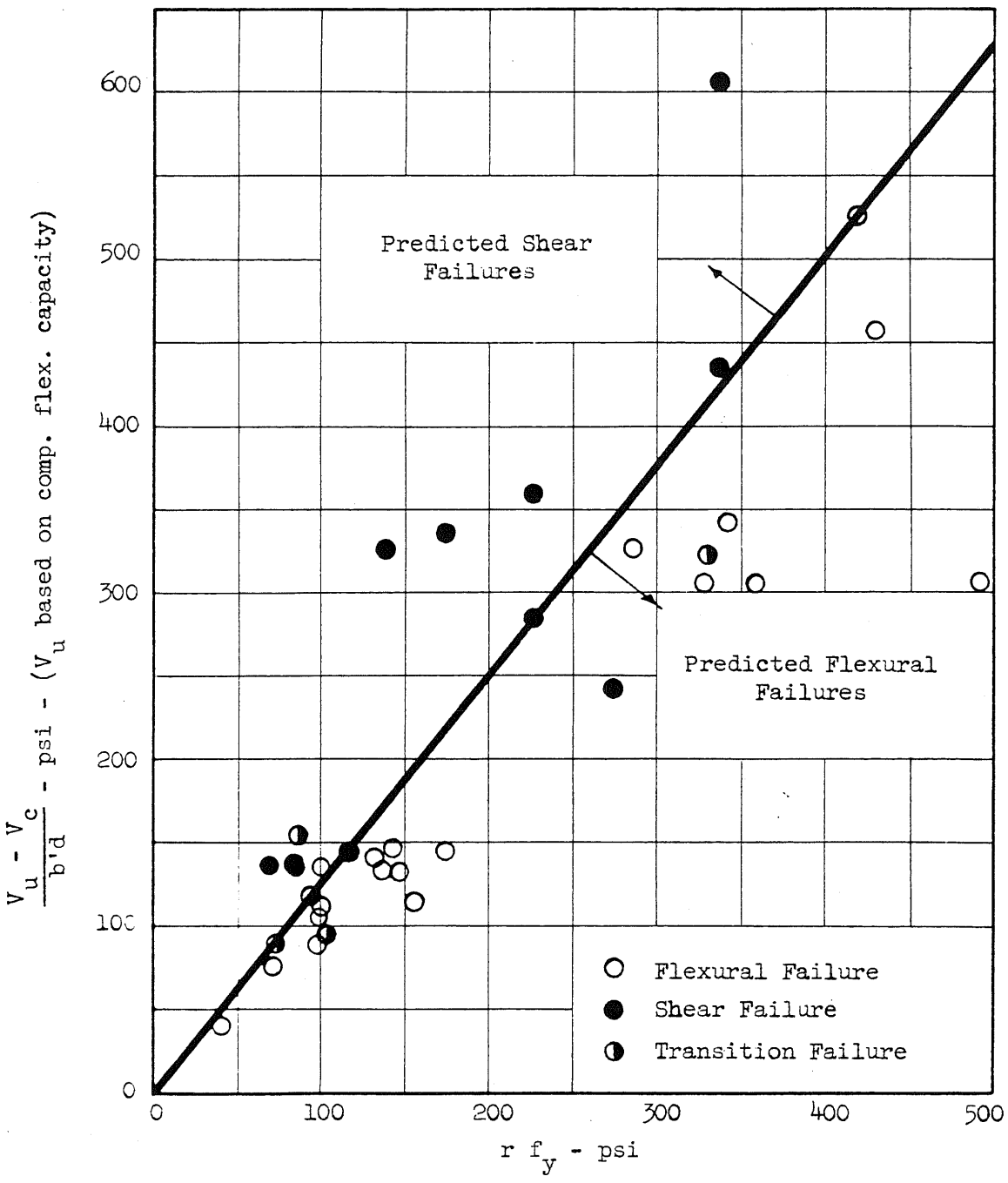

FIG. 61 PREDICTED AND OBSERVED MODES OF FAILURE